




**ADVERTIMENT.** L'accés als continguts d'aquesta tesi queda condicionat a l'acceptació de les condicions d'ús establertes per la següent llicència Creative Commons:  <https://creativecommons.org/licenses/?lang=ca>

**ADVERTENCIA.** El acceso a los contenidos de esta tesis queda condicionado a la aceptación de las condiciones de uso establecidas por la siguiente licencia Creative Commons:  <https://creativecommons.org/licenses/?lang=es>

**WARNING.** The access to the contents of this doctoral thesis it is limited to the acceptance of the use conditions set by the following Creative Commons license:  <https://creativecommons.org/licenses/?lang=en>

# **UAB**

## **Universitat Autònoma de Barcelona**

**Doctoral Program in Medicine**

**Department of Medicine**

Doctoral Thesis

### **THE ROLE OF SPINAL CORD RESERVE IN MULTIPLE SCLEROSIS**

Author

**Neus Mongay Ochoa**

Supervisors

**Deborah Pareto Onghena**

**Jaume Sastre Garriga**

Tutor

**Xavier Montalban Gairin**

Barcelona, 2024



## **The role of Spinal Cord Reserve in Multiple Sclerosis**



## AGRAÏMENTS

Em dono la llicència d'aprofitar aquest petit espai per ser subjectiva i no esta regida pels principis del mètode científic, així com per confessar, si se'm permet, que potser es una de les parts de la tesi que més m'ha agradat escriure.

No tinc enregistrat en el meu hipocamp quan vaig decidir que volia ser metgessa, potser era quelcom que ja sabia i prou. Però si recordo el moment en el que la Neurologia va activar tot el meu sistema límbic, generant una resposta unilateral: a segon de carrera, durant la classe del Professor Jose Luis Fernández sobre la fisiopatologia de la migranya. Jo, migranyosa des de la infància (a l'igual que un percentatge gens menyspreable dins dels companys de l'especialitat), em vaig quedar fascinada amb l'activació del sistema trigèmin-vascular que explicava el meu dolor. I el entendre el perquè, o si mes no, el com, em va alleugerar. Així doncs, asseguda en el Ministerio de Educación per triar plaça, en la meva llista nomes hi havia escrit Neurologia.

Ara, uns quants anys i aventures després, sento que el haver pogut desenvolupar aquesta tesi doctoral és un somni complit, així que tinc la necessitat de fer una menció especial a les persones que ho han fet possible.

A Xavier Montalban i Mar Tintoré per obrir-me les portes del Centre d'esclerosi múltiple de Catalunya, i donar-me l'oportunitat d'aprendre i formar part de l'equip qui hi ha enrere del nom Cemcat.

A Jaume Sastre-Garriga, per haver confiat en mi des del principi, per introduir-me en el mon de la Neuroimmunologia, tant en la seva vessant clínica com en la recerca, per ajudar-me a agafar embranzida, i enlairar-me.

A Deborah Pareto, la qual s'ha convertit en un referent per mi en tots els sentits; perquè ella ho sap, sense necessitat de dir-ho.

Als meus mentors durant la residència a l'Hospital de Bellvitge, per haver-me guiat en les primeres fases de l'aprenentatge i ajudat a convertir-me en la neuròloga que soc avui.

No puc deixar de mencionar a tot el personal que treballa en la Ressonància, als Tècnics, a les Administratives, a les Infermeres, totes elles persones amb funcions indispensables dins del camp de la Medicina en general, i la Neurologia en particular.

A Ceci, Ares, Clara, Vicky, Claudia, Nathane, Raquel, Ana, Silvia, Valentina, Marion, Belen, Leo, i totes les dones que amb la seva fortalesa i independència m'acompanyen en el meu camí, trencant el sostre de vidre, donant-me el suport emocional continuu que requereix la situació. Evitant qualsevol tipus de biaix, i no menys important per això, aquí també hi son l'Albert, Sergio, Edu, Pablo, Guille, Fer, Abel, Josep.

A la meva mare, al meu pare, al meu padrí, a la meva padrina, a Joan, a Jacint; sempre.

I com no, als pacients, evitant explícitament la paraula "nostres" pacients, perquè som nosaltres qui som, el SEUS metges.



## ABBREVIATIONS

|              |  |                  |  |
|--------------|--|------------------|--|
| <b>AI</b>    | Artificial intelligence                  | <b>JIM</b>       | Jacobian integration method                                |
| <b>BPF</b>   | Brain parenchyma fraction                | <b>LoA</b>       | Limit of agreement   |
| <b>CCaA</b>  | Cervical Canal Area                      | <b>MAGNIMS</b>   | Magnetic Resonance Imaging in Multiple Sclerosis           |
| <b>CIS</b>   | Clinical Isolated syndrome               | <b>MP-RAGE</b>   | Magnetization prepared – rapid gradient echo               |
| <b>CMSC</b>  | Consortium of Multiple Sclerosis Centres | <b>MRI</b>       | Magnetic Resonance Imaging                                 |
| <b>CNS</b>   | Central nervous system                   | <b>MS</b>        | Multiple Sclerosis   |
| <b>CSA</b>   | Cross-sectional area                     | <b>MSFC</b>      | Multiple sclerosis functional composite                    |
| <b>CSF</b>   | Cerebrospinal fluid                      | <b>NAIMS</b>     | North American Imaging in Multiple Sclerosis Cooperative   |
| <b>CV</b>    | Coefficient of variation                 | <b>Neuro-QoL</b> | Quality of life in neurological disorders                  |
| <b>DIR</b>   | Double-inversion recovery                | <b>PASAT</b>     | Paced auditory serial addition test                        |
| <b>DIS</b>   | Dissemination in space                   | <b>PIRA</b>      | Progression independent of relapse activity                |
| <b>DIT</b>   | Dissemination in time                    | <b>PDDS</b>      | Patient-determined disease steps                           |
| <b>DTI</b>   | Diffusion tensor imaging                 | <b>PPMS</b>      | Primary progressive multiple sclerosis                     |
| <b>DMT</b>   | Disease-modifying therapy                | <b>PRL</b>       | Paramagnetic rim lesion                                    |
| <b>DSC</b>   | Dice similarity coefficient              | <b>PROMs</b>     | Patient-reported outcomes measurements                     |
| <b>DWI</b>   | Diffusion-weighted image                 | <b>PST</b>       | Processing speed test                                      |
| <b>EDSS</b>  | Expanded Disability Status Scale         | <b>pwMS</b>      | People with multiple sclerosis                             |
| <b>FA</b>    | Flip angle                               | <b>RRMS</b>      | Relapsing-remitting multiple sclerosis                     |
| <b>FLAIR</b> | Fluid attenuated inversion recovery      | <b>SEL</b>       | Slowly expanding lesion                                    |
| <b>FOV</b>   | Field of view                            | <b>SIENA</b>     | Structural image evaluation using normalization of atrophy |
| <b>GT</b>    | Ground truth                             | <b>SCPF</b>      | Spinal cord parenchyma fraction                            |
| <b>GM</b>    | Grey matter                              | <b>SCT</b>       | Spinal cord Toolbox  |
| <b>HC</b>    | Healthy control                          | <b>SD</b>        | Standard deviation   |
| <b>ICC</b>   | Intraclass correlation coefficient       | <b>SDMT</b>      | Symbol digit modality test                                 |
| <b>IQR</b>   | Interquartile range                      | <b>SPM</b>       | Statistical parametric mapping                             |



|             |  |              |                    |
|-------------|--|--------------|--------------------|
| <b>SPMS</b> | Secondary progressive multiple sclerosis | <b>T2WI</b>  | T2-weighted image  |
| <b>STIR</b> | Short tau inversion recovery             | <b>T25FW</b> | Timed 25-foot walk |
| <b>TIV</b>  | Total intracranial volume                | <b>WM</b>    | White matter       |
| <b>TE</b>   | Echo time                                | <b>2D</b>    | Two-dimension      |
| <b>TR</b>   | Repetition time                          | <b>3D</b>    | Three-dimension    |
| <b>T1WI</b> | T1-weighted image                        | <b>9-HPT</b> | 9-hole peg test    |

## Index: Figures

|  |    |
|--|----|
| <b>Figure 1.</b> Schematic representation of the risk factors related to susceptibility for developing multiple sclerosis and the subsequent disability progression associated with the disease.....     | 17 |
| <b>Figure 2.</b> Spinal cord and spinal canal.....   | 30 |
| <b>Figure 3.</b> Spinal cord and spinal canal visualization with a sagittal brain 3D T1WI (A) and cervical cord 3DT1WI (B) in the same subject.....  | 31 |
| <b>Figure 4.</b> Conceptualization of the holistic concept of Central Nervous System (CNS) reserve .....   | 37 |
| <b>Figure 5.</b> Graphical representation of the proposed pipeline to estimate the cervical canal.....   | 47 |
| <b>Figure 6.</b> Cervical canal area mask obtained with the proposed pipeline (green) versus the manual segmentation (red) in a patient with multiple sclerosis.. ..                                     | 57 |
| <b>Figure 7.</b> Representation of individual and average ICC.....   | 58 |
| <b>Figure 8.</b> Bland & Altman plots showing the agreement between CCaA estimations assessed in different number of slices.....   | 59 |
| <b>Figure 9.</b> Violin plots with the distribution of the cervical canal area (CCaA) assessed at C2/C3 and C3/C4 intervertebral disc levels according to the different phenotypes.....                  | 62 |
| <b>Figure 10.</b> Exemplary case: Cervical canal area segmentation at C2/C3 and C3/C4 intervertebral disc levels derived from the MRI sequences employed for the analysis. ....                          | 64 |
| <b>Figure 11.</b> Spearman correlations with the 95% confidence interval between cervical canal area (CCaA) assessed in different MRI sequences and EDSS scores at C3/C4 intervertebral disc level. .... | 66 |
| <b>Figure 12.</b> Exemplary case. Qualitative differences in CCaA segmentation at C2/C3 intervertebral disc level and at C3/C4 level .....   | 71 |
| <b>Figure 13.</b> Mean cross-sectional area and sagittal profile of the spinal canal from C2 to C5 in cervical cord 2D T2WI, STIR, and brain 3D T1WI. ....   | 74 |

## Index: Tables

|  |    |
|--|----|
| <b>Table 1.</b> Standardised brain, spinal cord and optic nerve MRI protocols in the diagnosis and monitoring of multiple sclerosis.....   | 21 |
| <b>Table 2.</b> Distribution of phenotypes across the participating centres. ....  | 51 |
| <b>Table 3.</b> Acquisition parameters for the different MRI sequences. ....   | 52 |
| <b>Table 4.</b> Demographical, clinical and radiological characteristics. ....   | 56 |
| <b>Table 5.</b> Final cohorts at C2/C3 and C3/C4 intervertebral disc levels, as well as the excluded HC and pwMS.. ....  | 61 |
| <b>Table 6.</b> Multivariate regression models to investigate the association between EDSS and Cervical Canal Area (CCaA) at baseline, measured at C2/C3 and C3/C4 intervertebral disc levels .....  | 63 |
| <b>Table 7.</b> Absolute and consistency intraclass correlation coefficients (ICC) and their confidence interval (95% CI) to assess the equivalence between different MRI sequences at the two intervertebral disc levels (C2/C3 and C3/C4)..... | 65 |
| <b>Table 8.</b> Demographical, clinical and cervical canal measures using different MRI sequences at C2/C3 and C3/C4 intervertebral disc levels.....   | 66 |

# INDEX

---

|  |           |
|--|-----------|
| <b>ABSTRACT</b>  | <b>10</b> |
| <b>RESUM</b>   | <b>12</b> |
| <b>1. INTRODUCTION</b>   | <b>15</b> |
| 1.1 Multiple sclerosis at a glance                                       | 16        |
| 1.2 Magnetic resonance imaging: the tool of choice in MS                 | 19        |
| 1.3 Clinical approaches to measure progression                           | 22        |
| 1.4 Radiological hints to detect progression: an Up-To-Date overview     | 24        |
| 1.4.1 Brain atrophy: methodological aspects and clinical relevance       | 26        |
| 1.4.2 Spinal cord atrophy: methodological aspects and clinical relevance | 29        |
| 1.5 The concept of “Reserve” in MS                                       | 34        |
| <b>2. THESIS JUSTIFICATION</b>   | <b>39</b> |
| <b>3. HYPOTHESES</b>   | <b>41</b> |
| <b>4. OBJECTIVES</b>   | <b>43</b> |
| <b>5. METHODS</b>  | <b>45</b> |
| 5.1 Pipeline validation  | 46        |
| 5.2 Assessment of the spinal cord reserve in a multicentric cohort       | 49        |
| 5.3 Estimation of the cervical canal area in additional MRI sequences    | 52        |
| <b>6. RESULTS</b>  | <b>55</b> |
| 6.1 Pipeline validation  | 56        |
| 6.2 Assessment of the spinal cord reserve in a multicentric cohort       | 60        |
| 6.2.1 CCaA at C2/C3 intervertebral disc level                            | 60        |
| 6.2.2 CCaA at C3/C4 intervertebral disc level                            | 62        |
| 6.3 Estimation of the CCaA in additional MRI sequences                   | 63        |
| <b>7. DISCUSSION</b>   | <b>67</b> |
| <b>8. CONCLUSIONS</b>  | <b>77</b> |
| <b>9. FUTURE LINES OF RESEARCH</b>                                       | <b>79</b> |
| <b>10. BIBLIOGRAPHY</b>  | <b>83</b> |
| <b>11. ANNEX</b>   | <b>95</b> |
| 11.1 Publication   | 96        |
| 11.2 Oral communication  | 102       |
| 11.3 Funding and scholarships  | 104       |



## ABSTRACT

---

The present thesis addresses the methodological and clinical aspects of spinal cord reserve.

**Background:** The concept of brain reserve, represented by total intracranial volume (TIV), reflects maximal lifetime brain growth and serves as a proxy for neuronal or synaptic count. In multiple sclerosis (MS), a larger brain reserve, indicated by a greater TIV, is associated with a higher capacity to endure significant disease burden without cognitive decline. Recently, it has been postulated that a greater spinal cord reserve, assessed by the cervical canal area (CCaA), would also be protective against physical disability in MS.

**Objectives:** We aimed (i) to validate an analysis pipeline based on the Spinal Cord Toolbox (SCT) to obtain reproducible CCaA measures from brain and cervical cord sagittal magnetic resonance imaging (MRI) 3D T1-weighted images (T1WI), (ii) to apply the pipeline on a multicentre cohort of well-characterized people with MS (pwMS) and healthy controls (HC) to examine CCaA differences among groups and MS phenotypes, and explore its potential association with disability progression, and (iii) to evaluate the performance of our pipeline in estimating CCaA using alternative most commonly used MRI sequences in clinical practice.

**Materials and Methods:** Each objective was developed as a distinct project with its own cohort and methodology. For the first objective, 8 HC and 18 pwMS underwent baseline and follow-up brain and cervical cord sagittal 3D T1WI. CCaA measures obtained with the proposed pipeline were compared with manual segmentations using the Dice similarity coefficient (DSC). CCaA estimations from brain and cervical cord MRIs were also compared using the intraclass correlation coefficient (ICC). For the second objective, clinical and MRI data were collected at nine European MAGNIMS sites including 177 HC, 289 relapsing MS, and 139 progressive MS. CCaA was estimated at C2/C3 and C3/C4 levels. We compared the mean CCaA differences between groups, the association between Expanded Disability Status Scale (EDSS) and CCaA at baseline, and the relationship between CCaA and disability progression at 5-year follow-up, using multivariable regression models adjusted by age, sex, spinal cord parenchymal fraction, and cervical cord lesions. For the third objective, our pipeline was adapted to suit additional MRI sequences. The cohort included 52 pwMS who underwent sagittal brain 3D T1WI, and cervical cord sagittal 2D T1WI, 2D T2WI, and 2D short-tau inversion recovery (STIR) images. Semi-automated CCaA estimations were performed from reconstructed axial images at the C2/C3 and C3/C4 levels, and then compared to manual CCaA

masks using the DSC. The equivalence of CCaA estimations across sequences was assessed using the ICC.

**Results:** In the first study, the agreement between semi-automated and manual CCaA masks was excellent, with a mean DSC (range)=0.90 (0.73–0.97). CCaA estimations obtained from brain and cervical MRIs also showed a high agreement (ICC = 0.77; 95% CI, 0.45–0.90). In the second study, no significant differences in CCaA between HC and relapsing MS were observed, whereas progressive MS showed significantly lower CCaA, both at C2/C3 (HC: 214.62mm<sup>2</sup> [SD 8.42] vs. relapsing MS: 213.68mm<sup>2</sup> [SD 9.02] vs. progressive MS: 210.51mm<sup>2</sup> [SD 10.35], p=0.007) and C3/C4 levels (169.67mm<sup>2</sup> [SD 6.50] vs. 169.44mm<sup>2</sup> [SD 6.94] vs. 165.16mm<sup>2</sup> [SD 7.39], p<0.001). At C3/C4 level, CCaA and baseline EDSS were significantly associated ( $\beta$ -0.13, p<0.001); besides pwMS with clinical worsening at 5-year follow-up displayed a smaller CCaA at baseline (worsened vs. stable: 167.03 mm<sup>2</sup> [SD 7.53] vs. 169.13mm<sup>2</sup> [SD 7.13], p=0.03). Regarding the third study, CCaA estimation was not feasible on 2D T1WI. High agreement was found between semi-automated and manual CCaA masks derived from T2WI (DC range = 0.92 [0.89-0.93]) and STIR (DC range = 0.90 [0.88-0.92]). The equivalence of CCaA across sequences was higher at C3/C4 than at C2/C3: ICC T2WI – brain 3D T1WI was 0.67 (0.38-0.82) and 0.63 (0.26-0.82), while ICC STIR – brain 3DT1WI was 0.80 (0.64-0.89) and 0.52 (0.22-0.70), respectively. At C3/C4, T2WI CCaA and EDSS were significantly correlated (rho -0.34, p 0.023).

**Conclusions:** Our proposed pipeline provide reproducible CCaA measures from brain and cervical cord 3D T1WI MRI. With this methodology, we demonstrated that CCaA is associated with baseline EDSS and clinical worsening in a multicentric MS cohort, supporting the existence of spinal cord reserve. Moreover, progressive patients displayed a smaller CCaA, which could imply that a lower spinal cord reserve might be a feature of progressive MS. Finally, CCaA segmentation was also feasible on 2D sagittal T2WI and STIR, showing a good equivalence with estimations obtained from brain 3D T1WI.

## RESUM

---

La present tesi aborda els aspectes metodològics i clínics de la reserva medul·lar espinal.

**Antecedents:** El concepte de reserva cerebral, representat pel volum intracranial total (VIT), reflecteix el creixement màxim del cervell al llarg de la vida i serveix com a indicador del nombre de neurones o sinapsis. En l'esclerosi múltiple (EM), una reserva cerebral més gran, indicada per un VIT més gran, s'associa amb una major capacitat per suportar una càrrega significativa de la malaltia sense declivi cognitiu. Recentment, s'ha postulat que una reserva més gran de la medul·la espinal, avaluada per l'àrea del canal cervical (CCaA), també seria protectora contra la discapacitat física en l'EM.

**Objectius:** Ens vam proposar (i) validar una eina d'anàlisi basat en el software Spinal Cord Toolbox (SCT) per obtenir mesures reproduïbles de la CCaA a partir d'imatges de ressonància magnètica (IRM) sagitals 3D ponderades en T1 (T1WI) del cervell i la medul·la cervical, (ii) aplicar l'eina a una cohort multicèntrica ben caracteritzada de persones amb EM (paEM) i controls sans (CS) per examinar les diferències de CCaA entre grups i fenotips d'EM, així com explorar la seva possible associació amb la progressió de la discapacitat, i (iii) avaluar el rendiment de la nostra eina en l'estimació de la CCaA emprant seqüències d'IRM més comunament utilitzades en la pràctica clínica.

**Materials i mètodes:** Cada objectiu es va desenvolupar com un projecte diferenciat amb la seva pròpia cohort i metodologia. Per al primer objectiu, 8 CS i 18 paEM es van realitzar una IRM sagital 3D T1WI del cervell i la medul·la cervical en el moment basal i a l'any següent. Les mesures de CCaA obtingudes amb la nostra eina es van comparar amb segmentacions manuals utilitzant el coeficient de similitud de Dice (DSC). També es van comparar les estimacions de CCaA a partir d'IRM del cervell i de la medul·la cervical utilitzant el coeficient de correlació intraclasse (ICC). Per al segon objectiu, es van recopilar dades clíniques i d'IRM en nou llocs europeus del MAGNIMS, incloent-hi 177 CS, 289 EM recurrent (EMR) i 139 EM progressiva (EMP). La CCaA es va estimar als nivells intervertebrals C2/C3 i C3/C4. Vam comparar les diferències mitjanes de CCaA entre grups, l'associació entre l'Escala Expandida de Discapacitat (EDSS) i la CCaA en el moment basal, i la relació entre la CCaA i la progressió de la discapacitat en el seguiment de 5 anys, utilitzant models de regressió multivariable ajustats per edat, sexe, fracció parenquimal de la medul·la espinal i lesions de la medul·la cervical. Per al tercer objectiu, vam adaptar la nostra eina per utilitzar seqüències addicionals d'IRM. La



cohort incloïa 52 paEM que es van realitzar IRM sagitals 3D T1WI del cervell, i sagitals 2D T1WI, 2D T2WI, i 2D STIR de la medul·la cervical. Es van realitzar estimacions semiautomàtiques de la CCaA a partir d'imatges axials reconstruïdes als nivells C2/C3 i C3/C4, i després es van comparar amb màscares manuals de CCaA utilitzant el DSC. L'equivalència de les estimacions de CCaA a través de les seqüències es va avaluar utilitzant l'ICC.

**Resultats:** En el primer estudi, l'acord entre les màscares semiautomàtiques i manuals de CCaA va ser excel·lent, amb una DSC mitjana (rang) de 0.90 (0.73–0.97). Les estimacions de CCaA obtingudes a partir d'IRM del cervell i de la medul·la cervical també van mostrar un alt acord (ICC = 0.77; IC del 95%, 0.45–0.90). En el segon estudi, no es van observar diferències significatives en la CCaA entre CS i EMR, mentre que l'EMP va mostrar una CCaA significativament menor, tant als nivells C2/C3 (CS: 214.62mm<sup>2</sup> [DE 8.42] vs. EMR: 213.68mm<sup>2</sup> [DE 9.02] vs. EMP: 210.51mm<sup>2</sup> [DE 10.35], p=0.007) com C3/C4 (169.67mm<sup>2</sup> [DE 6.50] vs. 169.44mm<sup>2</sup> [DE 6.94] vs. 165.16mm<sup>2</sup> [DE 7.39], p<0.001). Al nivell C3/C4, la CCaA i l'EDSS basal estaven significativament associats ( $\beta$ -0.13, p<0.001); a més, els paEM amb empitjorament clínic als 5 anys mostraven una CCaA menor en el moment basal (empitjorats vs. estables: 167.03 mm<sup>2</sup> [DE 7.53] vs. 169.13mm<sup>2</sup> [DE 7.13], p=0.03). Pel que fa al tercer estudi, l'estimació de la CCaA no va ser factible en les IRM 2D T1WI. Es va trobar un acord excel·lent entre les màscares semiautomàtiques i manuals de CCaA derivades de T2WI (rang de DC = 0.92 [0.89-0.93]) i STIR (rang de DC = 0.90 [0.88-0.92]). L'equivalència de CCaA entre les seqüències va ser més alta a C3/C4 que a C2/C3: ICC T2WI – cervell 3D T1WI va ser 0.67 (0.38-0.82) i 0.63 (0.26-0.82), mentre que ICC STIR – cervell 3D T1WI va ser 0.80 (0.64-0.89) i 0.52 (0.22-0.70), respectivament. Al nivell C3/C4, la CCaA T2WI i l'EDSS estaven significativament correlacionats (rho -0.34, p 0.023).

**Conclusions:** La nostra eina proposada proporciona mesures reproduïbles de la CCaA a partir d'IRM 3D T1WI del cervell i de la medul·la cervical. Amb aquesta metodologia, vam demostrar que la CCaA està associada amb l'EDSS basal i l'empitjorament clínic en una cohort multicèntrica d'EM, donant suport a l'existència de la reserva de la medul·la espinal. A més, els pacients progressius mostraven una CCaA menor, cosa que podria implicar que una reserva menor de la medul·la espinal podria ser una característica de l'EM progressiva. Finalment, la segmentació de la CCaA també va ser factible en 2D T2WI i STIR, mostrant una bona equivalència amb les estimacions obtingudes de 3D T1WI del cervell.



# **1. INTRODUCTION**

---

# 1.Introduction

---

## 1.1 Multiple sclerosis at a glance

Multiple sclerosis (MS) is an immune-mediated, chronic and disabling neurological disease, with a great social and economic impact, since it stands as the primary cause of non-traumatic disability in young adults in Europe,<sup>1</sup> and its prevalence has increased across every world region in the last decade.<sup>2</sup>

The ultimate underlying cause of the disease remains elusive. Genetic susceptibility to MS only accounts for a fraction of the disease risk.<sup>3</sup> Notably, MS epidemiology suggests that non-genetic factors, including high latitude, female sex, low vitamin D levels, smoking, and childhood obesity are likely to play a major role in the disease development<sup>4</sup> (Figure 1). Furthermore, recent studies have highlighted the importance of seroconversion following Epstein-Barr virus infection, which appears to confer a 30-fold increase in the risk of developing MS, establishing it as one of the most prominent contributing factors to the disease.<sup>5</sup> Evidence of causality, however, remains inconclusive since the risk of MS in seronegative individuals, though minimal, is not entirely absent.<sup>5</sup>

The prediction of individual outcome, particularly the onset and magnitude of disability progression are not yet well-understood. Large natural history studies indicate that the presence of bad prognostic factors does not directly lead to disability, but serves in guiding the evolution.<sup>6</sup> Overall, poorer outcomes in MS are associated with a higher initial relapse rate, a shorter interval to the second relapse, higher level of disability in the first 5 years, and the involvement of more than 3 neural systems. In addition, the presence of oligoclonal bands, more than ten lesions on the baseline brain magnetic resonance imaging (MRI), and the presence of spinal cord lesions, as well as a persistent smoking habit, appear to predict a higher risk of disability accumulation.<sup>7,8</sup> Conversely, treatment initiation with a disease-modifying therapy (DMT) is associated with a reduction in the risk of long-term disability in patients with a first demyelinating event.<sup>9</sup> Recently, a variant allele (rs10191329 in the *DYSF-ZNF638* locus) has emerged as a predictor of MS severity.<sup>10</sup> This variant is associated with a shortened median time to require aid walking in homozygous carriers, and linked to an increased pathology in both brainstem and cortical regions.

All of these findings shed light on the complex interplay between genes, environment, lifestyle, and prognostic factors, reflecting the heterogeneous pathogenic mechanisms underlying the development and evolution of MS (Figure 1).

# 1.Introduction

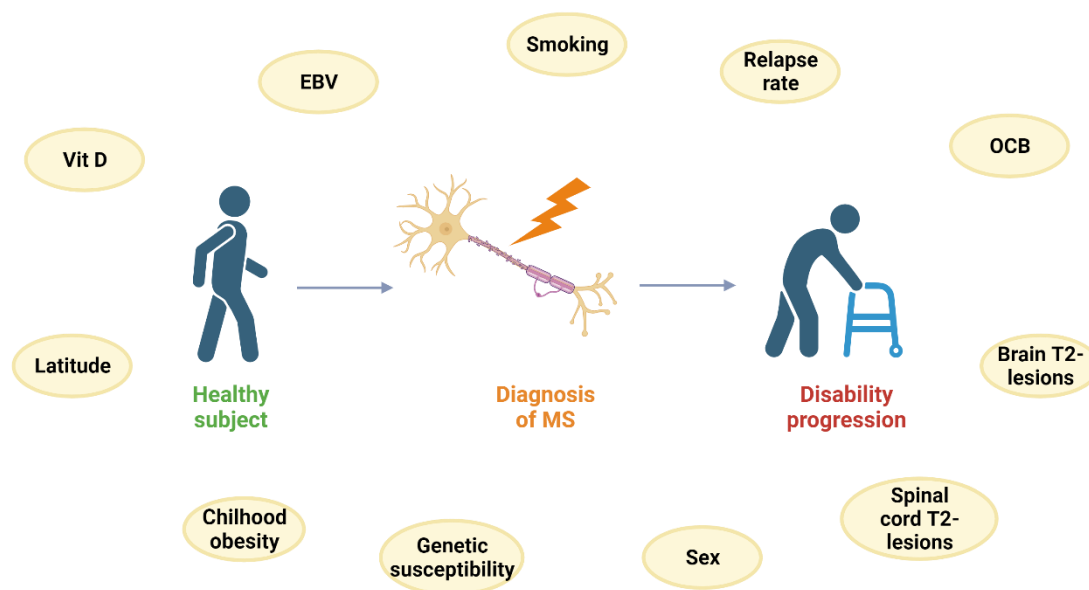


**Figure 1.** Schematic representation of the risk factors related to susceptibility for developing multiple sclerosis and the subsequent disability progression associated with the disease. EBV, Epstein-Barr virus; MS, multiple sclerosis; OCB, oligoclonal bands; Vit D, vitamin D. Created with BioRender.com

The characteristic pathological hallmark of MS is the presence of multiple perivenular inflammatory lesions, leading to demyelinating plaques, particularly noticeable in the early stages of the disease.<sup>11</sup> Clinically, neuroinflammation is characterized by acute episodes of neurological deficits, referred to as relapses.<sup>12</sup> These relapses depend on both the eloquent location and the extent of the new or enlarging acute inflammatory lesion(s) in the central nervous system (CNS), which are accurately assessed by MRI. Inflammation, which leads to oligodendrocyte damage and demyelination, is a predominantly T-cell mediated process,<sup>13</sup> although B-cells and innate immunity also play an important role.<sup>14</sup> Clinical deficits resulting from acute inflammatory demyelination could be partially reversible through remyelination<sup>12</sup> – a highly variable process across individuals and MS stages – that aims to promote both axonal survival and restoration of nerve conduction. Nevertheless, new myelin is less dense, contains thinner sheaths with widened internodes, and is more energetically demanding, which confers upon it an increased vulnerability compared to the healthy one.<sup>13</sup> In addition to these structural changes, the recovery of clinical symptoms could also be secondary to cortical plasticity,<sup>15</sup> which consists of a reorganisation of the functional activation of cortical regions to maintain clinical function. However, persistent demyelinating lesions are followed by axonal loss, underpinning the hypothesis that a lack of myelin-derived trophic support and mitochondrial dysfunction contribute to the degeneration of chronically demyelinated axons,<sup>16</sup> representing the pathological substrate of irreversible neurological deficits.

# 1.Introduction

---

Simultaneously with all these processes, neurodegeneration (neuronal cell death, axonal loss, astrocytic gliosis) begins beyond focal plaque formation in both the grey matter (GM) and white matter (WM).<sup>17</sup> This occurs at the early stages of the disease, leading to the accumulation of damage to the microstructure and a loss of volume in the brain and spinal cord.<sup>18</sup> In fact, histopathological studies and advanced MRI sequences have revealed that in normal-appearing WM there is diffuse myelin damage and axonal loss,<sup>13</sup> whereas in normal-appearing GM there is a loss of neural and synaptic density along with widespread demyelination.<sup>19</sup> Consequently, the progressive accumulation of disability in MS also occurs independently of relapse activity early in the disease course — a concept known as PIRA (Progression Independent of Relapse Activity)<sup>20</sup> – where relapses take place on a background of subtle progression before progression becomes dominant itself.<sup>21</sup> Indeed, PIRA is reported to occur in roughly 10% of all patients with a first demyelinating attack within the first 5 years of the disease,<sup>21</sup> contributing to at least 50% of all disability accrual events in typical relapsing-remitting MS (RRMS).<sup>22</sup> This phenomenon has become increasingly noticeable since the introduction of highly effective anti-inflammatory treatments and more aggressive immune reconstitution therapies, which achieve an almost complete suppression of focal inflammatory activity. In this current scenario, people with MS (pwMS) keep experiencing clinical deterioration despite being relapse-free and exhibiting neither new nor enlarging lesions on MRI. These changes contribute to a progressive clinical worsening that affects numerous spheres.<sup>20</sup> Eventually, focal and diffuse damage in the brain and spinal cord results in profound atrophy of the white and grey matter, leading to irreversible neurological disability.<sup>18</sup>

As a summary, the traditional two-stage view – relapsing or progressive – of MS and its division into the classical phenotypes (RRMS, secondary-progressive MS [SPMS], and primary progressive MS [PPMS]), are still useful for establishing a definite diagnosis, monitoring the evolution of the disease, identifying novel biomarkers, developing new drugs, evaluating social impact, and translating information to patients and their relatives. However, as our knowledge of pathological mechanisms broadens, it becomes more evident that this classification of the disease is somewhat artificial—a mere simplification of the spectrum.<sup>17</sup> Therefore, we are facing a complex disease, highly variable across patients in terms of relapses, neurodegeneration and treatment response, opening up a vast field for research.

# 1.Introduction

---

## 1.2 Magnetic resonance imaging: the tool of choice in MS

Histological analysis represents the gold standard technique for studying almost all pathophysiological processes, including inflammation and neurodegeneration in MS.<sup>11</sup> However, its inherent limitations are more than evident, as autopsy and biopsy samples of pwMS are rare and biased towards either a chronic burnt-out end or fulminant acute early stage.<sup>23</sup> In this context, the use of MRI has become a crucial element for in-vivo evaluation of pathology, playing an essential role in every aspect of the MS management, including diagnosis, monitoring disease progression, assessing treatment response, and research.<sup>24</sup> The latest published consensus protocol on MRI use for pwMS merges recommendations from the Magnetic Resonance Imaging in Multiple Sclerosis study group (MAGNIMS), Consortium of Multiple Sclerosis Centres (CMSC), and North American Imaging in Multiple Sclerosis Cooperative (NAIMS),<sup>25</sup> also extending the recommendations to the use of MRI in special populations and situations, such as patients with MS during childhood, pregnancy, and the postpartum period, as well as addressing safety concerns about the repetitive administration of intravenous gadolinium-based contrast agents.

The milestone in the diagnosis of MS involves demonstrating dissemination of lesions both in space (DIS) and time (DIT) in patients with a clinically isolated syndrome (CIS).<sup>26</sup> From the Barkhof-Tintore criteria,<sup>27,28</sup> where fulfilling DIS required the presence of at least three out of four MRI indicators (one gadolinium-enhancing lesion or nine T2-weighted images (T2WI) hyperintense lesions if there is no gadolinium-enhancing lesion, at least three periventricular lesions, at least one juxtacortical lesion, and/or at least one infratentorial lesion), to the latest revised version of McDonald criteria in 2017,<sup>29</sup> the role of MRI has become pivotal. Furthermore, since the 2010 McDonald criteria,<sup>30</sup> it has been possible to demonstrate DIS and DIT at a single scan if there are more than one T2WI lesions in at least two of four areas of the locations considered characteristic for MS (juxtacortical, periventricular, infratentorial, spinal cord) and a simultaneous presence of asymptomatic gadolinium-enhancing and non-enhancing lesions, establishing an earlier diagnosis.

The diagnostic value of spinal cord MRI in MS has been clearly established, and it plays an essential role in the 2017 McDonald criteria.<sup>29</sup> The relatively high presence of spinal cord lesions in patients with CIS, even in the absence of spinal cord symptoms, and the lower prevalence of such lesions in people with other neurological diseases or during healthy aging compared to those with MS or CIS, underscores the importance of spinal cord MRI. It serves

# 1.Introduction

---

both to demonstrate DIS and DIT, and to rule out alternative diagnoses, including vascular diseases, spinal cord compression, and inflammatory disorders.<sup>25</sup> The most affected segment in MS is the cervical cord, although demyelinating lesions have also been reported in thoracic spinal segments and the conus.<sup>31</sup> Conversely, few patients exhibit lesions that are exclusively located below the level of the fifth thoracic vertebra.<sup>31</sup> Therefore, scanning the upper half of the spinal cord (from C1 to T5) seems reasonable when there is no clinical suspicion of lower cord segment involvement, enabling shorter acquisition times compared to the entire spinal cord scan.<sup>25</sup>

Optic nerve MRI in pwMS with optic neuritis can detect T2WI hyperintense and gadolinium-enhancing lesions.<sup>25</sup> Additionally, asymptomatic demyelinating lesions in the optic nerve have been detected in CIS and MS patients without a personal history of optic neuritis.<sup>32</sup> The optic nerve is presently not considered one of the areas of the CNS used to demonstrate DIS within the 2017 McDonald criteria for the diagnosis of MS, but this may not be the case anymore in the forthcoming iteration of the MS diagnostic criteria,<sup>29</sup> as recent studies suggest that including optic nerve involvement as the fifth topography to demonstrate DIS in subjects improves the overall performance of MS diagnostic criteria.<sup>32,33</sup>

MRI is also the key tool to monitor the disease activity, treatment response and safety of disease-modifying therapies (DMT). Specific brain and spinal cord standardized protocols are described to these purposes.<sup>25</sup> Radiological activity, in the clinical setting, is primarily defined by the presence of gadolinium-enhanced T1-weighted images (T1WI) or new/enlarging T2WI lesions. Before starting or switching a DMT, a baseline brain MRI should be obtained. Then, a 3-6-months rebaseline MRI should be performed to avoid misinterpretation of lesions that developed prior to the onset of the therapeutic effect. From that timepoint, a yearly brain MRI while the patient is on the DMT is recommended to monitor the response and facilitate an early detection of patients at high risk of a suboptimal response to allow a prompt treatment switch or escalation. Another relevant use is to rule out or early diagnose potential neurological adverse events related to DMT. The main concern is the progressive multifocal leukoencephalopathy, an opportunistic infection that occurs nearly exclusively in immunocompromised individuals, thus making pwMS taking DMT a particularly at-risk group.<sup>34</sup>

Spinal cord MRI for assessing treatment efficacy and monitoring disease activity is not recommended on a regular basis, but is advised for special clinical conditions. This includes the detection of active spinal cord lesions secondary to a relapse, the exclusion of possible



# 1.Introduction

comorbidity involving the spine or spinal cord, and when pwMS experience disability worsening that cannot be explained by brain MRI.<sup>25</sup> Similarly, follow-up optic nerve MRI is only recommended in pwMS who have either new or chronic progressive visual symptoms, and in those with repeated isolated optic nerve relapses.<sup>25</sup> (Table 1)

| <b>DIAGNOSIS</b>  |   |  |
|-------------------|---|--|
|                   | <b>Recommended</b>  | <b>Optional</b>  |
| Brain             | -Axial T2WI<br>-3D Sagittal T2 FLAIR<br>-Axial T2WI FLAIR<br>-Axial or 3D sagittal T1WI post gadolinium injection | -High resolution T1WI<br>-DWI<br>-SWI (central vein sign)<br>-DIR (cortical or juxtacortical lesions)  |
| Spinal Cord       | -At least two of them: sagittal T2WI, PD weighted, or STIR<br>-Sagittal T1WI post gadolinium injection            | -Sagittal 3D T1WI (PSIR or MP-RAGE only for the cervical segment)<br>-Axial T2WI<br>-Sagittal T1WI before gadolinium injection<br>-Axial T1WI after gadolinium injection |
| Optic nerve       | Not recommended on a regular basis (see main text)  | -Axial and coronal fat-suppressed T2WI of STIR of optic nerve (2D or 3D)<br>-Axial and coronal fat-suppressed T1WI post gadolinium injection (2D or 3D)                  |
| <b>MONITORING</b> |   |  |
|                   | <b>Recommended</b>  | <b>Optional</b>  |
| Brain             | -Axial T2WI<br>-Sagittal T2 FLAIR<br>-Axial T2 FLAIR  | -Axial or 3D sagittal T1WI after Gadolinium injection<br>-DIR<br>- High resolution T1WI  |
| Spinal Cord       | Not recommended on a regular basis (see main text)  |  |
| Optic nerve       | Not recommended on a regular basis (see main text)  |  |

**Table 1.** Standardised brain, spinal cord and optic nerve MRI protocols in the diagnosis and monitoring of multiple sclerosis. DIR, double inversion recovery, DWI, diffusion-weighted image; FLAIR, fluid-attenuated inversion recovery; MRI, magnetic resonance imaging; PSIR, phase-sensitivity inversion; STIR, short tau inversion recovery; SWI, susceptibility weighted imaging; T1WI, T1-weighted imaging; T2WI, T1-RT, T1-relaxation time; T2-weighted imaging; 2D, two-dimension; 3D, three-dimension

# 1.Introduction

---

The term 'conventional MRI' encompasses sequences used in clinical practice to describe pathology by relying on contrast changes in the acquired images.<sup>18</sup> These images, predominantly T1WI and T2WI, reflect a biophysical contrast mechanism. When using conventional MRI in the MS clinic, it is generally possible to identify: (i) the number, volume, and location of focal T2WI hyperintense lesions; (ii) the number, volume, and location of contrast-enhancing T1WI lesions; (iii) the number, volume, and location of T1-hypointense lesions (also called black holes); and (iv) the presence of global/regional atrophy (a qualitative assessment without a quantification of volume loss).<sup>35</sup> However, sensitivity to these characteristics can vary based on several technical factors.<sup>36</sup> In contrast, conventional MRI is largely insensitive to the heterogeneity of focal MS lesions and to the pathology affecting CNS tissue beyond demyelinating lesions, such as normal-appearing GM and WM, or different CNS tissue compartments, such as myelin, axons, and glia.<sup>37</sup> Actually, there are no MRI biomarkers that distinguish PPMS from RRMS, nor reliably predict the evolution of RRMS to SPMS.

In this context, there is an expanding research community engaged in the field of MS using advanced MRI sequences in combination with novel computational algorithms and artificial intelligence to explore innovative approaches for understanding the disease. Advanced imaging techniques, which can be defined as imaging modalities that are not yet implemented in daily routine practice,<sup>17</sup> provide an opportunity to assess the microscopic features of brain and spinal cord in pwMS. These techniques could be used to better understand the underlying mechanism behind neuroinflammation and neurodegeneration, facilitating the development of highly effective anti-inflammatory, neuroprotective, and reparative therapies.

## 1.3 Clinical approaches to measure progression

Clinically, the identification of progression in MS is retrospective,<sup>38</sup> relying on a history of gradual worsening of disability observed over months or years ( $\geq 6/12$  months for RRMS,  $\geq 12$  months for PPMS patients). Currently, there are no universally accepted criteria, and the classification of a patient into a progressive form is often delayed by months or even years,<sup>39</sup> which may hinder a prompt switch to a more suitable DMT. In fact, it has been seen that up to two-thirds of patients with insidious worsening of disability are still considered by clinicians to have RRMS.<sup>40</sup>

# 1.Introduction

---

The Expanded Disability Status Scale (EDSS) score is the most widely used instrument in clinical practice and clinical trials to measure MS-related disability.<sup>41</sup> Score increases in EDSS help to identify disability progression, and must be confirmed after 3-6 months to distinguish true progression from reversible disability associated with a relapse or assessment errors. However, the EDSS has limitations including reliance on ambulation functions above 4.0, limited sensitivity to progression at extreme scores, the lack of accuracy when evaluating non-physical symptoms of MS such as cognitive impairment, fatigue or depression, and a certain degree of inter-evaluator variability within the neurological examination.<sup>42,43</sup> In a recent study, the best combined criteria for defining SPMS were: an increase of one EDSS point when EDSS is  $\leq 5.5$  or 0.5 when EDSS is  $\geq 6$  in the absence of relapses, a minimum EDSS score of 4.0 and pyramidal functional system score of 2, and confirmed progression over  $\geq 3$  months, including confirmation within the leading functional system.<sup>44</sup>

Other clinical tests have been designed to measure disability progression. The Multiple Sclerosis Functional Composite (MSFC) score comprises quantitative measures of leg function/ambulation (Timed 25-Foot Walk [T25FW]), arm/hand function (9-hole Peg test [9-HPT]), and cognition (Paced Auditory Serial Addition Test [PASAT]),<sup>45</sup> providing a more comprehensive neurological assessment. Subsequently, a visual pathway test (low contrast letter acuity) was also included, and PASAT was replaced by Symbol Digit Modalities Test (SDMT).<sup>46</sup> Although the MSFC may be influenced by learning effects and the methods to calculate z-scores, a recent meta-analysis demonstrated that MSFC change can be a sensitive and effective tool to assess the clinical severity and progression of MS disease.<sup>47</sup> Nowadays, MSFC is almost exclusively used in clinical trials and other research contexts.<sup>41</sup>

The isolated used of EDSS score and disease duration could result in misclassifying patients with low physical impact but a substantial burden of invisible symptoms as having ‘benign’ MS. A possible approach is to include in the examination patient-reported outcomes measurements (PROMs),<sup>48</sup> a complementary measure to the EDSS, which assess health-related quality of life, including symptoms, cognitive status, and social aspects, offering a more accurate picture of the patient's functional status.<sup>49</sup> PROMs are increasingly used as secondary or tertiary outcomes in MS clinical trials of DMTs and symptomatic treatments, and to measure disease progression, whereas in rehabilitation trials are used as primary or coprimary outcomes.<sup>50</sup>

Recently, innovative wearable digital devices (i.e., accelerometers, gyroscopes, GPS tracking devices, etc), but also smartphones applications and biosensors, which are able to

# 1.Introduction

---

measure different functions and activities, are being developed to assess the effects of disability progression on patients' daily lives,<sup>51</sup>. These digital devices are under intense investigation, and their first results seem promising.<sup>52,53</sup>

## 1.4 Radiological hints to detect progression: an Up-To-Date overview

From the radiological perspective, the identification of progression in MS is also retrospective. Therefore, there is an increasing need to find reliable biomarkers for the early identification of MS progression and, more challenging, to predict its evolution.

The first studies aimed at predicting disease progression primarily focused on the formation and evolution of chronic or persistent T1WI hypointense lesions – commonly known as black holes – which do not enhance after gadolinium-contrast injection.<sup>54</sup> They represent areas of focal axonal damage and irreversible tissue destruction. Black holes are more frequently observed in patients with longer disease durations and progressive phenotypes.<sup>54</sup> The relationship between black holes and disability has been established in several studies,<sup>55,56</sup> showing a correlation between the increase in EDSS score within the follow-up and black hole volume at baseline. Besides, the evolution of newly formed lesions into persistent black holes is currently under investigation as a possible measure of neuroprotection in several treatment trials.<sup>57</sup>

The role of T2WI visible lesions has also been assessed in terms of disability prediction. Notably, it was demonstrated that the number of T2WI hyperintense WM lesions at MS onset, and the increase in lesion load within the first years, appear to predict the risk of long-term disability worsening. In fact, progressive MS has been shown to exhibit a higher lesion load than RRMS.<sup>58</sup> However, the clinic-radiological paradox, i.e., the weak relationship between radiological findings and clinical outcomes, remains an unresolved issue in MS.<sup>59</sup> One hypothesis posits that lesion location, in addition to lesion load, plays a key role in explaining disability. In particular, progressive MS phenotypes are most often characterized by a worsening pyramidal syndrome of the lower limbs and, to a lesser extent, the upper limbs,<sup>60</sup> suggesting corticospinal tract involvement. Studies consistently show that the highest lesion frequency occurs in the corona radiata and between the C2 and C4 vertebral levels, a patterns observed across all MS phenotypes.<sup>58</sup> Other studies demonstrated that in CIS suggestive of MS,

# 1.Introduction

---

lesion topography at disease onset, particularly in infratentorial regions (mainly the brainstem),<sup>61</sup> and spinal cord,<sup>62</sup> also seems to predict disability progression. Additionally, the presence of gadolinium-enhanced lesions at the baseline MRI and new spinal cord lesions over time are independently associated with SPMS at 15-year follow-up.<sup>63</sup>

Chronically active slowly expanding lesions (SELs) are a subtype of focal WM lesions with a hypocellular core that progressively increase in size and hypointensity on T1WI,<sup>64</sup> leading to a smouldering, slow radial expansion, further myelin damage, axonal loss, and gliosis.<sup>65</sup> They can be identified in volumetric T1WI and T2WI MRI.<sup>64</sup> SELs rarely show gadolinium enhancement, and are likely to become persistent black holes. Overall, they represent 30% to 50% of the lesion burden in pathohistological studies,<sup>65</sup> and are more frequent in PPMS compared to RRMS.<sup>64</sup> In both SPMS and PPMS patients, a higher definite SEL volume was associated with increasing disability progression assessed by EDSS scores,<sup>66,67</sup> suggesting that these lesions could be in vivo predictors of axonal loss observed in chronic active lesions.<sup>68</sup>

Paramagnetic rim lesions (PRLs) represent another subset of chronic active WM lesions in MS.<sup>69</sup> These lesions characteristically show a persistent active demyelination, with destruction of oligodendrocytes and accumulation of residual and detrimental iron products within activated microglia at the edge of the lesion, forming a distinctive rim.<sup>69</sup> These features can be detected in vivo using T2\*WI,<sup>70</sup> susceptibility-weighted imaging (SWI),<sup>71</sup> and quantitative susceptibility mapping (QSM).<sup>72</sup> The rim appears as hypointense, ring-like structures that surround the WM lesion. Some PRLs have been observed to slowly expand over time, more so than non-PRLs, although their shrinkage has also been documented.<sup>73</sup> Interestingly, PRLs are specific to MS and are rarely seen in other inflammatory or infectious neurological conditions.<sup>74</sup> PRLs are estimated to occur in about 40% of pwMS,<sup>75</sup> and the presence of  $\geq 2$  of them has been associated with greater motor and cognitive disability.<sup>76</sup>

Cortical lesions are common in MS, even at early stages of the disease.<sup>77</sup> Imaging cortical lesions in vivo is technically challenging, so its application in clinical settings is still limited.<sup>38</sup> Their detection has been improved using novel MRI sequences such as double inversion recovery (DIR), phase sensitive inversion recovery (PSIR), 3D magnetization-prepared rapid acquisition with gradient echo (MP-RAGE) and ultra-high field (7 Tesla) MRI.<sup>38,78</sup> Although only a small proportion of cortical lesions are detected compared to those found in histopathological studies, this proportion is still clinically relevant.<sup>78</sup> In fact, they have not been found in other neurologic conditions that can mimic MS, such as migraine or

# 1.Introduction

---

neuromyelitis optica spectrum disorders.<sup>78</sup> Besides, the presence of a single cortical lesion can identify with high specificity those CIS patients who will develop MS.<sup>79</sup> Additionally, cortical lesions positively better correlate with physical disability and cognitive impairment than WM lesion burden.<sup>80</sup>

Recent radiological studies using 3T<sup>81</sup> and ultra-high field<sup>82</sup> MRI have revealed that within the cervical cord, WM lesions seem to be more frequent than GM lesions in RRMS. In contrast, progressive MS phenotype displays a comparable absolute lesion volume in both GM and WM compartments. Notably, GM lesions are particularly associated with more severe disability and are correlated with higher EDSS scores,<sup>81</sup> which highlights the significant impact of GM damage on clinical outcomes in MS.

Neuronal and axonal damage, regardless of the aetiology or pathological mechanism, results in what is known in histopathology as tissue atrophy.<sup>57</sup> Nowadays, it is possible to quantify the damage beyond the aforementioned lesions in the normal-appearing WM and GM with advanced MRI sequences, but further studies are needed to integrate them into clinical practice. Conversely, a widely accepted measure of tissue loss is the assessment of brain and spinal cord volume changes over time,<sup>18</sup> as it represents the net effect of all destructive pathogenic processes.<sup>57</sup> Indeed, brain and spinal cord atrophy correlate more strongly with the patient's level of disability and cognitive decline than other measurements,<sup>38</sup> such as lesion load, aiding in predicting disease progression.

## 1.4.1 Brain atrophy: methodological aspects and clinical relevance

Brain volume measurements have gained significant interest due to their reliable association with disability and the development of a range of methods that are sensitive and reproducible in measuring even small changes in tissue volume changes.<sup>83</sup>

The accuracy of MRI volume measurements is influenced by image resolution and contrast. High-resolution 3D volumetric acquisitions, with a voxel dimension around 1×1×1mm, are preferred over 2D, to minimize partial volume errors and improve alignment or re-slicing in serial studies. T1WI is the most commonly used sequence for whole-brain atrophy measurements,<sup>57</sup> due to its clear contrast between brain tissues and cerebrospinal fluid (CSF). Fluid-attenuated inversion recovery (FLAIR) sequence is also used since it creates a distinct signal difference between cerebral and extra-cerebral matter.<sup>84</sup> It is well-established that WM lesions can impact regional atrophy calculations, since they may be misidentified as GM or

# 1.Introduction

---

CSF due to their reduced intensity in T1WI. Lesion filling techniques are often employed for correction.<sup>57</sup> Other factors affecting brain volume measurements include the oedema associated with lesion formation, which can lead to a transient elevation and then decrease of brain volume on oedema resolution<sup>85</sup> (the latter being referred to as pseudoatrophy),<sup>18</sup> patient hydration status, and the effect of corticosteroids or newly initiated DMTs, which can cause a transient decrease in whole-brain volume (a particular case of pseudoatrophy).<sup>85</sup> Therefore, these variables must be considered when analysing brain atrophy.

After MRI acquisition, there are different approaches to assess brain volumes. Initially, atrophy measures relied on partial,<sup>86</sup> indirect<sup>87</sup> or global<sup>88</sup> techniques unable to focus on specific brain tissue types. The development of segmentation methods with predefined atlases<sup>84</sup> has enabled separate assessments of WM and volumes of cortical and deep GM structures (thalamus, caudate nucleus, putamen, and hippocampus, among others).

Manual outlining is a straightforward method for assessing volume changes.<sup>84</sup> It requires minimal specialized software and aligns well with the operator's perceptions, particularly for small structures like the spinal cord or third ventricle.<sup>84</sup> Conversely, this approach demands an experienced observer, is prone to operator biases, exhibits lower precision compared to other automated techniques, and entails longer analysis times.<sup>84</sup> Despite these drawbacks, manual outlining is often used as a benchmark for evaluating new segmentation methods, due to the lack of a normative dataset and high intersubject brain volume variability.<sup>89</sup>

Semi-automated methods, which combine automated processes with some manual intervention, improve speed and reproducibility.<sup>84</sup> However, there is a trend towards fully automated image segmentation methods that integrate the assessment of lesion load and atrophy,<sup>90</sup> providing good reproducibility and reduced reliance on time-consuming operator input. Open-source tools such as FreeSurfer, FMRIB Software Library (FSL), Statistical Parametric Mapping (SPM), and Structural Image Evaluation, Using Normalisation, of Atrophy (SIENA),<sup>91,92</sup> aim to automate the analysis process, though some manual intervention for quality control and parameter optimization may still be necessary. These tools are extensively utilized in research for their flexibility and comprehensive feature sets. There are also commercial platforms, like Brainlab,<sup>93</sup> Philips IntelliSpace Portal,<sup>94</sup> and General Electric Healthcare Advanced Workstation Server,<sup>94</sup> which provide advanced visualization and analysis capabilities, often tailored for clinical applications. More recently, the introduction of Artificial Intelligence (AI) tools, such as machine learning and deep learning, present several advantages over current analysis techniques.<sup>95</sup> They can efficiently utilize various MRI

# 1.Introduction

---

contrasts and measures to explore tissue composition, structure, and function. Additionally, AI algorithms can identify intricate patterns from large datasets, generalize from these patterns, rank variable importance, and make predictions on new data.<sup>95</sup> All of the mentioned tools enable efficient and precise processing of MRI data, supporting a wide range of applications in academic research. However, they are not yet incorporated into clinical practice due to their complexity, integration challenges with existing clinical systems, and the need for specialized training.

Taken together, a loss of 0.4% per year is suggested as a pathological brain atrophy cutoff using SIENA.<sup>18</sup> This loss differs when using other methodologies, showing a range from 0.4% to 1.35% of yearly volume loss.<sup>96,97</sup> Besides, establishing a single cutoff is controversial, as it assumes that the rate of brain volume loss remained constant over the disease course of MS.<sup>83</sup> Evidence indicates that whole-brain volume loss is faster within the first 5 years of the disease compared to later stages.<sup>83</sup> Interestingly, short-term changes brain volume changes (even over just 1 year) are predictive of MS conversion in CIS patients,<sup>98</sup> and disability worsening in RRMS and PPMS.<sup>99</sup> Clinically, whole brain atrophy consistently correlates with cognitive dysfunction and mood disturbances in pwMS.<sup>100</sup> Despite the lack of an absolute cutoff for whole-brain volume loss, the quantification of the atrophy provides insightful results for understanding disease progression.

When examining CNS compartments separately, atrophy exhibits varying rates, extent, and severity. While MS was traditionally viewed as a primarily WM disorder, volume loss occurs in both the GM and WM from the earliest stages of the disease.<sup>101</sup> In fact, GM atrophy assessment appears more clinically relevant than WM atrophy or lesion volume load.<sup>92</sup> In a 4-year follow-up study, GM atrophy rate was 8.1 times greater in RRMS patients compared to HC, 12.4 times greater in RRMS patients converting to SPMS, and 14 times greater in SPMS patients,<sup>102</sup> indicating an acceleration of GM volume loss throughout the disease course. In contrast, WM atrophy rates remain relatively constant across all disease stages.<sup>101</sup>

Several studies have shown that in pwMS there is both diffuse cortical atrophy and focal thinning of the cerebral cortex.<sup>101</sup> Furthermore, the cortical areas with earlier volume changes were the cingulate cortex, insula and the transverse temporal gyrus, and also the thinning of these areas displayed the strongest correlation with the lesion load.<sup>103</sup> This pattern of brain volume loss is distinct from that seen in normal ageing,<sup>104</sup> demonstrating that atrophy in MS is not a mere acceleration of age-related volume loss.



# 1. Introduction

---

It is now standard practice to include the reduction in whole-brain volume loss as a secondary or tertiary end point in phase III randomized controlled trials for developing new DMTs in MS,<sup>105</sup> and even as primary outcome in phase II trials.<sup>85,106</sup> Nevertheless, it has not yet been adopted into routine clinical practice.<sup>92</sup> One reason for this is the lack of a standardized protocol for MRI acquisition across centres, resulting in significant variations in quality, resolution, and acquisition parameters. Additionally, new techniques and software are constantly being developed, making it difficult to establish a single standardized methodology that remains relevant over time.<sup>107</sup> Therefore, establishing consensus on the most appropriate MRI protocol and analysis techniques remains an ongoing challenge. The long-term goal of atrophy quantification is clinical translation, which requires multicentre validation and determination of clinical meaningfulness. International collaboration efforts, such as the MAGNIMS study group, aim to address these challenges by developing multicentre studies with larger cohorts, aiming to address the unmet needs in the field of MRI measurement.

## 1.4.2 Spinal cord atrophy: methodological aspects and clinical relevance

The spinal cord and spinal canal have anatomical peculiarities that should be outlined beforehand.

The spinal cord and the surrounding tissues are located within the spinal canal; the spinal cord extends caudally from the foramen magnum and occupies two thirds in length of the spine.<sup>108</sup> The lower section of the canal contains the filum terminale and the cauda equina. The spinal cord is divided into 4 regions and 31 segments: cervical (8 segments), thoracic (12 segments), lumbar (5 segments) and sacral (6 segments) (Figure 2A). Its diameter varies along its length, with cervical and lumbar enlargements. Unlike the brain, the spinal cord has GM surrounded by WM. The emergent ventral and dorsal roots form spinal nerves on either side of the cord. The main blood supply comes from the single anterior spinal artery, supplying the anterior two-thirds, and two posterior spinal arteries, supplying the posterior one-third.<sup>109</sup> The spinal cord is covered by the three membranes of the CNS: the dura mater, arachnoid and the innermost pia mater. The epidural space, containing fat and Batson's plexus veins, separates the dura mater from the osseous spinal canal. The subdural space is a potential space between the dura mater and the arachnoid, while the subarachnoid space, filled with CSF, lies between the arachnoid and pia mater.

# 1.Introduction

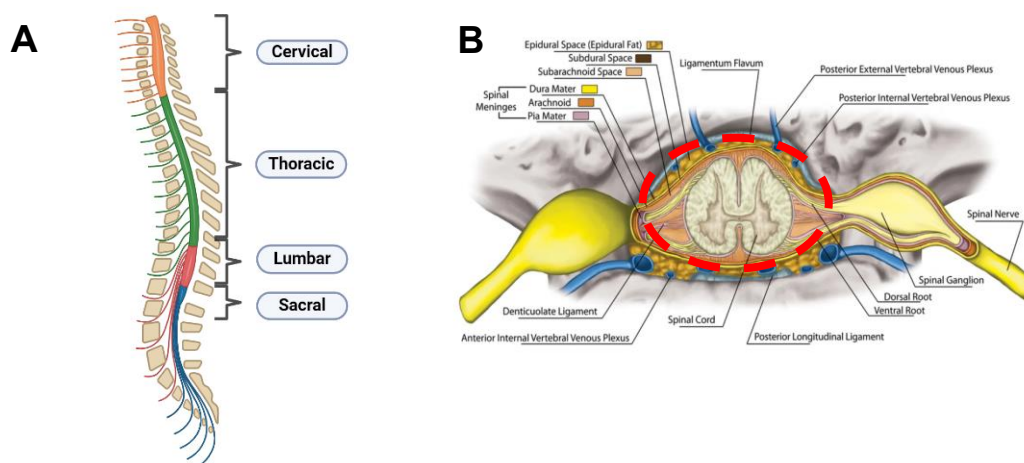


**Figure 2.** Spinal cord and spinal canal. (A) Division of the spinal cord into 4 regions and 31 segments. Created with BioRender.com (B) Schematic representation of the spinal cord and surrounding tissues within the spinal canal (red dashed line). Image adapted from the Netter atlas of human anatomy, 7<sup>th</sup> edition, 2018.

The spinal canal, also known as the vertebral canal or spinal cavity,<sup>110</sup> is delimited anteriorly by the vertebral bodies, intervertebral discs, and the posterior longitudinal ligament; posteriorly, by the vertebral laminae and the ligamentum flavum; and laterally, by the pedicles and intervertebral foramina, which allows the passage of spinal nerves and blood vessels (Figure 2B). The spinal canal diameter varies by region.<sup>111</sup> In the cervical region, it decreases from C1 to C3, and achieves a more stable diameter from C3 to C7.<sup>112</sup> The thoracic canal also becomes narrower in the cranio-caudal direction. Compared to the cervical and thoracic regions, the lumbar vertebral group has a larger spinal canal diameter on average.

Overall, the spinal cord and spinal canal are small structures surrounded by numerous and distinct tissues that make the MRI acquisition and its subsequent interpretation technically challenging. In addition to their small cross-sectional dimensions, the spinal cord exhibits a physiological motion due to the flow of the CSF, respiration and cardiac pulsation which can generate artifacts in MRI. Motion artifacts due to cardiac and pulmonary activity could be partially controlled with cardiac and respiratory gating.<sup>113</sup> Additionally, differences in the magnetic susceptibility between bone, soft tissues and air represent a source of “noise”, image distortion and loss of signal intensity, causing further field inhomogeneities and affecting the MRI quality. Several post-processing approaches have been described to optimize image quality,<sup>114</sup> but the results are not as robust as in brain MRI.

# 1.Introduction

---

The spinal cord is an area of preferential damage in MS.<sup>62</sup> Traditionally, clinical trials and clinical practices related to MS have primarily focused on monitoring changes in the brain. Nevertheless, there is an increasing recognition of the importance of evaluating the entire neuroaxis to gain a more comprehensive understanding of disability in MS.<sup>62</sup> Despite the aforementioned additional challenges to obtain a good quality spinal cord MRI, measurement of spinal cord atrophy is becoming more relevant, given its robust correlation with disability worsening.

In literature, the most representative measurement of spinal cord atrophy is the cross-sectional area (CSA, in mm<sup>2</sup>),<sup>115</sup> although the spinal cord volume (mm<sup>3</sup>) has also been used. The preferred spinal cord MRI sequences for this purpose are T1WI gradient-echo (e.g., inversion-recovery or magnetisation prepared rapid gradient-echo), and T2WI.<sup>25</sup> The C2/3 intervertebral disc level of the cervical cord is the most commonly used to assess atrophy in MS due to its high concentration of lesions, increased rate of atrophy, and relative technical ease compared to assessment of the whole cord.<sup>81</sup> The 3D T1WI brain MRI sequence, recommended for volumetric assessment of the brain, often captures a few upper cervical cord levels. Since the spinal cord MRI is less frequently performed than brain MRI due to technical challenges and enlarged acquisition time, a recent study has shown a good correlation between CSA at the C1 level assessed in 3D T1WI brain MRI and CSA at the C2/C3 level assessed in T2\*WI MRI.<sup>116</sup> However, the current recommendation for evaluating spinal cord atrophy is to use of dedicated cervical cord MRI when available.<sup>18</sup>(Figure 3)

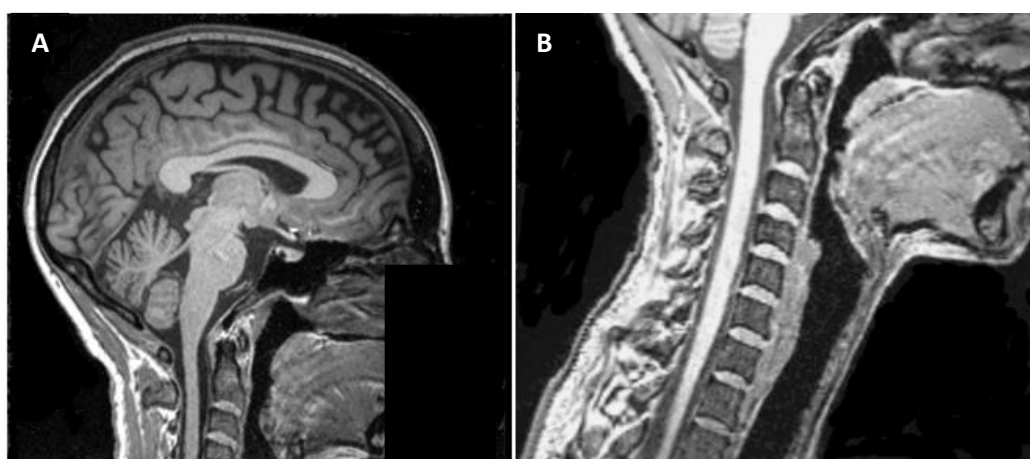


**Figure 3.** Spinal cord and spinal canal visualization with a sagittal brain 3D T1WI (A) and cervical cord 3DT1WI (B) in the same subject. T1WI, T1-weighted image; 3D, 3-dimensional.

There are manual, semi-automated and fully-automated methods to measure spinal cord area, but there is still a significant degree of heterogeneity in the methodology among studies.<sup>115</sup>

# 1.Introduction

---

The first accurate and reproducible method was developed by Losseff and coworkers.<sup>117</sup> It is based on the strong signal contrast between the spinal cord and CSF, and also accounts for the partial volume effect. This method determines the true boundary position by drawing a contour at a signal intensity halfway between the cord and CSF.<sup>117</sup> Subsequently, other methods have emerged, such as Cordial,<sup>118</sup> used to estimate the spinal cord volume, but not very extensively employed. The JIM (Jacobian integration method)<sup>119</sup> and SCT (Spinal Cord Toolbox)<sup>120</sup> software toolboxes are used to calculate the spinal cord volume, area, and length, which often require reference marks and manual correction to provide reliable measures. However, there is a lack of large studies comparing different approaches to establish a consensus in spinal cord atrophy measurements across MRI sequences.<sup>115</sup>

The use of more advanced MRI sequences, such as the phase-sensitive inversion recovery (PSIR),<sup>121</sup> has enabled the study the spinal cord GM and WM atrophy separately. Recently, some fully-automated segmentation tools have been proposed,<sup>122,123</sup> showing better performance than manual outlining, as they reduce the intra-operator biases. However, the presence of demyelination lesions in the cervical cord can cause blurring in the MRI, hampering the estimation of the area, especially in progressive patients with areas of diffuse demyelination in the cervical segments.<sup>121,124</sup>

A relevant aspect in the evaluation of cervical cord atrophy across subjects is the normalization of measurements,<sup>125</sup> given the large intersubject variability of spinal cord areas. The normalization allows to reduce biological variation of structural measurements unrelated to disease, and maximizes the statistical power to detect group differences, enabling more effective assessment of differences between pwMS and healthy controls.<sup>126</sup> Factors such as age, sex, height, and body mass index influence spinal cord CSA, GM and WM.<sup>126</sup> Several studies indicated that the body mass index has no significant impact on the spinal cord area,<sup>127</sup> while the influence of body height, though statistically significant, is minimal and may be subject to sex differences.<sup>127</sup> Height has been suggested as a normalization parameter,<sup>128</sup> particularly when estimating spinal cord volumes. However, in the assessment of spinal cord CSA, adjustments based on age and sex appear to be adequate in controlling intersubject variability.<sup>126</sup>

Studies on cervical cord atrophy have calculated that the rate of volume loss is approximately 1.78% per year,<sup>115</sup> compared to the reported rates of brain atrophy, which commonly range from 0.4 to 1.35% per year.<sup>96,97</sup> Of note, the atrophy rates for the brain and spinal cord are estimated using different methodologies. Therefore, while the absolute rate values are not directly comparable, these findings suggest that spine atrophy may occur at a rate

# 1.Introduction

---

even higher than brain volume loss. The atrophy rate also seems to vary along the spinal cord length. It has been reported that the spinal cord CSA shows an average reduction of about 2 mm<sup>2</sup> per decade at the C2/C3 level, and 1.3 mm<sup>2</sup> at the T9-T10 level, while the average spinal cord GM reduction is of the order of 0.3–0.4 mm<sup>2</sup> per decade at both the levels.<sup>129</sup> In progressive MS patients, the magnitude of spinal cord CSA is even larger (2.08% per year).

It was in 1996 when Losseff and coworkers demonstrated a strong graded correlation between spinal cord CSA measured at the C2 level and the EDSS,<sup>117</sup> which is heavily weighted towards ambulatory function. In fact, progressive patients and those with higher EDSS scores exhibited smaller areas compared to RRMS patients or those with low EDSS scores. Since then, studies evaluating spinal cord atrophy have consistently showed a significant relationship between cervical cord CSA and disability worsening, assessed with different measurements, including 9-HPT,<sup>130</sup> T25FW,<sup>131</sup> SDMT and quality of life.<sup>132</sup> The regional analysis has also highlighted a differential accumulation of cord atrophy across cervical levels at different disease stages, with subtle tissue loss starting at C1/C2 in early RRMS, progressively involving the upper cord segments in RRMS, and subsequently affecting the lowest cervical segments in progressive MS.<sup>133</sup> This cranio-caudal gradient may be due to a higher myelin content and WM fiber density, with subsequent spreading of cord damage to caudal segments.<sup>133</sup> Therefore, spinal cord atrophy is measured from the early stages of MS, seems to be independent of the cortex and deep GM volume loss,<sup>134</sup> and correlates more strongly with disability than brain atrophy.<sup>38</sup>

Even in the absence of WM loss, there is a detectable loss of tissue in the GM in relapsing MS that is more prominent during the progressive phase of the illness.<sup>124</sup> Spinal cord GM area seems to be the strongest predictor of disability across studies in models including normalized brain GM and WM volumes, brain T1 lesion load, spinal cord WM area, and number of spinal cord lesions,<sup>124</sup> underscoring the clinical relevance of these findings.

Furthermore, an association between cord atrophy and reduced peripapillary retinal nerve fibre layer thickness has been identified, indicating that cervical cord atrophy reflects, at least in part, global pathological processes and not only specific damage of long tracts.<sup>135,136</sup>

While research on brain atrophy in MS has been extensively conducted, studies focusing on spinal cord atrophy are comparatively limited. However, findings suggest that the rate of spinal cord atrophy seems to be higher. This underscores the significance of incorporating spinal cord CSA as an outcome measure in clinical trials. In clinical practice, it could be useful

# 1.Introduction

---

in monitoring treatment response, disease activity and progression, once standardized atrophy measurements protocols are available.

## 1.5 The concept of “Reserve” in MS

As previously discussed, predicting cognitive and physical disability progression in MS remains a significant challenge. A considerable body of research is dedicated to developing new clinical, neuroimaging, and serum/CSF biomarkers to gain deeper insights into the pathophysiology of neurodegeneration. Among these biomarkers, brain and spinal cord atrophy measurements have shown robust associations with clinical outcomes. However, these measurements only partially correlate with functional impairment and disease trajectories,<sup>137,138</sup> leaving a proportion of disability worsening unexplained.

Indeed, the clinic-radiological paradox in MS highlights a common observation in daily practice: the association between clinical findings and the extent of radiological damage is generally weak.<sup>139</sup>

The wide variability and unpredictability in clinical disability progression in MS may be attributed to the complex interplay of different factors. These factors include persistent or smouldering inflammation of the CNS, an imbalance between neuronal damage and regeneration, and the functional reserve or resilience of the CNS, which modulates the accumulation of neuro-axonal loss.<sup>140</sup> Consequently, some individuals may experience rapid neurological decline, while others show minimal or no detectable clinical progression over the years despite similar degrees of lesion load and tissue damage.

Efforts in MS research have been primarily directed towards quantifying damage in the brain and spinal cord. However, there is currently no direct metric available to accurately gauge the quantity of remaining functionally intact neurons.<sup>139</sup> As a result, in addition to assessing measures like atrophy and focal lesions, elucidating the integrity of the residual CNS tissue emerges as a pivotal aspect in understanding the maintenance of functional capacity in pwMS.<sup>139</sup>

The term “*reserve*” refers to an organ’s ability to withstand damage or degeneration without manifesting noticeable deficits. In neurology, the concept of brain reserve<sup>141</sup> refers to individual differences in the structural properties of the brain. It is defined as the capacity of the brain to compensate the effects of aging, neurodegenerative disorders or injury. This

# 1.Introduction

---

concept has been firstly explored in Alzheimer's disease and other dementias.<sup>142</sup> For instance, in Alzheimer's disease the presence of amyloid plaques and neurofibrillary tangles must exceed a quantitative threshold before the clinical onset of dementia becomes apparent.<sup>141</sup> Similarly, in vascular dementia, it has been demonstrated that symptoms onset is not evident until an aggregate volume of at least 50-100cc of infarction has been found.<sup>141</sup> In other words, a considerable amount of tissue destruction needs to occur before the system is compromised and disease becomes clinically evident. But the variability in the threshold of clinically eloquent tissue destruction is related to the functionality and volume of *remaining* tissue (i.e., reserve) that can compensate for that damage.

The surrogate measure of the brain reserve was originally the head circumference, and presently the total intracranial volume (TIV),<sup>143</sup> which reflects the maximal lifetime brain growth and shows a strong correlation with brain size in healthy subjects. TIV is also considered a proxy for neuronal or synaptic count,<sup>144</sup> and linked to the presence of more redundant neural structures. Redundancy in biological systems implies the existence of duplicate elements that provide an alternative functionality in case of failure.<sup>145</sup> In the context of neurological disorders, redundancy involves having extra neurons, synapses and pathways, making the brain more robust or resistant to aging and disease-related changes. Subsequently, a larger TIV indicates a greater brain reserve, allowing individuals to withstand a higher disease burden before reaching a critical threshold.<sup>143</sup> Evidence points to the fact that elderly individuals with a larger TIV (or greater brain reserve) tend to exhibit better cognitive function and a reduced risk of clinical dementia in the face of similar disease-related damage.<sup>146,147</sup> It is essential to note that brain reserve is also heavily influenced by genetic factors. Considering that men typically have a larger TIV than women, research studies evaluating TIV often incorporate adjustments based on sex to ensure accurate and unbiased analyses.<sup>143</sup>

In the aforementioned examples, the threshold effect assumes uniform brain tissue or neuronal loss across individuals,<sup>141</sup> but repeated observations indicate that there is not a direct relationship between the degree of brain pathology or damage and the clinical manifestations of that damage.<sup>148</sup> In fact, a clinical study with postmortem evaluation revealed that approximately one-third of older subjects within the studied cohort, despite not exhibiting dementia symptoms, displayed histopathological changes consistent with Alzheimer's disease.<sup>142</sup> It suggests that some individuals are more resilient to neurodegenerative disorders, which highlights the complexity of individual variability in the onset of such conditions. In this context, another relevant concept has emerged: the cognitive reserve.<sup>148</sup> It proposes that certain

# 1.Introduction

---

factors, such as cognitive activities, education, social engagement, and intellectual stimulation throughout life, contribute to building a reserve of neural resources that act as protective factors. This may explain critical threshold differences in the onset of clinical symptoms after acquired brain injury.<sup>148</sup> Cognitive reserve is also related to neuroplasticity, which involves the functional brain reorganization in response to damage.<sup>149</sup> This implies that individuals with a higher cognitive reserve may delay the onset of cognitive decline due to their ability to recruit or reorganize alternative brain networks as needed.

Indeed, cognitive reserve closely parallels the concept of brain reserve, but with some remarkable differences. While brain reserve is typically regarded as a passive trait,<sup>148</sup> given at birth, linked to brain size, unmodifiable, and involves an increased number of redundant neuronal networks, cognitive reserve operates as a more dynamic process. It may be based on the more efficient utilization of brain networks or an enhanced neuroplasticity potential,<sup>148</sup> depending on lifetime intellectual enrichment.

The brain reserve has also been explored in MS. Many pwMS experience cognitive impairment,<sup>150</sup> particularly in memory and cognitive efficiency (slowed processing speed, difficulty multitasking), while others endure significant disease burden without cognitive decline.<sup>151</sup> This is evident, in part, by the relatively modest or incomplete correlation between MS disease burden (e.g., T2WI lesion volume, cerebral atrophy) and cognitive performance.<sup>152</sup> Recent findings demonstrate that pwMS with a larger TIV mitigated the detrimental link between MS disease burden and cognitive efficiency in both cross-sectional<sup>143</sup> and longitudinal<sup>153</sup> studies.

The cognitive reserve hypothesis also contributes to explaining the discrepancy between disease burden and cognitive status in MS.<sup>148</sup> It suggests that pwMS with greater education are better protected against disease-related cognitive impairment.<sup>154</sup> In fact, engagement in cognitive leisure activities during early adulthood has been shown to moderate the negative effect of disease burden on current cognitive status.<sup>155</sup> Indeed, a higher cognitive reserve appears to have a protective role against verbal learning and memory impairment, as well as information processing inefficiency,<sup>156</sup> by moderating the effects of brain atrophy<sup>157</sup> and WM lesion load.<sup>158</sup> Consequently, the adverse impact of disease burden on cognition is more pronounced in individuals with lower intellectual enrichment compared to those with higher enrichment,<sup>154</sup> leading to divergent trajectories of cognitive decline over time. Longitudinal research further emphasizes the clinical importance of considering a patient's level of lifetime enrichment,<sup>153</sup> which may serve as a useful predictor of future cognitive decline.



# 1.Introduction

---

In parallel with the cognitive reserve, the concept of physical reserve has been recently delineated as a conceptual and empirical framework to assess individual differences in the ability to withstand physical decline over time in elderly subjects.<sup>159</sup> Gait speed is the proposed measure for this reserve, as it has been shown to be associated with fall risk, disability and mortality in this subpopulation.<sup>159</sup>

Despite the fact that the CNS encompasses both the brain and spinal cord, and the role of the spinal cord is recognized as central in MS, there was no equivalent construct for spinal cord reserve as there is for brain reserve. Thus, the study of reserve in neurology was primarily restricted to the brain, neglecting the undeniable contribution of the spinal cord to disability in MS (Figure 4).

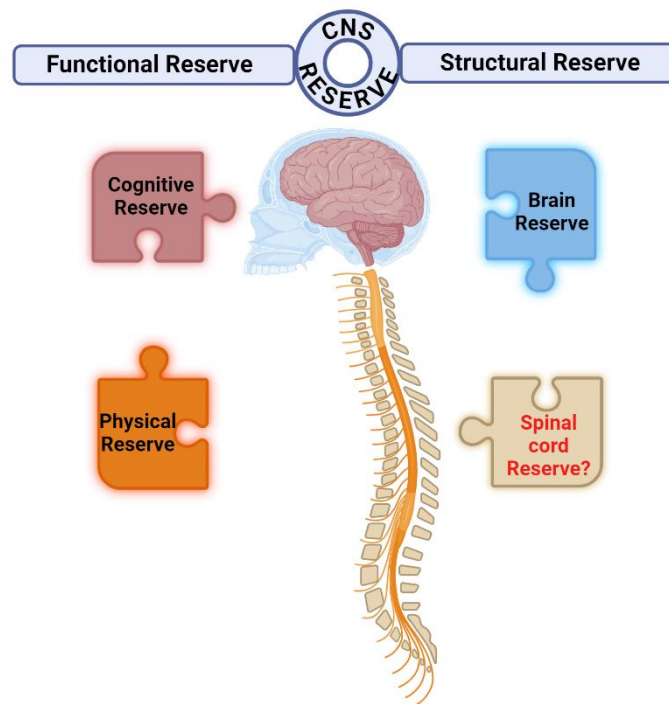


**Figure 4.** Conceptualization of the holistic concept of Central Nervous System (CNS) reserve, comprising both structural and functional reserves. Functional reserve includes the cognitive and physical life-long enrichment, while structural reserve encompasses both intracranial volume and spinal canal. To date, there had been no formal attempt to develop the concept of spinal cord reserve.

An exploratory study has investigated for the first time the possible existence of a spinal cord reserve,<sup>160</sup> in analogy to the brain reserve concept. In this case, the surrogate tested measure was the cervical canal area (CCaA), assessed as the mean cross-sectional area over 11 slices centred at the C2/C3 intervertebral disc level. The main hypothesis posited that a larger CCaA would be associated with a lower level of disability. CCaA was estimated in a large international

# 1.Introduction

---

multicentre MRI dataset of pwMS and HC. For this purpose, an in-house semi-automated segmentation pipeline based on the SCT was developed. The studied revealed no differences in CCaA between pwMS and HC,<sup>160</sup> suggesting that the area of the spinal canal is not affected by the disease process, a prerequisite for considering it a valid proxy for the maximal lifetime growth of the premorbid spinal cord. Besides, CCaA was found to be associated with disability, as measured by the Patient-Determined Disease Steps (PDDS), in linear models adjusted for spinal cord parenchyma fraction (SCPF), brain T2WI lesion volume, age, and sex. PDDS is a well-validated PROM extensively used in MS research. CCaA also correlated with the lower extremity subscale of the quality of life in neurological disorders (Neuro-QoL) and with processing speed test (PST).<sup>160</sup>

In summary, this study represented the first step to support the existence of the spinal cord reserve, opening up a significant field of research upon which this thesis is built.

## **2. THESIS JUSTIFICATION**

## 2. Thesis justification

---

One central focus in MS research involves the identification of biomarkers to measure disease progression. The ultimate goal is to develop new drugs that can decelerate, attenuate, or control the neurodegenerative processes leading to disability worsening in pwMS. Additionally, there is an ongoing effort to identify non-modifiable risk factors present from the disease onset, which also play a role in predicting its course over time. Assessing these factors at the time of diagnosis could guide the initiation of DMT towards more efficient drugs, particularly for patients at a higher risk of disability progression.

Despite substantial efforts to establish significant correlations between brain MRI-derived parameters and clinical disability in MS, results have been suboptimal, highlighting the need for additional metrics. One potential explanation is that spinal cord involvement is not fully incorporated into the formal evaluation of MS. While advancements in measuring spinal cord volume loss and lesion burden have enhanced our understanding of disability accumulation in MS, the variability in disability worsening among patients remains poorly understood.

In this context, the concept of reserve has emerged as an important contributor in elucidating the variability in clinical outcomes in MS. While brain reserve is well-established in MS research, the role of spinal cord reserve remains largely unexplored, despite the integral role of the spinal cord in MS pathology and disability. Of note, there was no recognized equivalent to brain reserve for the spinal cord.

The first study to explore the spinal cord reserve used the CCaA as a proxy measure. It found that there were no differences in CCaA between pwMS and HC. Besides, this measure was correlated with disability, as assessed through patient-reported outcomes. It is important to note that this study employed a cross-sectional analysis, assessed the CCaA in 3D T1WI brain MRIs, and did not provide information about MS phenotypes or EDSS. Consequently, there is ample room for further investigation of this measure with improved approaches, different analysis designs, and additional MRI sequences.

Therefore, there is a considerable body of literature exploring brain reserve and cognitive reserve, but there is currently no established counterpart for the spinal cord. Considering the significance of spinal cord measurements in predicting MS prognosis, there exists an unmet need for a comprehensive analysis of the potential role of spinal cord reserve in disease progression. This thesis aims to shed light on this aspect and will possibly provide valuable insights to the field.

### **3. HYPOTHESES**

### 3. Hypotheses

---

The primary working hypothesis of the current thesis posits the existence of a spinal cord reserve that can be measured in each patient by estimating the mean cervical canal area (CCaA), thereby extending the concept of brain reserve to the spinal cord.

Furthermore, the spinal cord reserve is linked to disability in MS and could be considered as a non-modifiable risk factor for disability progression, particularly in terms of the progressive spastic paraparesis that some patients may exhibit either from the onset or during the course of the disease.

Specifically, we hypothesize that:

1. The CCaA, the surrogate measure of spinal cord reserve, can be estimated after implementing an accurate analysis pipeline that enables semi-automated estimations from brain and cervical cord MRI acquisitions.
2. The CCaA can be assessed with the developed analysis pipeline with MRIs from different centres and settings, potentially allowing us to demonstrate the existence of spinal cord reserve and its association with disability in a large international cohort of MS patients.
3. Our analysis pipeline can be applied to different MRI sequences, beyond volumetric T1WI, to accurately estimate the CCaA.

## **4. OBJECTIVES**

## 4. Objectives

---

The main objective of this thesis is to test the possible existence of a spinal cord reserve and its relationship with disability in MS. In addition, there are 3 secondary objectives:

1. ***Pipeline validation***: it involves developing, implementing and validating the in-house semi-automated segmentation pipeline designed to obtain quantitative measures of the CCaA. Subsequently, the CCaA will be assessed in brain MRIs, and the resulting measurements will be compared to those obtained using dedicated cervical cord MRI. Finally, the consistency of the CCaA measurements during a 1-year period (scan-rescan test) will be also evaluated.
2. ***Assessment of the spinal cord reserve in a multicentric cohort***: it consists of investigating the potential of the CCaA as a proxy for spinal cord reserve in a longitudinal multicentric cohort of pwMS (including all MS phenotypes) and healthy controls. The CCaA will be examined at two different intervertebral disc levels – C2/C3 and C3/C4 – and disability will be measured with the EDSS score, the most widely used scale for neurological examination in MS.
3. ***Estimation of the CCaA in additional MRI sequences***: it involves exploring the feasibility of measuring the CCaA in the most commonly used MRI sequences in clinical practice, such as 2D sagittal T1WI, T2WI and STIR.



## **5. METHODS**

## 5. Methods

---

We used the SCT to assess the CCaA across the three studies. The SCT is a comprehensive software specifically designed for the analysis of spinal cord MRI data,<sup>120</sup> providing tools for image processing, such as segmentation, registration, and statistical analysis. It utilizes specialized templates and transformations that facilitate accurate and reproducible measurements. High-resolution spinal cord templates serve as references for various segments, allowing for precise alignment and comparison across different subjects and imaging modalities.<sup>161,162</sup> Transformations within SCT use sophisticated algorithms to map individual spinal cord images onto these templates, ensuring consistent identification of anatomical landmarks and features.<sup>120</sup> Key aspects of SCT are its robust segmentation tools, which delineate spinal cord boundaries and substructures, and its advanced registration techniques, which adjust for anatomical variability and motion artifacts. These capabilities make SCT an essential tool for researchers and clinicians aiming to obtain reliable and detailed assessments of spinal cord morphology and pathology. In the following sections, we discuss how we adapted the SCT to estimate the CCaA.

### 5.1 Pipeline validation

Our group has developed an in-house semi-automated segmentation tool based on the SCT (<https://www.nitrc.org/projects/sct/>) to obtain quantitative measures of the CCaA. To validate the reproducibility of the proposed pipeline and, to this end, address the first objective of this thesis, we tested it in an initial cohort of 10 HC and 21 pwMS, who underwent baseline and one year follow-up brain and cervical spine sagittal 3D T1WI MP-RAGE. All MRI scans were acquired in a 3-Tesla system (Tim Trio; Siemens) using the following acquisition parameters: TR = 2300 ms, TE = 2.98ms, TI = 900 ms, flip angle = 9°, voxel size = 1 x 1 x 1mm<sup>3</sup>; brain field-of-view (FOV) = 240 x 256 x 176, cervical FOV = 240 x 25 x 128. Additionally, all subjects underwent a brain 2D FLAIR scan (TR = 9000 ms, TE = 93 ms, TI = 2500 ms, flip angle = 120°, voxel size = 0.49 x 0.49 x 3.0 mm<sup>3</sup>). The positioning protocol was the same across all subjects. The project was approved by the local ethics committee, and subjects signed an informed consent.

The CCaA was measured in all acquisitions using the following in-house pipeline based on the SCT (Version 5.0.1).<sup>120</sup> (Figure 5)

## 5. Methods

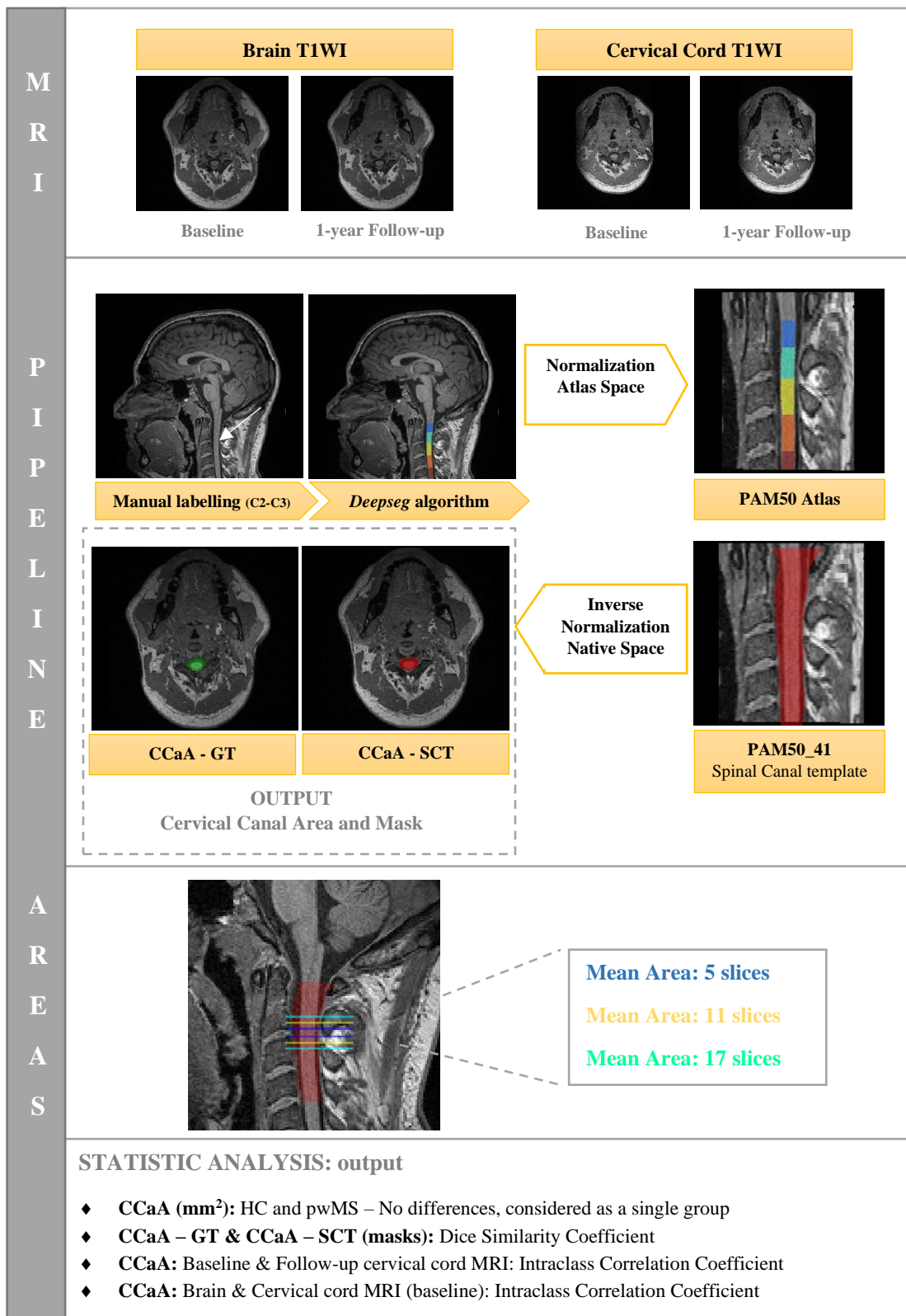


**Figure 5.** Graphical representation of the proposed pipeline to estimate the cervical canal, including the MRI sequences, a flowchart, the assessment of the means cervical canal area over the different number of slices, and the statistical analysis performed. CCaA: cervical canal area, GT: ground truth, SCT: Spinal Cord Toolbox, HC: healthy controls, pwMS: patients with multiple sclerosis.

## 5. Methods

---

First, a segmentation of the cervical cord was obtained with the *DeepSeg* algorithm. Then, the posterior tip of the C2/C3 intervertebral disc was manually labelled by 2 evaluators (a neurologist with a 7 years' experience and an MRI technician with 11 years' experience). The output from the *DeepSeg* algorithm, along with these manual intervertebral disc landmarks, was used to normalize the images to the PAM50 atlas,<sup>162</sup> an unbiased multimodal MRI template of the full spinal cord (C1–L2 vertebral level) and brainstem where several spinal cord structures have been predefined. Previously, a spinal canal template covering from C1 to C5 was created by our research group in the same space as the PAM50 atlas and was added to the predefined structures (PAM50\_41). A spinal canal segmentation mask was created in the same space as the atlas and added to the predefined structures, including the spinal canal template. Then, the images were normalized using the inverse normalization matrix, as proposed by SCT, and finally, the spinal canal mask was transferred from the atlas space to the native space.

Additionally, the total intracranial volume was assessed in all subjects using the T1WI sequences with statistical parametric mapping software (SPM; <http://www.fil.ion.ucl.ac.uk/spm/software/spm12>); the lesion volume was estimated using 2D FLAIR MRI with the Lesion Segmentation Toolbox, included in the SPM software (<https://www.applied-statistics.de/lst.html>).

CCaA was then estimated as the mean cross-sectional area across either 5, 11, or 17 slices centered on the C2/C3 intervertebral disc, representing the 3 groups of comparisons. Anatomically, 5 slices usually cover the C2/C3 cervical disc, 11 slices cover from the lower margin of C2 to the upper margin of C3; and 17 slices cover from the odontoid basis to the midpoint of the posterior arch of C3 (a certain intersubject variability is detected in those limits according to the individual anatomy). To identify outlier CCaA estimations, we removed all measures with a value beyond 1.5 times the interquartile range.<sup>163</sup> Then, CCaA estimations in HC and pwMS were compared by a multivariable regression model adjusted for age and sex; CCaA estimations from baseline and follow-up cervical cord scans and from brain and cervical MRIs were also compared using a paired t test. To assess the reproducibility of the proposed pipeline, we compared the CCaA estimations obtained from the cervical cord and brain T1WI at 2 different time points with the proposed pipeline manual segmentations performed by 1 evaluator, considered the ground truth (GT), using the Dice similarity coefficient (DSC).<sup>164</sup> In addition, a second evaluator manually outlined the CCaA to assess the interoperator variability. Additionally, we compared the CCaA mean obtained with the manual GT at baseline for the

## 5. Methods

---

cervical cord and brain scans using a paired t test. The GT, considered the reference value, was measured at the midpoint of C2/C3.

Finally, CCaA estimations obtained on baseline and follow-up cervical cord T1WI were compared; brain and cervical cord acquisitions were also compared using the individual and average intraclass correlation coefficient (ICC)<sup>165</sup> and the Bland-Altman method with their limits of agreement (LoA). Statistical analysis was performed with STATA 16.1 software (StataCorp). Before we performed a t test, the normal distribution of different variables was evaluated using the Shapiro-Wilk test, and the homogeneity of variances was determined by the Levene test. To appraise assumptions of linear regression, we checked the normality of residuals using the Shapiro-Wilk test; homoscedasticity was evaluated with the Breusch-Pagan test; independence of observations was determined using the Durbin-Watson test; and collinearity was assessed by the variance inflation factor. The p value for significance was set at  $p < 0.05$ .

### 5.2 Assessment of the spinal cord reserve in a multicentric cohort

In this study the cohort comprised pwMS recruited between 2010 and 2016 from nine European sites ([www.magnims.eu](http://www.magnims.eu)): (1) the Amsterdam MS Centre (the Netherlands); (2) the Cemcat, Hospital Vall d'Hebron, Barcelona (Spain); (3) St. Josef Hospital Ruhr University, Bochum (Germany); (4) Queen Square Institute of Neurology, UCL, London (UK); (5) the Department of Neurology, Neurocentre of Southern Switzerland, Lugano; (6) the Department of Neurology, University of Heidelberg, Mannheim (Germany); (7) the Neuroimaging Research Unit, San Raffaele Scientific Institute, Milan (Italy); (8) the MRI Centre "SUN-FISM," University of Campania "Luigi Vanvitelli," Naples (Italy); and (9) the Nuffield Department of Clinical Neurosciences, Oxford (UK). All MS phenotypes were included. HC were recruited among friends and relatives of pwMS. This multicentric cohort has already been used in previous studies to characterize the evolution of cervical cord atrophy,<sup>133</sup> and the distribution of brain grey-matter atrophy across MS phenotypes.<sup>166</sup>

The project was approved by the local Ethics Committee in each Centre, and all subjects gave written informed consent before enrolment.

To be included, pwMS had to have stable treatment during the last six months and received no corticosteroids during the last month. CIS patients suggestive of MS had to have a

## 5. Methods

---

first episode suggestive of central nervous system demyelination and a clinical assessment within 3 months from clinical symptoms onset. Exclusion criteria for HC and pwMS were history of cervical cord/brain trauma, severe cord compression (radiologically defined) on previous MRI scans, diagnosis of MS mimickers; major comorbidities, and any other medical conditions interfering with MRI.

All classical MS phenotypes were recruited. Among them, there were a low number of patients with PPMS; therefore, patients were categorized into relapsing MS phenotype (including CIS and RRMS), and progressive MS phenotype (including SPMS and PPMS), using present criteria for phenotype classification in all centres.<sup>167</sup>

Disability was measured by the EDSS score at baseline and 5-year follow-up. Confirmed clinical worsening at follow-up was defined as EDSS score increase of  $\geq 1.5$  when baseline was = 0.0, EDSS score increase of  $\geq 1.0$  when baseline EDSS was  $\leq 5.5$ , or EDSS score increase of  $\geq 0.5$  when baseline EDSS was  $\geq 6.0$ , as reported elsewhere.<sup>133</sup>

Although a strict standardization of contrast parameters was not implemented, the acquisition MRI strategy of the volumetric cord sequence was similar across sites, with the use of an isotropic (1mm<sup>3</sup>) inversion-prepared scan,<sup>133,168</sup> and there were no major hardware/software updates during the study. All subjects underwent a 3D T1WI at inclusion, covering the entire cervical cord using a 3T scanner.<sup>133</sup>

All images were visually checked by an experienced neurologist (NM). Images were excluded in presence of: cervical spondylosis with compromise of the cervical canal involving the C2-C4 segment, extreme physiological variations of the CCaA (specifically when the vertebral cavity reaches a stable diameter lower than C2/C3 vertebral level),<sup>111,127</sup> and marked cervical hyperextension on acquisition. Images were also excluded due to poor MRI quality or off-center FOV.

The CCaA was then estimated in all participants with our in-house semi-automated segmentation pipeline based on the SCT.<sup>169</sup> It was calculated as the mean cross-sectional area over 11 slices centred on two different intervertebral disc levels: C2/C3 and C3/C4. As part of the segmentation quality control, a coefficient of variation (CV) was calculated for each CCaA measurement at the two different levels, removing subjects who displayed a  $CV > 0.075$ .<sup>160</sup> Segmentation process failures were also removed.

## 5. Methods

The output of the pipeline also provided the mean spinal cord CSA area, which was used to calculate the SCPF as the ratio of SCA to the CCaA, and then reported as percentage. Of note, SCA and SCPF were also assessed both at C2/C3 and C3/C4 intervertebral levels.

The statistical analysis was conducted separately at C2/C3 and C3/C4 intervertebral disc levels. First, a descriptive analysis and a comparison between included and excluded participants were performed. The analysis included the percentage of patients in each phenotype, the mean age and disease duration, as well as the median and interquartile range (IQR) of EDSS and number of cord lesions (0,1,2,3...). Subsequently, comparisons between included HC and pwMS were performed in terms of demographic, clinical and MRI characteristics. Age- and sex-adjusted linear models were built to test for differences in CCaA between HC, relapsing MS and progressive MS.

Multivariable linear regression models adjusted for age, sex, SCPF and number of cord lesions were used to evaluate the association between EDSS and CCaA at baseline, firstly with the whole cohort, and then by phenotypes. As the distribution of the phenotype differed between centres, no attempt was made to adjust by centre to avoid model overadjustment (Table 2).

| Site      | HC<br>n (%) | CIS<br>n (%) | RRMS<br>n (%) | SPMS<br>n (%) | PPMS<br>n (%) | Total – n |
|-----------|-------------|--------------|---------------|---------------|---------------|-----------|
| Amsterdam | 47 (34.1)   | 0 (0)        | 47 (34.1)     | 44 (31.8)     | 0 (0)         | 138       |
| Bochum    | 6 (27.3)    | 4 (18.2)     | 12 (54.5)     | 0 (0)         | 0 (0)         | 22        |
| London    | 10 (28.6)   | 0 (0)        | 0 (0)         | 13 (37.1)     | 12 (34.3)     | 35        |
| Milano    | 55 (27.9)   | 0 (0)        | 84 (42.7)     | 32 (16.2)     | 26 (13.2)     | 197       |
| Oxford    | 17 (53.1)   | 0 (0)        | 15 (46.9)     | 0 (0)         | 0 (0)         | 32        |
| Napoli    | 13 (31.7)   | 6 (14.6)     | 21 (51.2)     | 0 (0)         | 1 (2.5)       | 41        |
| Mannheim  | 6 (23.1)    | 0 (0)        | 20 (76.9)     | 0 (0)         | 0 (0)         | 26        |
| Lugano    | 15 (17.2)   | 1 (1.1)      | 60 (69.0)     | 7 (8.1)       | 4 (4.6)       | 87        |
| Barcelona | 8 (29.6)    | 8 (29.6)     | 11 (40.7)     | 0 (0)         | 0 (0)         | 27        |

**Table 2.** Distribution of phenotypes across the participating centres. Of note, each one contributed with a different proportion of multiple sclerosis phenotypes. Total number of subjects = 605 (before the quality check control). CIS, clinically isolated syndrome; HC, healthy controls; n, number; PPMS, primary progressive multiple sclerosis; RRMS, relapsing-remitting multiple sclerosis; SPMS, secondary progressive multiple sclerosis; %, percentage.

Additionally, we employed the jackknife resampling method to evaluate the robustness and stability of the association between the CCaA and baseline EDSS in the entire cohort.

## 5. Methods

---

We also compared the CCaA at baseline between pwMS who presented clinical worsening at 5-year follow-up to those who remained stable by using a multivariate linear regression model adjusted for age, sex, SCPF, and number of cord lesions.

To appraise assumptions of linear regression, we checked the normality of residuals using the Shapiro-Wilk test; homoscedasticity was evaluated with the Breusch-Pagan test, and collinearity was assessed by the variance inflation factor. The p value for significance was set at  $p < 0.05$ . Statistical analysis was performed with STATA 16.1 software (StataCorp).

### 5.3 Estimation of the cervical canal area in additional MRI sequences

The cohort included pwMS from the outpatient clinic of the Centre of Multiple Sclerosis of Catalonia who underwent an MRI study from August 2021 to September 2023. To be included, the MRI study had to comprise the following sequences: brain sagittal 3D T1WI, and cervical sagittal 2D T1WI, T2WI, and STIR. All MRI scans were acquired in a 3.0 T system (Siemens - MAGNETOM Prisma Fit - syngo MR XA30). The acquisition parameters are detailed in Table 3.

|                     | Brain 3D<br>T1WI | Cervical 2D<br>T1WI | Cervical 2D<br>T2WI | Cervical 2D<br>STIR |
|---------------------|------------------|---------------------|---------------------|---------------------|
| TR (ms)             | 2300             | 695                 | 3000                | 3500                |
| TE (ms)             | 2.98             | 9.2                 | 86                  | 37                  |
| FOV (mm)            | 240 x 256        | 337 x 300           | 315 x 280           | 315 x 280           |
| FA (°)              | 9                | 150                 | 160                 | 150                 |
| Interslice gap (mm) | 0                | 0.5                 | 0.5                 | 0.5                 |
| Voxel Size (mm)     | 1x1x1            | 0.4688x0.4688x3     | 0.625x0.625x3       | 0.7292x0.7292x3     |

**Table 3.** Acquisition parameters for the different MRI sequences. TR, repetition time; TE, echo time; FOV, field of view; FA, flip angle, T1WI, T1-weighted image; T2WI, T2-weighted image; STIR, short-tau inversion recovery image; mm, millimetres; ms, milliseconds; °, angle.

All different MS phenotypes were recruited. Among them, the predominant phenotype was relapsing-remitting MS; therefore, patients were categorized into relapsing MS phenotype (including CIS and relapsing-remitting MS), and progressive MS phenotype (including SPMS and PPMS), using present criteria for phenotype classification.<sup>167</sup> Exclusion criteria were history of cervical cord/brain trauma, spondylotic cervical disease with cervical stenosis or cord



## 5. Methods

---

compression on previous MRI scans, major comorbidities, history of drug/alcohol abuse, pregnancy, and any other conditions interfering with MRI (claustrophobia, contraindications). Clinical variables (age, sex, disease duration, EDSS, phenotype) were gathered at the closest time point to the MRI study.

MRIs were visually inspected by an experienced neurologist (NM). Images were excluded from analysis due to poor MRI quality, off-center FOV, presence of spondylotic cervical disease producing central canal stenosis / cord compression, and marked cervical hyperextension during acquisition as this affects the neuroanatomic alignment of spinal levels with the vertebrae.<sup>170</sup>

CCaA was then estimated in every MRI sequence as the mean cross-sectional area over 11 slices centred both at C2/C3 and C3/C4 intervertebral disc levels, using our validated in-house semi-automated pipeline based on the SCT.<sup>169</sup> Of note, CCaA estimations were performed using the axial reconstructions from the original sagittal acquisitions. For the current study, a specific spinal canal template was created in the same space as the PAM50 atlas, termed PAM50\_42, to estimate CCaA using 2D sagittal T2WI. As a quality control for segmentation, a CV was calculated for each CCaA estimation; those with  $CV > 0.075$  were removed.<sup>160</sup> Segmentation process failures were excluded. Only subjects with CCaA estimations in all tested MRI sequences were included.

The output of the pipeline also provided the mean SCA derived from each MRI sequence, which was used to calculate the SCPF as the ratio of SCA to the CCaA, reported as a percentage. Additionally, SCA and SCPF were assessed at both the C2/C3 and C3/C4 intervertebral levels. To validate the performance of the pipeline, the CCaA was manually outlined by an experienced operator (NM) in all studied MRI sequences at the C2/C3 intervertebral disc level to obtain a manual ground truth CCaA mask (CCaA-GT).

The manual masks (CCaA-GT) and semi-automated CCaA estimations (CCaA-SCT) from cervical cord sagittal 2DT1WI, T2WI, and STIR sequences were compared using the DSC to validate the performance of the pipeline. The reliability of CCaA-SCT from the clinical MRI sequences was explored using the absolute and consistency intraclass correlation coefficients (ICC) against CCaA-SCT obtained from brain 3D T1WI, which was considered the reference MRI sequence.

On clinical grounds, a comparative analysis of the demographic and clinical variables was first conducted between relapsing and progressive MS using parametric and non-

## 5. Methods

---

parametric tests, as appropriate. Multivariate regression models adjusted for age, sex, and SCPF were then built to evaluate CCaA-SCT differences between MS phenotypes. We did not consider to adjust by treatment effect, since the CCaA is a non-modifiable factor, whose area do not change over time. Finally, the association between CCaA-SCT from all MRI sequences and disability, measured by the EDSS score, was evaluated using Spearman correlation. All calculations were performed at two intervertebral discs levels: C2/C3 and C3/C4. The p-value for significance was set at  $p < 0.05$ . Statistical analysis was performed with STATA 16.1 software (StataCorp).

## 6. RESULTS

## 6. Results

The results from each project are presented in the subsections below.

### 6.1 Pipeline validation

When assessing the mean CCaA in the initial cohort, our pipeline failed in only 3 subjects, because the position of the brain scan was too high and did not cover the upper segment of the cervical cord completely. After the removal of outlier subjects, the final cohort included CCaA estimations from 8 HC and 18 pwMS. Clinical and MRI data are shown in Table 4.

|                                     | HC<br>n=8     | pwMS<br>n=18  | p value <sup>1</sup> |
|-------------------------------------|---------------|---------------|----------------------|
| <b>Sex (female) - n (%)</b>         | 5 (62.5%)     | 11 (61.1%)    | 0.97                 |
| <b>Age - mean (SD)</b>              | 30.89 (1.44)  | 33.84 (1.98)  | 0.36                 |
| <b>CCaA – mean (SD)</b>             |               |               |                      |
| Cervical MRI acquisition            | 218.15 (4.84) | 218.47 (5.23) | 0.73                 |
| Brain MRI Acquisition               | 214.57 (3.97) | 216.75 (3.47) | 0.48                 |
| <b>TIV – mean (SD)</b>              | 1422.3 (0.10) | 1392.9 (0.12) | 0.55                 |
| <b>T2 lesion volume – mean (SD)</b> | -             | 2.31 (4.09)   | -                    |

**Table 4.** Demographical, clinical and radiological characteristics. 1p values correspond to univariate comparisons using parametric and non-parametric tests, as convenience. CCaA is expressed in mm<sup>2</sup>; TIV is expressed in mL. T2 lesion volume are expressed in mm<sup>3</sup>. CCaA, cervical canal area; HC, healthy controls; pwMS, patients with multiple sclerosis; SD, standard deviation; TIV, total intracranial volume.

Having evaluated the assumptions of linear regression (Shapiro-Wilk test,  $p = 0.80$ ; Levene test,  $p = 0.74$ ; Breusch-Pagan test,  $p = 0.94$ ; Durbin-Watson test,  $p = 0.84$ ; and variance inflation factor = 1.07), age- and sex-adjusted linear regression models confirmed that there were no significant differences in the CCaA between HC and pwMS, estimated in both the cervical cord (mean absolute difference = 0.33 mm<sup>2</sup>,  $b = 0.10$ ,  $p = 0.54$ ) and brain acquisitions (mean absolute difference = 2.18 mm<sup>2</sup>,  $b = 0.36$ ,  $p = 0.14$ ). Consequently, to perform the statistical analysis between different sequences with a larger sample size, we considered HC and patients with MS as a single group (26 subjects).

In the assessment of the reproducibility of the proposed pipeline, the degree of overlap between the CCaA masks generated by the proposed pipeline and the manual GT was excellent with a DSC mean of 0.90 (range, 0.73–0.97). The distribution across the 4 different acquisitions is shown in Figure 6. Agreement between the 2 evaluators was also excellent, with a DSC of 0.95 (range, 0.78–1). Furthermore, we did not find significant differences when comparing

## 6. Results

CCaA estimations obtained with the pipeline and the GT by a t test, either at the baseline cervical cord T1WI (mean absolute difference =  $9.56 \text{ mm}^2$ ,  $t [25] = 1.77$ ,  $p = 0.09$ ) or brain T1WI (mean absolute difference =  $6.35 \text{ mm}^2$ ,  $t[25] = 0.82$ ,  $p = 0.42$ ).

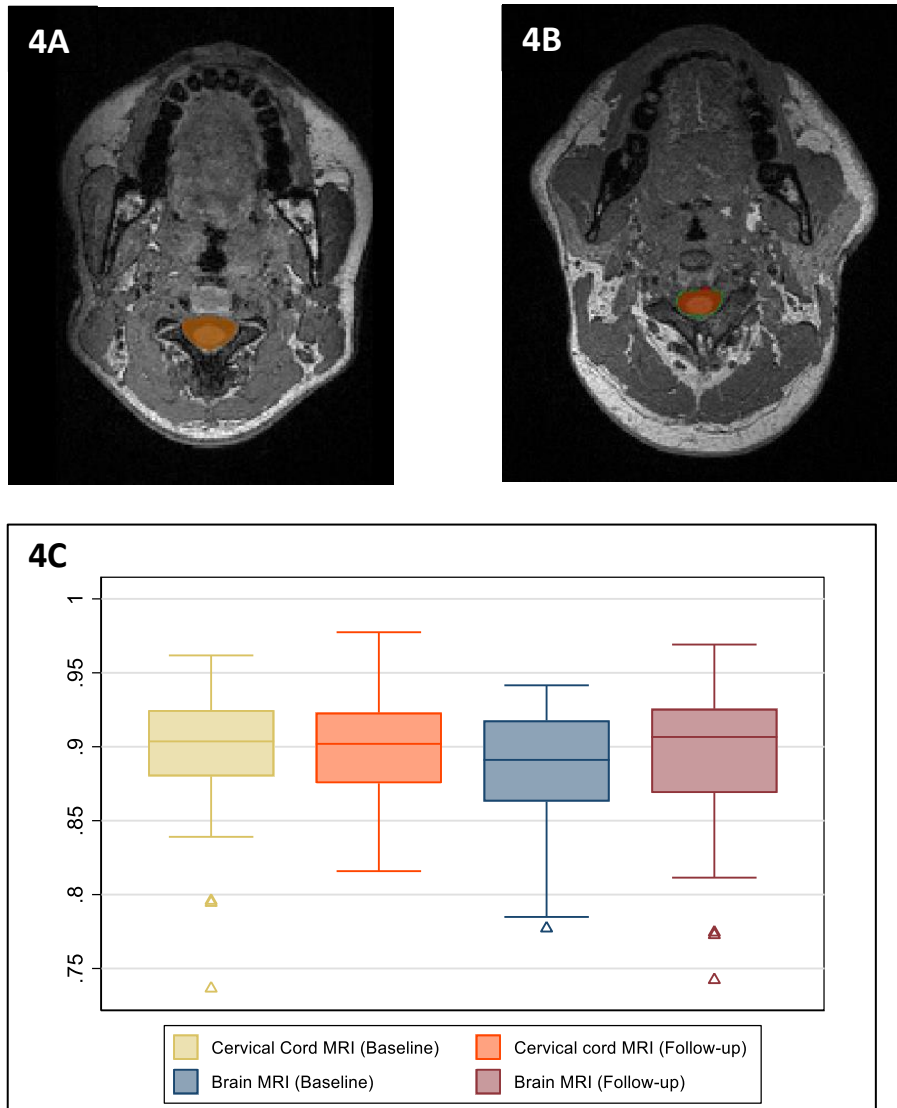


**Figure 6.** Cervical canal area mask obtained with the proposed pipeline (green) versus the manual segmentation (red) in a patient with multiple sclerosis. A: spinal MRI acquisition, showing a dice similarity coefficient of 0.92. B: brain MRI acquisition, showing a dice similarity coefficient of 0.88. Figure 4C: distribution of Dice Similarity Coefficients between Cervical Canal Area masks from the in-house pipeline and the Ground Truth over the 4 acquisitions, both in healthy controls and patients with multiple sclerosis.

## 6. Results

When we compared CCaA estimations obtained from baseline and 1-year follow-up cervical cord MRIs, the highest agreement was obtained with 11 and 17 slices (ICC = 0.76; 95% CI, 0.44–0.88, and ICC = 0.78; 95% CI, 0.56–0.90, respectively). Average ICCs are represented in Figure 7, and they are consistently higher than individual ICCs.

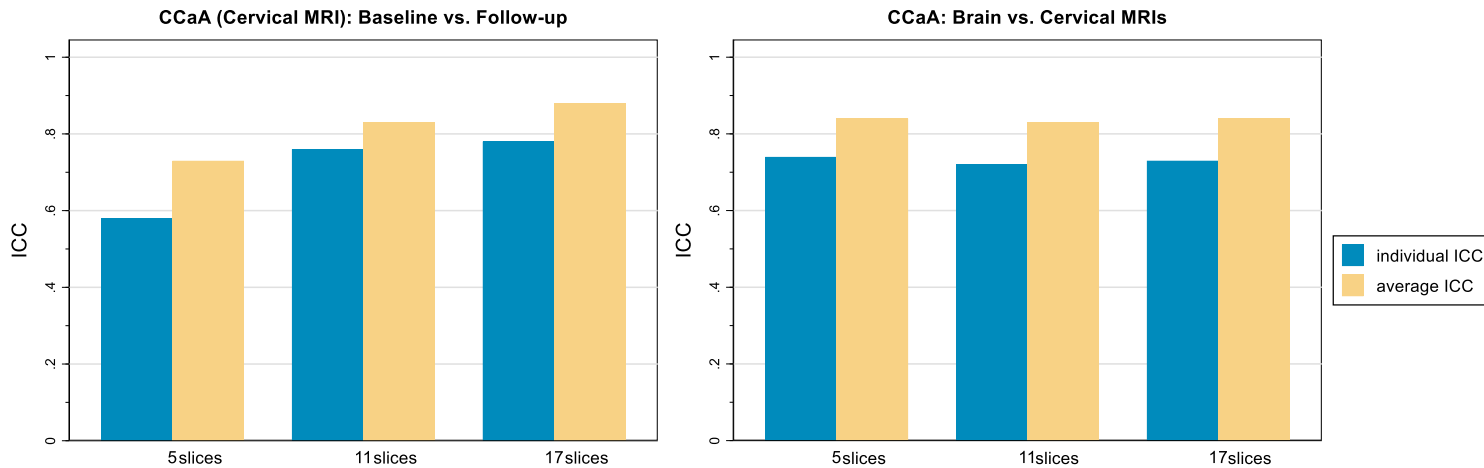


**Figure 7.** Representation of individual ICC (blue) and average ICC (yellow), calculated in 5, 11 and 17 slices. On the left, ICC between baseline and follow-up cervical MRI. On the right, degree of concordance of CCaA analysed in brain and cervical acquisitions. ICC: intraclass correlation coefficient. CCaA: cervical canal area.

Estimations of the CCaA with 17 and 11 slices were also highly similar when using the Bland-Altman method, in contrast to LoA obtained with 5 slices, with a narrower and better-centered LoA (Figure 8, left side). When comparing CCaA estimations obtained from cervical cord T1WI acquisitions at baseline (mean = 218.37 [SD, 5.02] mm<sup>2</sup>) and follow-up (mean = 217.09 [SD, 5.62] mm<sup>2</sup>), we did not find significant differences (mean absolute paired difference = 1.28 mm<sup>2</sup>,  $t[25] = 1.22$ ,  $P = .23$ ). CCaA estimations obtained from brain and cervical cord MRIs had a high agreement, independent of the number of slices used to estimate the CCaA (Figure 7). However, the Bland-Altman method showed a better agreement with CCaA estimations of 17 and 11 slices, than with those obtained with 5 slices (Figure 8, right side). When analysing absolute means, we found minimal but significant differences between CCaA estimations from brain (mean = 216.07 [SD, 3.7] mm<sup>2</sup>) and cervical MRIs (mean = 218 [SD, 5.0] mm<sup>2</sup>) (mean absolute paired difference = 2.30,  $t[25] = 2.97$ ,  $p = 0.006$ ).

## 6. Results

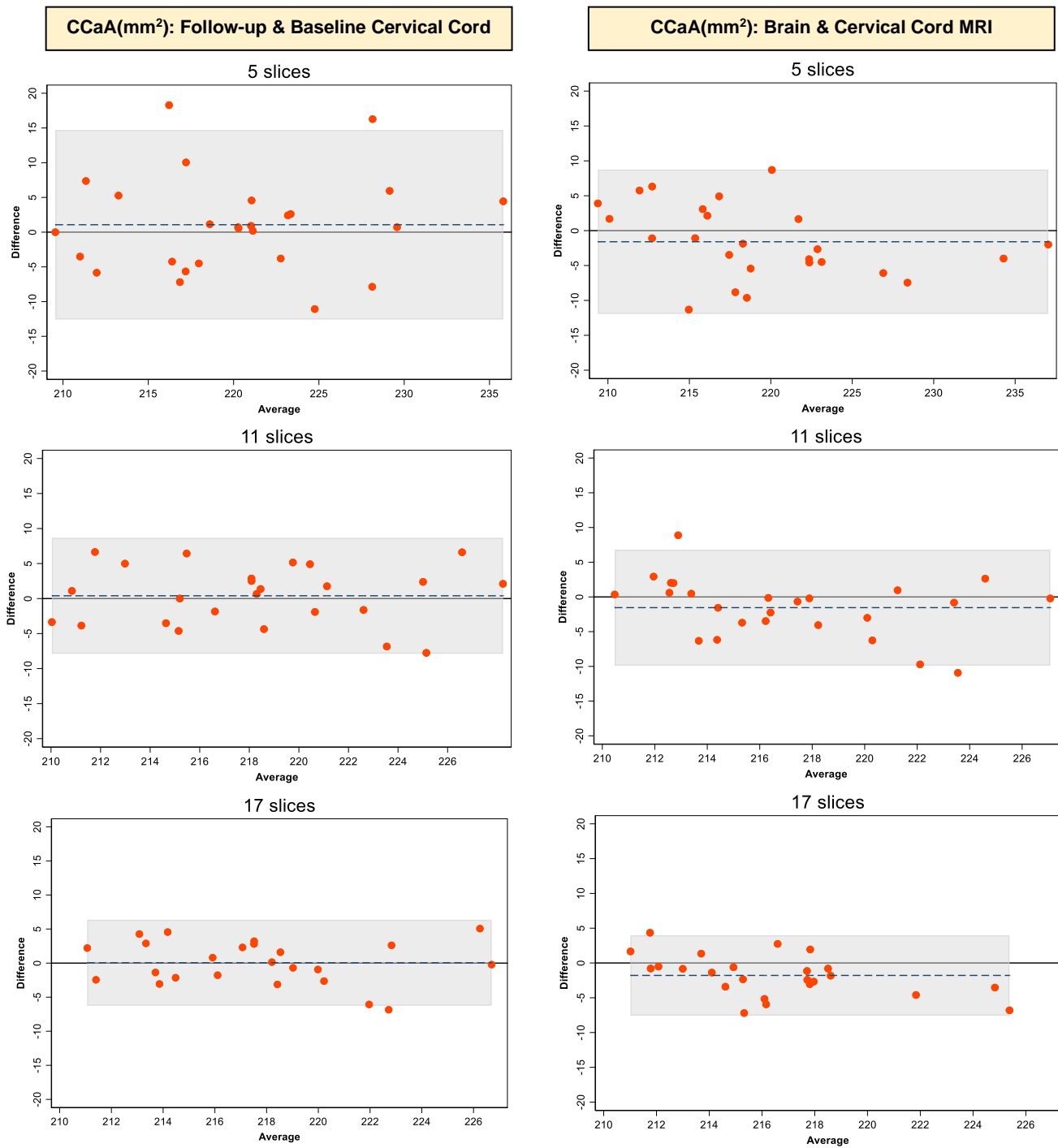


**Figure 8.** Bland & Altman plots showing the agreement between CCaA estimations assessed in different number of slices. On the left, it is shown the agreement between baseline and follow-up cervical cord MRI. On the right, between brain and cervical cord MRIs. Notice that the x-axis scale of the plot analysing CCaA estimations on 5 slices is bigger than the others

## 6. Results

---

### 6.2 Assessment of the spinal cord reserve in a multicentric cohort

An initial set of 177 HC and 428 pwMS (289 [67.5%] relapsing MS, and 139 [32.5%] progressive MS) had a cervical cord 3D T1WI. After the visual quality check, 139 MRIs were removed (35 HC [19.8%], 72 [24.9%] relapsing MS and 32 [23.0%] progressive MS). Among these, 15/139 showed signs of cervical spondylosis, 5/139 had a vertebral cavity with a diameter stabilization below the C2/C3 vertebral level, 13/139 exhibited marked cervical hyperextension, 85/139 had poor MRI quality, and 21/139 had an off-centre FOV. Following quality control, the segmentation process failed in 9 subjects. Out of 457 final participants, 18 MRIs (3.9%) were removed only from the analyses of C2/C3 level, and 7 (1.5%) were removed from the analyses of C3/C4 level, since these CCaA segmentations displayed a  $CV > 0.075$ .

Baseline demographical, clinical and MRI data of the final cohorts at both intervertebral levels can be found in Table 5. Patients with progressive MS were significantly older with a longer disease duration, a higher disability, and a greater number of cervical cord lesions. Excluded participants had overlapping characteristics to the final cohort (Table 5).

#### 6.2.1 CCaA at C2/C3 intervertebral disc level

The final cohort comprised 135 HC and 304 pwMS (207 [68.1%] relapsing MS and 97 [31.9%] progressive MS). In age and sex-adjusted regression models, there were no significant differences in CCaA between HC and relapsing MS ( $214.62\text{mm}^2$  [SD 8.42] vs.  $213.68\text{mm}^2$  [SD 9.02],  $p=0.40$ ), but progressive MS showed significantly lower CCaA than HC ( $214.62\text{mm}^2$  [SD 8.42] vs.  $210.51\text{mm}^2$  [SD 10.35],  $p=0.007$ ) (Figure 9).

CCaA and baseline EDSS were associated in an age- and sex-adjusted linear model ( $\beta=-0.11$ ;  $p=0.023$ ; adjusted- $R^2=0.37$ ). However, when adjusting by SCPF and number of cord lesions, the significance disappeared (Table 6). The analysis by phenotypes including all adjusting variables showed a significant association between EDSS and CCaA in relapsing MS ( $\beta=-0.19$ ;  $p=0.002$ ; adjusted- $R^2=0.35$ ), but not in progressive MS (Table 6). The application of jackknife resampling in the linear regression analysis resulted in identical coefficients of predictor variables, standard errors, and confidence intervals as those in the original model. However, the relationship between CCaA and baseline EDSS did not reach significance at this level either.

At 5-year follow-up, 85 patients (32.7%) experienced disability progression. We did not find differences in CCaA between patients with clinical worsening and those who remained stable ( $212.01\text{mm}^2$  [SD 9.83] vs.  $213.36\text{mm}^2$  [SD 9.16],  $p=0.28$ ).



## 6. Results

|                                 | C2/C3 Level               |                       |                        | C3/C4 Level               |                       |                         | Excluded subjects        |                      |                        |              |
|---------------------------------|---------------------------|-----------------------|------------------------|---------------------------|-----------------------|-------------------------|--------------------------|----------------------|------------------------|--------------|
|                                 | Healthy controls<br>N=135 | Relapsing MS<br>N=207 | Progressive MS<br>N=97 | Healthy controls<br>N=142 | Relapsing MS<br>N=208 | Progressive MS<br>N=100 | Healthy controls<br>N=45 | Relapsing MS<br>N=81 | Progressive MS<br>N=40 | 1,p<br>value |
| Sex (female)<br>n (%)           | 76 (56.3)                 | 140 (67.6)            | 50 (51.5)              | 80 (56.3)                 | 139 (66.8)            | 51 (51)                 | 28 (62.2)                | 48 (59.2)            | 26 (65)                | >0.05        |
| Age [years]<br>mean (SD)        | 40.4 (13.2)               | 42.1 (11.5)           | 55.2 (8.9)             | 40.0<br>(13.2)            | 42.0 (11.5)           | 55.3 (9.3)              | 38.6 (14.7)              | 43.9 (13.0)          | 53.0 (9.8)             | >0.05        |
| EDSS<br>baseline p50<br>(IQR)   | -                         | 2.5 (1.5 – 3.5)       | 6 (5 – 6.5)            | -                         | 2.5 (1.5 – 3.5)       | 6 (5 – 6.5)             | -                        | 2.75 (1.5 –<br>4)    | 6 (4.75 –<br>6.75)     | >0.05        |
| D.D [years]<br>mean (SD)        | -                         | 11.2 (9.1)            | 19.9 (9.1)             | -                         | 11.1 (9.1)            | 20.02 (9.3)             | -                        | 11.9 (8.0)           | 18.7 (11.9)            | >0.05        |
| Cord lesions<br>p50 (IQR)       | -                         | 2 (0 – 3)             | 3 (2 – 6)              | -                         | 2 (0 – 3)             | 3 (2 – 6)               | -                        | 2 (1 – 3)            | 4 (1 – 6)              | >0.05        |
| TIV [mL]<br>mean (SD)           | 1468.9 (64.1)             | 1440.9 (78.9)         | 1374.7 (61.4)          | 1470.7<br>(64.9)          | 1439.3 (80.1)         | 1375.5 (64.3)           | 1495.2 (68.7)            | 1426.3<br>(75.3)     | 1373.5<br>(72.5)       | >0.05        |
| Brain T2LV<br>[mL] mean<br>(SD) | -                         | 8.2 (10.0)            | 16.2 (15.6)            | -                         | 8.2 (10.1)            | 16.5 (15.7)             | -                        | 8.8 (11.2)           | 13.5 (10.4)            | 0.01         |

**Table 5.** Final cohorts at C2/C3 and C3/C4 intervertebral disc levels, as well as the excluded HC and pwMS. <sup>1</sup>p values correspond to univariate comparisons using parametric and non-parametric tests, as convenience. <sup>2</sup>Data from excluded patients is compared to the C2/C3 cohort for each phenotype. CIS, clinically isolated syndrome; D.D, disease duration; IQR, interquartile range; MS, multiple sclerosis; PPMS, primary progressive MS; p50, percentile 50 (median); RRMS, relapsing-remitting MS; SD, standard deviation; SPMS, secondary-progressive MS; TIV, total intracranial volume; T2LV, T2-lesion volume. -Dash indicates not information available. Of note, relapsing MS includes CIS and RRMS; progressive MS includes PPMS and SPMS.

## 6. Results

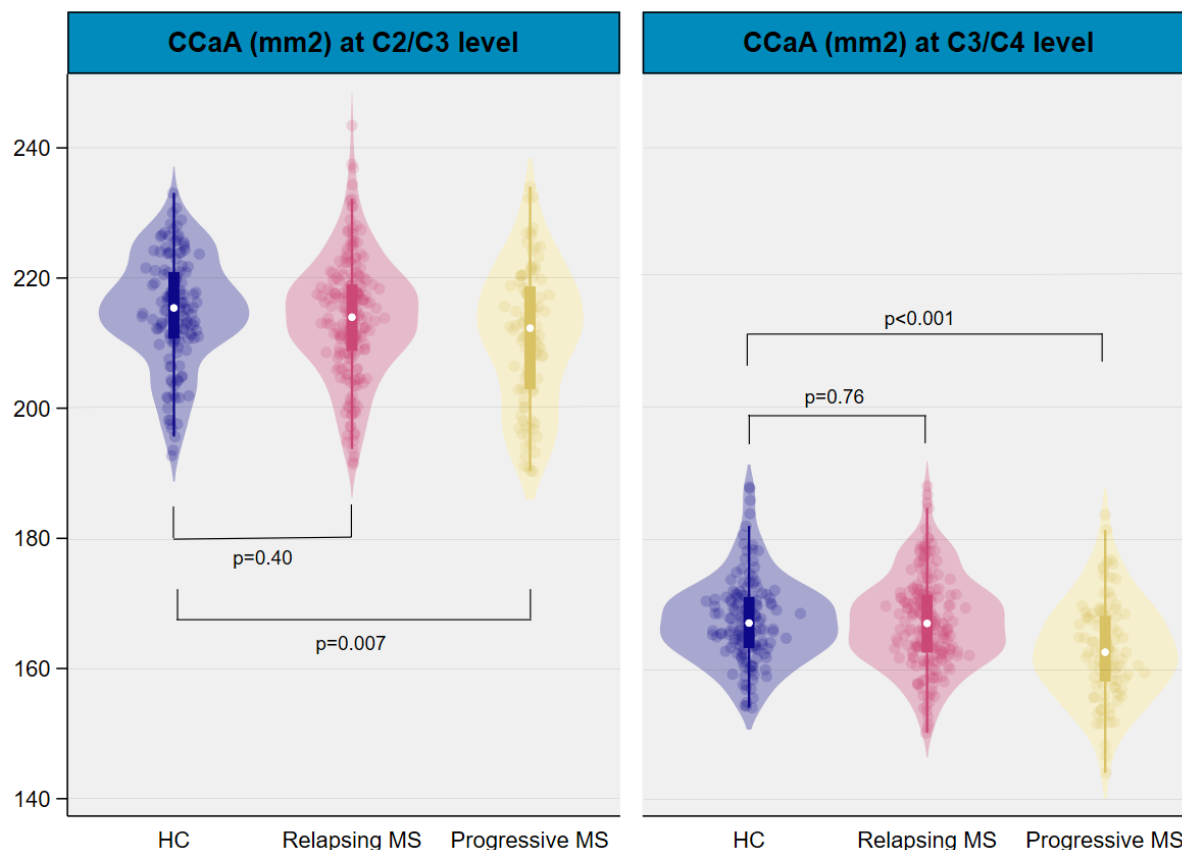


**Figure 9.** Violin plots with the distribution of the cervical canal area (CCaA) assessed at C2/C3 and C3/C4 intervertebral disc levels according to the different phenotypes. Dots represent individual values. White dots show the median, inner boxes represent Q1 and Q3, and vertical whiskers indicate  $Q3 \pm 1.5$  IQR. P values were obtained in age- and sex-adjusted regression models (see main text). HC, healthy controls; MS, multiple sclerosis.

### 6.2.2 CCaA at C3/C4 intervertebral disc level

The final cohort comprised 142 HC and 308 pwMS (208 [67.5%] relapsing MS and 100 [32.5%] progressive MS). As in the C2/C3 level, there were no significant differences in CCaA when comparing HC and relapsing MS ( $169.67 \text{ mm}^2$  [SD 6.50] vs.  $169.44 \text{ mm}^2$  [SD 6.94],  $p=0.76$ ), but again, progressive MS displayed a significant smaller CCaA ( $169.67 \text{ mm}^2$  [SD 6.50] vs.  $165.16 \text{ mm}^2$  [SD 7.39],  $p<0.001$ ) (Figure 7).

CCaA and baseline EDSS showed a significant association using a multivariate regression model adjusted by age, sex, SCPF and number of cord lesions, both when including the whole cohort ( $\beta=-0.13$ ;  $p=0.009$ ; adjusted- $R^2=0.43$ ) (Table 6), and the relapsing phenotype ( $\beta=-0.16$ ;  $p=0.02$ ; adjusted- $R^2=0.33$ ). As in the C2/C3 level, the association was not significant in progressive MS (Table 6). Jackknife resampling analysis revealed that the coefficients of the predictor variables, along with the standard errors and confidence intervals, remained

## 6. Results

unchanged with and without jackknife adjustment in the whole cohort, consistent with the original model, which enhances the association between the CCaA and baseline EDSS.

At 5-year follow-up, 86 patients (32.7%) showed disability progression. Patients with clinical worsening showed a significant smaller CCaA at baseline compared to those who remained stable when adjusting by age and sex (167.03mm<sup>2</sup> [SD 7.53] vs. 169.13mm<sup>2</sup> [SD 7.13], p=0.03). However, when adjusting by SCPF and number of cord lesions, the significance disappeared.

|                                 | <b>C2/C3</b>        |                     |                       | <b>C3/C4</b>        |                     |                       |
|---------------------------------|---------------------|---------------------|-----------------------|---------------------|---------------------|-----------------------|
|                                 | <b>EDSS</b>         |                     |                       | <b>EDSS</b>         |                     |                       |
|                                 | <b>Whole cohort</b> | <b>Relapsing MS</b> | <b>Progressive MS</b> | <b>Whole cohort</b> | <b>Relapsing MS</b> | <b>Progressive MS</b> |
| <b>CCaA</b>                     | $\beta$ -0.05       | $\beta$ -0.19***    | $\beta$ 0.22          | $\beta$ -0.13***    | $\beta$ -0.16*      | $\beta$ 0.11          |
| <b>Age</b>                      | $\beta$ 0.50***     | $\beta$ 0.48***     | $\beta$ -0.007        | $\beta$ 0.48***     | $\beta$ 0.45***     | $\beta$ -0.05         |
| <b>Sex (Male)</b>               | $\beta$ 0.05        | $\beta$ 0.09        | $\beta$ -0.32         | $\beta$ 0.06        | $\beta$ 0.10        | $\beta$ -0.09         |
| <b>SC lesions</b>               | $\beta$ 0.28***     | $\beta$ 0.16**      | $\beta$ 0.26*         | $\beta$ 0.26***     | $\beta$ 0.13*       | $\beta$ 0.04          |
| <b>SCPF</b>                     | $\beta$ -0.11*      | $\beta$ -0.02       | $\beta$ -0.07         | $\beta$ -0.05       | $\beta$ -0.07       | $\beta$ -0.07         |
| <b>Adjusted-R<sup>2</sup></b>   | 0.44                | 0.35                | 0.10                  | 0.43                | 0.33                | 0.01                  |
| <b>Model p-value</b>            | <0.001              | <0.001              | 0.03                  | <0.0001             | <0.0001             | 0.32                  |
| <b>Shapiro-Wilk test (CCaA)</b> | 0.001               | 0.17                | 0.11                  | 0.12                | 0.37                | 0.89                  |
| <b>Breusch-Pagan test</b>       | 0.06                | 0.16                | 0.26                  | 0.05                | 0.23                | 0.22                  |
| <b>Collinearity (IF)</b>        | 1.08                | 1.07                | 1.05                  | 1.16                | 1.13                | 1.11                  |

**Table 6.** Multivariate regression models to investigate the association between EDSS and Cervical Canal Area (CCaA) at baseline, measured at C2/C3 and C3/C4 intervertebral disc levels. The table shows adjusted beta coefficients for each variable in every single regression model. At each vertebral level, the linear models are built in three different ways: using the entire cohort, or only relapsing MS or progressive MS. EDSS represents the dependent variable. Assumptions of linear regression are also being appraised. CCaA, cervical canal area; EDSS, Expanded Disability Status Scale; IF, inflation factor; MS, multiple sclerosis; SC, spinal cord; SCPF, spinal cord parenchyma fraction; Significance of  $\beta$  coefficient: \*\*\*p<0.001, \*\*p<0.01, \*p<0.05

### 6.3 Estimation of the CCaA in additional MRI sequences

We aimed to obtain CCaA-SCT from brain sagittal 3D T1WI, cervical cord sagittal 2D T1WI, T2WI, and STIR sequences from the initial cohort of 52 pwMS who met the inclusion

## 6. Results

criteria. However, the pipeline failed when employing 2D T1WI due to the low contrast between structures. Therefore, all analyses were conducted solely using CCaA-SCT derived from the other MRI sequences (Figure 10).

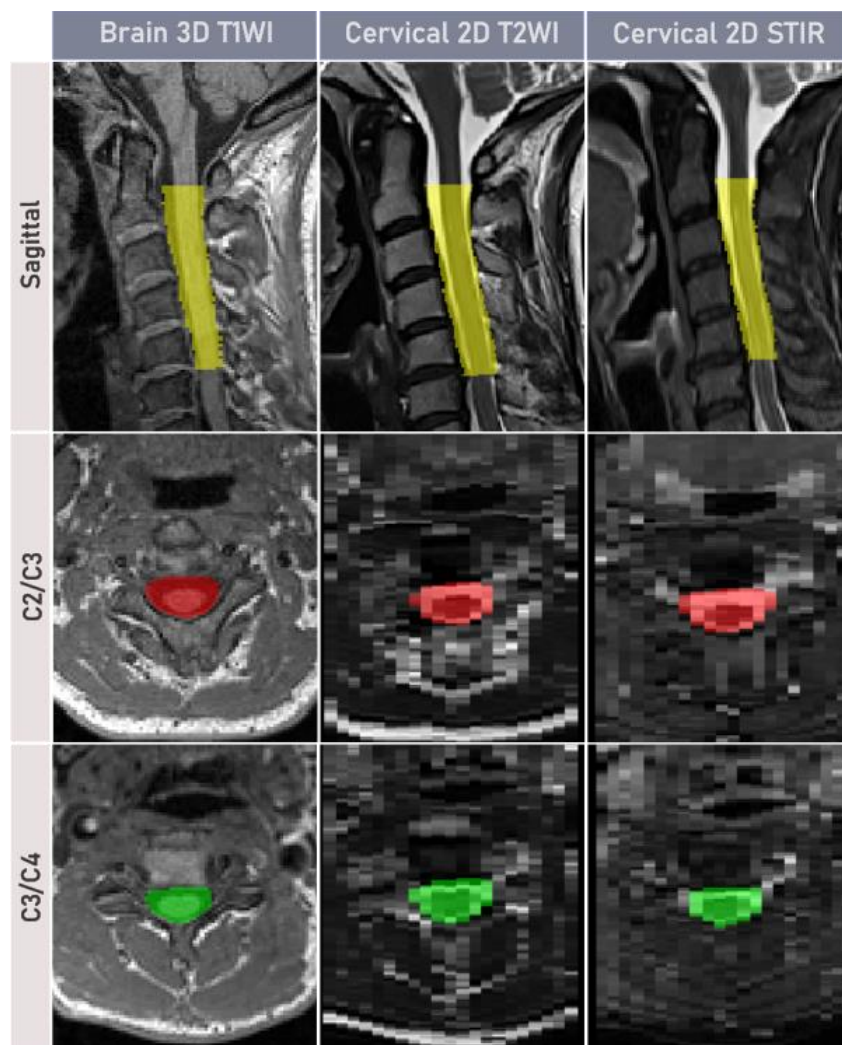


**Figure 10.** Exemplary case: Cervical canal area segmentation at C2/C3 and C3/C4 intervertebral disc levels derived from the MRI sequences employed for the analysis. T1WI, T1-weighted image; T2WI, T2-weighted image; STIR, short-tau inversion recovery.

Out of the 52 pwMS, five subjects (9.6%) were excluded from the analysis due to poor MRI quality in one or more sequences. The segmentation process failed in one T2WI and one STIR sequence at the C2/C3 level, and in one brain T1WI at the C3/C4 level. Additionally, eleven (23.4%) CCaA-SCT (four in brain 3D T1WI, two in T2WI and five in STIR) displayed a CV greater than 0.075 at the C2/C3 level, and two (4.3%) at the C3/C4 level (one in brain T1WI, and one in STIR). Consequently, after quality control, the final cohort comprised 34 MS

## 6. Results

patients at the C2/C3 level and 44 at the C3/C4 level with CCaA-SCT data derived from brain 3D T1WI, and cervical cord 2D T2WI and STIR sequences.

In the assessment of agreement between manual and semi-automated CCaA masks, the degree of overlap was excellent between CCaA-GT and CCaA-SCT using cervical cord T2WI (DSC range = 0.92 [0.89-0.93]) and STIR sequences (DSC range = 0.90 [0.88-0.92]).

Regarding the equivalence between CCaA-SCT from cervical cord 2D T2WI, STIR and brain 3D T1WI, the absolute and consistency ICC are detailed in Table 7. As shown, absolute ICCs appeared to be poor at both intervertebral disc levels. In contrast, consistency ICCs ranged from moderate to good,<sup>165</sup> showing a higher reliability at C3/C4 level across the three comparison groups.

|       |                                    | T2WI – 3D<br>T1WI | STIR – 3D<br>T1WI | T2WI – STIR      |
|-------|------------------------------------|-------------------|-------------------|------------------|
| C2/C3 | <b>Absolute ICC</b><br>(95% CI)    | 0.19 (-0.1-0.53)  | 0.21 (-0.19-0.54) | 0.63 (0.27-0.68) |
|       | <b>Consistency ICC</b><br>(95% CI) | 0.63 (0.26-0.82)  | 0.52 (0.22-0.70)  | 0.65 (0.30-0.82) |
| C3/C4 | <b>Absolute ICC</b><br>(95% CI)    | 0.13 (-0.07-0.43) | 0.18 (-0.03-0.36) | 0.80 (0.63-0.89) |
|       | <b>Consistency ICC</b><br>(95% CI) | 0.67 (0.38-0.82)  | 0.80 (0.64-0.89)  | 0.80 (0.63-0.89) |

**Table 7.** Absolute and consistency intraclass correlation coefficients (ICC) and their confidence interval (95% CI) to assess the equivalence between different MRI sequences at the two intervertebral disc levels (C2/C3 and C3/C4). Of note, brain 3D T1WI is the reference sequence. T1-weighted image; T2WI, T2-weighted image; STIR, short-tau inversion recovery.

The analysis of clinical variables, including demographic, disease-related, and MRI data for both intervertebral disc levels, is presented in Table 8. Overall, in the progressive MS group, there was a lower proportion of females, with greater disability and longer disease duration. At the C3/C4 level using the T2WI, progressive MS exhibited a significant smaller CCaA compared to relapsing MS when adjusting for age, sex, and SCPF (mean CCaA absolute difference 5.32mm<sup>2</sup>, 95%CI 0.96-9.68, p 0.044). Although there were also consistent mean numerical CCaA differences (smaller CCaA in the progressive group) measured with the other sequences at both C2/C3 and C3/C4 levels, they did not reach statistical significance.

## 6. Results

|                      | C2/C3 level          |                        |        | C3/C4 level          |                        |        |
|----------------------|----------------------|------------------------|--------|----------------------|------------------------|--------|
|                      | Relapsing MS<br>N=23 | Progressive MS<br>N=11 | p      | Relapsing MS<br>N=27 | Progressive MS<br>N=17 | p      |
| Sex [female]: n (%)  | 21 (91.3)            | 7 (63.70)              | 0.048  | 24 (89.9)            | 11 (64.7)              | 0.052  |
| Age [years]          | 49.01 (10.91)        | 50.25 (5.86)           | 0.72   | 47.84 (12.13)        | 50.82 (5.05)           | 0.34   |
| EDSS: p50 (IQR)      | 2 (1.5 – 3)          | 5 (4 -6)               | <0.001 | 2 (1 – 3)            | 5.5 (4.5 – 6.5)        | <0.001 |
| DD [years]           | 15.13 (7.77)         | 21.06 (11.56)          | 0.08   | 14.56 (7.84)         | 20.50 (10.25)          | 0.03   |
| CCaA – Brain 3DT1WI  | 214.22 (6.43)        | 210.95 (4.09)          | 0.15   | 168.65 (7.07)        | 166.85 (4.03)          | 0.87   |
| CCaA – Cervical T2WI | 233.49 (8.19)        | 231.82 (9.23)          | 0.16   | 193.58 (7.79)        | 189.26 (5.38)          | 0.041  |
| CCaA – Cervical STIR | 230.49 (11.87)       | 226.23 (14.48)         | 0.11   | 192.73 (7.81)        | 189.37 (6.63)          | 0.66   |

**Table 8.** Demographical, clinical and cervical canal measures using different MRI sequences at C2/C3 and C3/C4 intervertebral disc levels. Comparisons of variables between multiple sclerosis phenotype groups were conducted using parametric and non-parametric test, as convenience. CCaA is measured in mm<sup>2</sup>. If not indicated otherwise, variables are reported as mean (SD). CCaA, cervical canal area; DD, disease duration; MS, multiple sclerosis; p50, median value; IQR, interquartile range; SD, standard deviation, T1WI, T1-weighted image; T2WI, T2-weighted image; STIR, short-tau inversion recovery; mm<sup>2</sup>, squared millimetres

Lastly, we explored the role of CCaA measurements as a surrogate marker for spinal cord reserve. At the C3/C4 level, a significant correlation was observed between CCaA-SCT and EDSS when employing T2WI: rho -0.34, p 0.023 (Figure 11). However, no significant correlation was found using STIR or brain 3D T1WI, despite observing a consistent trend. Additionally, at the C2/C3 level, no significant correlations were observed.

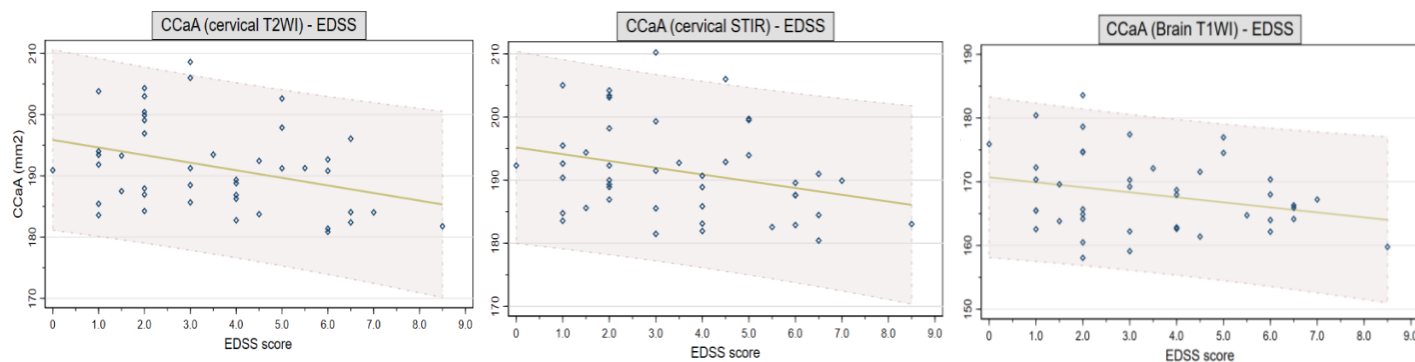


**Figure 11.** Spearman correlations with the 95% confidence interval between cervical canal area (CCaA) assessed in different MRI sequences and EDSS scores at C3/C4 intervertebral disc level. CCaA is measured in mm<sup>2</sup>. T1WI, T1-weighted image; T2WI, T2-weighted image; STIR, short-tau inversion recovery.

## **7. DISCUSSION**

## 7. Discussion

---

The current thesis builds on the first formal attempt to define the concept of spinal cord reserve in MS through a comprehensive analysis of the CCaA as a surrogate marker, drawing on the established concept of brain reserve. For this purpose, we first developed and validated a methodology based on the SCT to obtain reproducible measures of the CCaA from brain and cervical cord sagittal 3D T1WI. Secondly, we applied the pipeline on a multicentre cohort of well-characterized pwMS and HC to examine CCaA differences among groups and MS phenotypes, and explore its potential association with disability progression. Finally, we evaluated the performance of our pipeline in estimating CCaA using the most commonly employed MRI sequences in clinical practice. The ultimate goal of this thesis was to validate the CCaA as a reliable marker for spinal cord reserve, thereby advancing the understanding of disability progression in MS through three consecutive and complementary projects.

The basis of this thesis lies in a preliminary cross-sectional study that analysed the CCaA in a multicentre cohort, demonstrating that CCaA was independently related to self-perceived disability.<sup>160</sup> In that study, CCaA was estimated from brain MRI acquisitions, no information on disease phenotypes was available, and EDSS scores were unavailable, as disability was measured by the PDDS. To our knowledge, no other studies have been published in this field. Consequently, the present thesis was undertaken to confirm these initial findings, and was conceptualized to address the methodological, neuroimaging and clinical translation aspects inherent to the concept of spinal cord reserve.

The first step involved establishing a methodology to reliably estimate CCaA with an acceptable balance of time and efforts. Therefore, our group created an in-house semi-automated segmentation pipeline based on SCT. We validated this tool by comparing the generated masks with the corresponding manual GT both from brain and cervical cord 3D T1WI. The overlap was excellent, and significant differences were not found when comparing both measurement methods, indicating that the proposed pipeline seems to appropriately measure the CCaA.

To date, CCaA variations across time have not been analysed before, though changes were not expected a priori under physiological conditions.<sup>111</sup> We verified its consistency during a 1-year period by assessing the measurement in baseline and follow-up cervical T1WIs. Consequently, the CCaA could be used in future studies as a proxy for the premorbid status of the spinal cord, because stability across time is a prerequisite for such use. Similar to other cervical cord area measurement methods,<sup>133</sup> we considered it more appropriated to calculate the mean area over a few sections rather than just one. Increasing the number of sections used



## 7. Discussion

---

would typically reduce measurement variability. However, in the case of the spinal canal, variability could increase because sections may cover regions where the canal area physiologically increases toward the foramen magnum. To determine the optimal number of sections, we calculated ICCs using CCaA estimations with the SCT across 5, 7, and 11 slices centred at the midpoint of the C2/C3 vertebral disc. The study showed a good level of concordance between time points, obtaining the highest individual ICC when using 11 and 17 slices for the analysis, compared with 5 slices. We considered that differences in the ICC between the number of slices were related to minor inaccuracies in subject repositioning; hence, the lower the number of slices used to calculate the CCaA, the greater the variability found among patients. In addition, we tested the robustness of CCaA estimations obtained from brain and spine scans, obtaining good agreement between them. Similar ICC values across the different numbers of slices used to calculate the CCaA may be because no repositioning is needed between brain and spine acquisitions.

Overall, ICCs obtained were lower than those reported in other validation studies.<sup>168,171</sup> A possible explanation might be that the individual ICC has been reported instead of the average, which tends to minimize variations and provides higher ICCs. Moreover, although the degree of agreement between CCaA estimations from brain and cervical MRIs was not excellent and there were significant differences between both measurements, the mean difference was inferior to 3 mm<sup>2</sup> in the paired t-test analysis. As the in-house pipeline failed in 3 subjects when using 17 slices, it might be advisable to use the 11-slice approach, which provides similar reproducibility parameters.

Once we had a validated tool to obtain reproducible measures of CCaA, we proceeded to apply it in a multicentre cohort with different scanners and MRI protocols. We aimed to study for the first time CCaA variations across all MS phenotypes and HC. For this purpose, we had cervical cord 3D T1WI, so we assessed the CCaA as the mean CSA centred at both the C2/C3 and C3/C4 intervertebral disc levels. Our CCaA estimations are fully in line with those documented by Kato and coworkers<sup>111</sup> in a study with 1211 HC. They reported a CCaA for 40-year-old males of 211.4 mm<sup>2</sup> at the C2/C3 level, and 170.7 mm<sup>2</sup> at the C3/C4 level, compared to our values of 214.62mm<sup>2</sup> at the C2/C3 level, and 169.67mm<sup>2</sup> at the C3/C4 level.

In the examination of CCaA across phenotypes, we observed no differences in CCaA between HC and relapsing MS. This finding supports the use of CCaA as a surrogate measure of maximal spinal cord lifetime growth, and reinforces its use to test the concept of spinal cord reserve in MS.

## 7. Discussion

---

In contrast, progressive MS displayed a significantly lower CCaA than HC and relapsing MS. We have verified this finding by measuring the CCaA at 2 different intervertebral disc levels, C2/C3 and C3/C4. In light of these results, it seems that a smaller CCaA could be a feature of progressive forms of MS, and it might be one of the factors related to the progressive spastic paraparesis that these patients present either from the beginning or through the evolution of the disease.<sup>172,173</sup> However, this finding needs further testing in cohorts including higher number of patients with progressive phenotypes.

In this second study, we included all MS phenotypes, and disability was measured by EDSS, the most widely used instrument in clinical practice and clinical trials.<sup>41</sup> Spearman's correlation and multivariate linear regression models (mainly at C3/C4 level) did confirm the association between baseline EDSS and CCaA. These findings may support the existence of the spinal cord reserve, hence a larger CCaA could be protective against disability in MS. In the subgroup analysis by phenotypes, the association between CCaA and EDSS did not reach statistical significance in the progressive phenotype. This may be due to the fact that, in the present cohort, patients with progressive MS exhibited a very narrow range of EDSS scores (50% of progressive patients had EDSS scores of 6.0 or 6.5), thus hampering statistical associations.

The jackknife resampling technique yielded nearly identical results to the original multivariate regression model using the entire cohort. Coefficients of predictor variables and the adjusted R-squared value remained unchanged. Confidence intervals generated through jackknife adjustment closely matched those from the original model. Consistent coefficients across iterations suggest high reliability, indicating minimal influence from specific data points. Overall, the jackknife method has enhanced the robustness of the association between CCaA (at C3/C4 level) and baseline EDSS.

We observed that patients with disability progression at 5-year follow-up exhibited smaller CCaA at baseline in age- and sex-adjusted linear models. These results are again supportive of the concept of spinal cord reserve and point towards considering CCaA as a non-modifiable contributor for clinical progression. Admittedly, when adjusting also by SCPF and the number of cervical cord lesions, linear models did not reach significance. The potential of spinal cord atrophy<sup>133,174,175</sup> and the presence of cervical cord lesions<sup>176,177</sup> as disability predictors has been well-demonstrated. In that sense, the role of CCaA in disability worsening is likely to be modest, especially when compared to the other two mentioned, more robust, pathology-driven, variables.

## 7. Discussion

---

In the quality check, the main reason of exclusion was poor MRI quality. As discussed in the *Introduction*, spinal cord has some particularities that make the imaging process technically challenging. Therefore, an accurate quality check is still crucial to obtain reliable data for subsequent statistical analysis. Additional exclusion criteria in this study were the presence of cervical spondylosis and anatomical variations of the spinal canal, which were not as relevant as the MRI quality in our cohort. Conversely, the number of excluded subjects based on the CV criteria was very low compared to our previous study,<sup>160</sup> where the CCaA segmentation was performed in brain MRIs. CCaA segmentation in dedicated cervical cord MRI has been proven to provide more stable measurements,<sup>169</sup> which outlines the use of spinal cord MRI in MS.

We obtained consistent, but not fully identical results when analysing data from C2/C3 and C3/C4 CCaA segmentations. Interestingly, results derived from the C3/C4 analysis showed stronger correlations, higher beta coefficients, and more frequent statistically significant associations in multivariate linear regression models. We hypothesized that such differences are related to the fact that the cervical canal anatomy varies along its length, showing significant decreases from C1 to C3, and achieving a more stable diameter from C3 to C7.<sup>111,127</sup> Consequently, C3/C4 CCaA measurements exhibit reduced variability across the 11 slices used to calculate the spinal canal area, which is reflected by smaller SDs (see *Results*). Additionally, fewer participants are excluded based on the CV criteria in C3/C4 CCaA segmentations, possibly due to the more stable measurements at this level (Figure 12). All these findings support segmentations at C3/C4 level to obtain CCaA estimations.

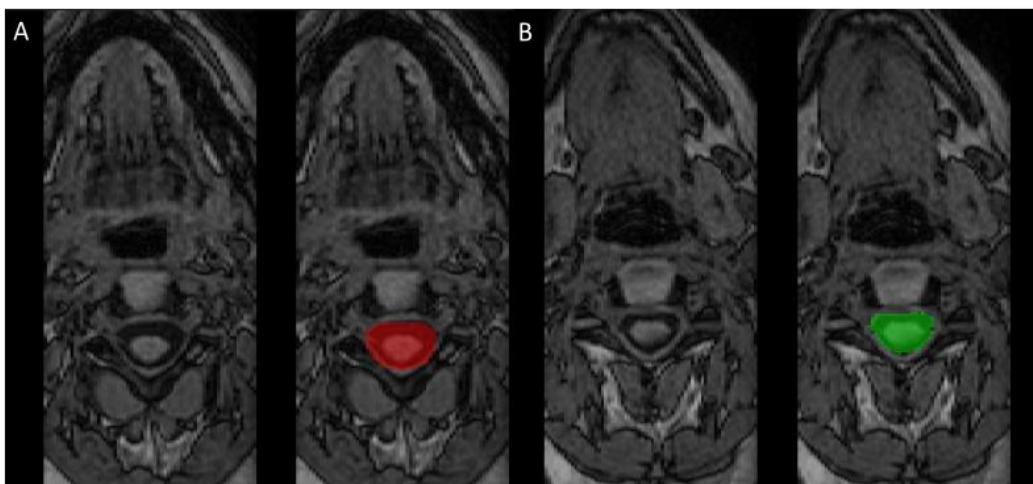


**Figure 12.** Exemplary case. Qualitative differences in CCaA segmentation at C2/C3 intervertebral disc level (red) and at C3/C4 level (green). A: we observed an overestimation of the CCaA in the segmentation at this level. B: CCaA segmentation is more accurate at C3/C4 in the same subject. CCaA, cervical canal area.

## 7. Discussion

---

Generally, the assessment of spinal cord CSA or volume has relied on 3D T1WI owing to the high contrast between the spinal cord and CSF,<sup>117</sup> facilitating accurate delineation by automated or semi-automated segmentation softwares.<sup>115</sup> We also employed T1WI to segmentate the CCaA for the first two studies in this thesis. However, we acknowledge that the contrast between the CSF and the spinal canal structures (mainly the soft tissues and bone)<sup>110</sup> is remarkably poorer in T1WI. Conversely, other clinical MRI sequences commonly used in clinical practice,<sup>25</sup> such as 2D T1WI, T2WI, and STIR, offer improved image contrast between these compartments, although their utility has not been studied yet in this field.

In this context, we designed the third study to assess the performance of our validated pipeline for measuring the CCaA using non-volumetric spinal cord sequences as an alternative to the brain sagittal 3D T1WI. We observed an excellent degree of overlap when comparing manual and semi-automated CCaA masks obtained from cervical T2WI and STIR acquisitions. Furthermore, we obtained good consistency ICCs when comparing CCaA segmentations from cervical cord T2WI and STIR sequences against brain 3D T1WI. Clinically, progressive MS patients also displayed a significantly smaller CCaA, and there was a significant negative correlation between CCaA and EDSS score, particularly when using T2WI.

We could not obtain CCaA estimations from cervical 2D T1WI. We hypothesized that the pipeline failed to localize different structures due to the low contrast between the CSF and the surrounding tissues. An important step in the image processing is the segmentation of the cervical cord using the *DeepSeg* algorithm of the SCT. Indeed, this step failed in almost all subjects. Therefore, volumetric acquisitions seem to be required to estimate the CCaA from T1WI.

Conversely, we did obtain CCaA measurements derived from T2WI and STIR sequences. To validate the segmentations, we compared the CCaA-SCT and CCaA-GT masks through the DSC, obtaining an excellent degree of overlap with the masks derived from both acquisitions. A higher contrast between the CSF and other structures allows a valid and consistent segmentation of the spinal canal even when the MRI sequences are not isotropic. However, as CCaA was conducted using the axial reconstructions from the original sagittal acquisitions, the resulting axial images showed poor resolution. Several AI tools are currently being explored as potential solutions to generate T1-like contrast images and high isotropic resolution from any type of MRI contrast or orientation.<sup>178</sup>

Regarding the absolute values of the CCaA obtained with the different sequences, those from the brain 3D T1WI are fully in line with the previously reported spinal canal areas at the

## 7. Discussion

---

two explored intervertebral disc levels.<sup>111,160</sup> However, CCaA measurements from T2WI and STIR sequences are substantially larger (Table 10), as indicated by the low absolute ICCs (Table 9). Interestingly, consistency ICCs between the T2WI and STIR sequences and brain 3D T1WI are good, suggesting a systematic rather than a random or unpredictable difference.<sup>165</sup> Therefore, while there is good agreement among CCaA estimated from different sequences, their absolute measures are not interchangeable when exploring the spinal cord reserve. We attribute these systematic differences to the fact that the spinal canal template used to segmentate the CCaA is not the same when using T1WI or T2WI, as these two sequences are weighted towards different aspects of tissue composition. Another factor may be that brain acquisitions are volumetric, while T2WI and STIR sequences tested are not. However, in an exploratory analysis, we artificially modified the voxel size of brain acquisitions to make them non-isotropic (1x1x3 mm<sup>3</sup>), and subsequent CCaA estimations did not differ from the original ones (data not shown).

As a secondary aim, to further test the clinical validity of the present findings, we explored the usefulness of the different MRI sequences to assess the spinal cord reserve. Progressive MS patients displayed a significantly smaller CCaA compared to relapsing patients, adjusted for age, sex, and SCPF when using CCaA derived from T2WI at the C3/C4 level. This suggests that a smaller spinal canal, and thus a lower spinal cord reserve, might be a feature of progressive MS, consistent with observations in the second project. In addition, CCaA measurements appeared to be correlated with the EDSS score, supporting the role of CCaA as a proxy for spinal cord reserve, so that a larger CCaA seems to be a protective factor against physical disability in MS.<sup>160</sup> We observed similar trends when using the other sequences and repeating the analyses at the C2/C3 level, although the results did not reach significance.

As previously reported, ICCs and correlation results are stronger when investigated at the C3/C4 in comparison to the C2/C3 intervertebral disc level. Again, we attributed these differences to the anatomical variations of the spinal canal along its length,<sup>111,127</sup> particularly in the cervical region.

The output of the pipeline included the mean cross-sectional area of the spinal canal from C2 to C5 (Figure 13). The described cervical canal area variations are more evident when exploring the spinal canal using T2WI and STIR sequences. In contrast, the spinal canal variations outlined with the brain acquisition appeared to continue decreasing below the C3/C4 level. These findings underscore the importance of selecting appropriate vertebral levels and imaging sequences for accurate measurement of the CCaA.

## 7. Discussion

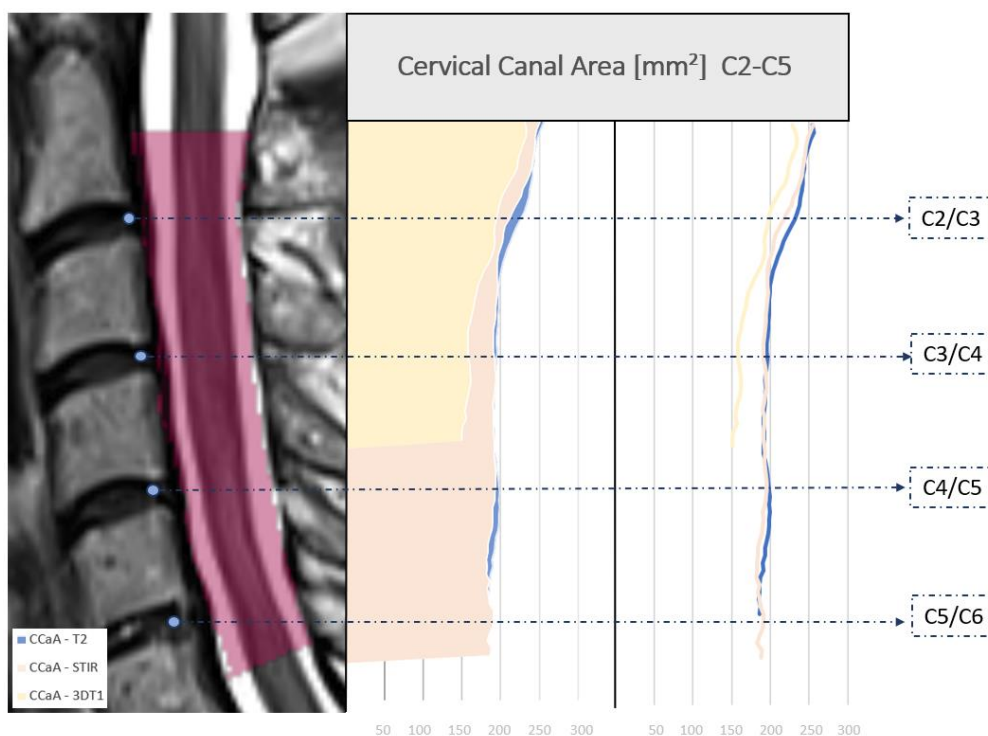


**Figure 13.** Mean cross-sectional area and sagittal profile of the spinal canal from C2 to C5 in cervical cord 2D T2WI, STIR, and brain 3D T1WI (sagittal profile extends to the lowest point of C4, shown in yellow). The figure includes a cervical cord T2WI. T1WI, T1-weighted image; T2WI, T2-weighted image; STIR, short-tau inversion recovery.

Taken together, these results demonstrated that our in-house built semi-automated segmentation pipeline has proven to provide reliable and reproducible CCA measures from brain and cervical cord 3D T1WI, as well as from cervical cord 2D T2WI and STIR sequences. While the absolute mean values across these sequences differ significantly, they are statistically associated. However, CCA estimations from the different sequences are not interchangeable. Conversely, since the tool has also proven accurate with non-volumetric MRI sequences, it could potentially be used in clinical settings to estimate individual spinal cord reserve during the evaluation of a pwMS.

In the statistical analysis of CCA, we found overlapping but not identical results when exploring the spinal canal in different MRI acquisitions and at different intervertebral disc levels. At the C2/C3 level, CCA estimations derived from both brain and cervical cord MRIs do not appear to be clinically different. In contrast, at the C3/C4 level, CCA from brain MRI tends to be underestimated compared to measures from dedicated cervical cord MRIs. This discrepancy is likely due to the fact that lower cervical levels in brain MRIs are located at the

## 7. Discussion

---

periphery of the FOV, where gradient nonlinearity effects are substantial,<sup>171</sup> leading to an underestimation of the CCaA in this acquisition. Although it is possible to reliably measure the cervical cord area and CCaA using brain acquisitions,<sup>168</sup> we recommend dedicated cervical cord MRI when analysing the CCaA at the C3/C4 level.

In addition, we did not consider estimating the CCaA in lower intervertebral disc levels even in cervical cord acquisitions. As it is reported in the literature,<sup>179,180</sup> degenerative cervical pathology and cervical disc herniations mostly occurred in the lower segments of the cervical column, being more commonly observed at C5/C6 level. Consequently, assessing the CCaA below the C5 intervertebral level could lead to underestimations of the real spinal canal area.

Clinically, we found intriguing results across MS phenotypes regarding CCaA measurements. HC and relapsing pwMS did not show significant differences in CCaA measures, suggesting that CCaA may indeed reflect the premorbid status of the spinal cord. However, a consistent trend emerged when analysing progressive MS: subjects with smaller CCaA measurements were associated with progressive forms of the disease. This suggests that a smaller CCaA may serve as a non-modifiable risk factor, potentially contributing, in conjunction with other factors, to the development of a progressive phenotype. Furthermore, we consistently observed a significant negative correlation between the CCaA and the EDSS score, both in cervical cord 3D T1WI and 2D T2WI. Besides, pwMS who experienced disability progression at 5-year follow-up displayed smaller CCaA at baseline MRI. All of these findings collectively represent the underpinnings of spinal cord reserve, wherein the CCaA arises as a reliable surrogate marker with an impact on physical disability, particularly in relation to the ambulatory function in MS, and disability progression throughout the disease course.

Overall, the current thesis contributes to the forefront of research by providing foundational evidence that supports the existence of a spinal cord reserve in MS. We have uncovered interesting associations between the spinal canal area, MS phenotypes, and disability. Furthermore, we believe that the spinal cord reserve may represent a novel radiological feature to better understand physical disability development, and its role might be further extended to other neurological disorders.

The three studies that comprise this thesis, along with the aforementioned results, share certain limitations that should be considered in the interpretation of the findings. Firstly, our pipeline entails manual labelling of the C2/C3 and C3/C4 intervertebral disc levels, which substantially increases processing times, especially in larger cohorts, compared to a fully

## 7. Discussion

---

automated segmentation process. Nonetheless, this operator intervention ensures meticulous delineation of levels and facilitates rigorous quality assessment of MRI data.

Another shared limitation lies in the retrospective design of all three studies. This aspect is particularly relevant when analysing the association between CCaA and clinical outcomes, primarily EDSS scores and disability progression. Retrospective designs inherently possess limitations in establishing causality or temporal relationships. Therefore, a prospective design, coupled with longer follow-up times, is warranted to better elucidate the impact of spinal cord reserve on disability.

Furthermore, it is important to note that both methodological studies, including the validation of the pipeline and the CCaA estimation in different MRI sequences, featured relatively small sample sizes, which may account for the variability observed in the range of ICCs obtained. Increasing the sample size will improve the reliability and robustness of these methodological approaches.

Lastly, progressive patients were generally older across our studies, had longer disease duration, and exhibited a narrower range of EDSS scores. Addressing such biases in future investigations is paramount for a more nuanced comprehension of the role of CCaA in this specific patient cohort. Besides, further studies are needed to establish the difference in CCaA among SPMS and PPMS patients.



## **8. CONCLUSIONS**

## 8. Conclusions

---

The main conclusions of this thesis are:

1. Our segmentation pipeline based on the SCT provides reproducible and reliable CCaA estimations from both brain and cervical cord 3D T1WI. Therefore, brain CCaA estimations might be considered to assess spinal cord reserve when dedicated cervical sequences are not available.
2. Progressive MS patients exhibited a smaller CCaA, suggesting that a lower spinal cord reserve might be a feature of progressive MS phenotype.
3. CCaA was associated to EDSS, using spinal cord acquisitions and a longitudinal follow-up, which confirms the possible existence of a spinal cord reserve.
4. CCaA segmentation is feasible on 2D sagittal T2WI and STIR, showing a good equivalence to volumetric brain T1WI. This potentially facilitates the estimation of individual spinal cord reserve in a clinical setting.

## **9. FUTURE LINES OF RESEARCH**

## 9. Future lines of research

---

As discussed in previous sections of this thesis, the analysis of individual MRI metrics, such as volume loss or lesion burden, does not fully account for disability in MS. A relevant factor that contributes to explaining the different disease trajectories over time in pwMS is the concept of reserve. This is understood as the capacity to maintain functionality despite disease, serving as an indirect marker of the remaining functionally intact neurons after pathological insults.

Considerable research in the existing literature has focused on brain reserve and cognitive reserve in MS. Additionally, the concepts of physical reserve and lifelong enrichment are being explored. Within this context, we have built the current thesis to establish the methodological and clinical basis for spinal cord reserve in MS.

Overall, different types of reserve are being investigated independently, yet there is a lack of a holistic perspective to assess cognitive and physical disability in MS. Therefore, we advocate for a paradigm shift toward a more comprehensive understanding by considering both brain and spinal cord perspectives as structural reserves, and cognitive and physical perspectives as functional reserves. Collectively, the integrated combination of these four types of reserve will constitute the CNS reserve. This new conceptual framework will open a window in research, broadening the field of disability in MS. It will offer new perspectives and approaches to better understand this complex disease, potentially leading to more effective strategies for assessing and managing disability in pwMS. By considering the interplay between brain, spinal cord, cognitive, and physical reserves, researchers and clinicians can develop a deeper understanding of how MS affects individuals differently and tailor interventions to maintain and improve quality of life for pwMS.





## **10. BIBLIOGRAPHY**

## 10. Bibliography

---

1. Thompson AJ, Baranzini SE, Geurts J, Hemmer B, Ciccarelli O. Multiple sclerosis. *Lancet*. 2018;391(10130):1622-1636. doi:10.1016/S0140-6736(18)30481-1
2. Walton C, King R, Rechtman L, et al. Rising prevalence of multiple sclerosis worldwide: Insights from the Atlas of MS, third edition. *Mult Scler J*. 2020;26(14):1816-1821. doi:10.1177/1352458520970841
3. Sawcer S, Franklin RJM, Ban M. Multiple sclerosis genetics. *Lancet Neurol*. 2014;13(7):700-709. doi:10.1016/S1474-4422(14)70041-9
4. Olsson T, Barcellos LF, Alfredsson L. Interactions between genetic, lifestyle and environmental risk factors for multiple sclerosis. *Nat Rev Neurol*. 2017;13(1):25-36. doi:10.1038/nrneurol.2016.187
5. Bjornevik K, Münz C, Cohen JI, Ascherio A. Epstein–Barr virus as a leading cause of multiple sclerosis: mechanisms and implications. *Nat Rev Neurol*. 2023;19(3):160-171. doi:10.1038/s41582-023-00775-5
6. Degenhardt A, Ramagopalan S V., Scalfari A, Ebers GC. Clinical prognostic factors in multiple sclerosis: a natural history review. *Nat Rev Neurol*. 2009;5(12):672-682. doi:10.1038/nrneurol.2009.178
7. Tintore M, Rovira À, Río J, et al. Defining high, medium and low impact prognostic factors for developing multiple sclerosis. *Brain*. 2015;138(7):1863-1874. doi:10.1093/brain/awv105
8. Ramanujam R, Hedström A-K, Manouchehrinia A, et al. Effect of Smoking Cessation on Multiple Sclerosis Prognosis. *JAMA Neurol*. 2015;72(10):1117. doi:10.1001/jamaneurol.2015.1788
9. Cobo-Calvo A, Tur C, Otero-Romero S, et al. Association of Very Early Treatment Initiation With the Risk of Long-term Disability in Patients With a First Demyelinating Event. *Neurology*. 2023;101(13). doi:10.1212/WNL.0000000000207664
10. Harroud A, Stridh P, McCauley JL, et al. Locus for severity implicates CNS resilience in progression of multiple sclerosis. *Nature*. 2023;619(7969):323-331. doi:10.1038/s41586-023-06250-x
11. Filippi M, Brück W, Chard D, et al. Association between pathological and MRI findings in multiple sclerosis. *Lancet Neurol*. 2019;18(2):198-210. doi:10.1016/S1474-4422(18)30451-4
12. Dobson R, Giovannoni G. Multiple sclerosis – a review. *Eur J Neurol*. 2019;26(1):27-40. doi:10.1111/ene.13819
13. Lassmann H. Pathology and disease mechanisms in different stages of multiple sclerosis. *J Neurol Sci*. 2013;333(1-2):1-4. doi:10.1016/j.jns.2013.05.010
14. Hemmer B, Kerschensteiner M, Korn T. Role of the innate and adaptive immune responses in the course of multiple sclerosis. *Lancet Neurol*. 2015;14(4):406-419. doi:10.1016/S1474-4422(14)70305-9
15. Tomassini V, Matthews PM, Thompson AJ, et al. Neuroplasticity and functional recovery in multiple sclerosis. *Nat Rev Neurol*. 2012;8(11):635-646. doi:10.1038/nrneurol.2012.179
16. Irvine KA, Blakemore WF. Remyelination protects axons from demyelination-associated axon degeneration. *Brain*. 2008;131(6):1464-1477. doi:10.1093/brain/awn080
17. Giovannoni G, Popescu V, Wuerfel J, et al. Smouldering multiple sclerosis: the ‘real MS.’ *Ther Adv Neurol Disord*. 2022;15:175628642110667. doi:10.1177/17562864211066751
18. Sastre-Garriga J, Pareto D, Battaglini M, et al. MAGNIMS consensus recommendations on the use of brain and spinal cord atrophy measures in clinical practice. *Nat Rev Neurol*.



## 10. Bibliography

---

- 2020;16(3):171-182. doi:10.1038/s41582-020-0314-x
19. Vercellino M, Plano F, Votta B, Mutani R, Giordana MT, Cavalla P. Grey Matter Pathology in Multiple Sclerosis. *J Neuropathol Exp Neurol*. 2005;64(12):1101-1107. doi:10.1097/01.jnen.0000190067.20935.42
  20. Kappos L, Wolinsky JS, Giovannoni G, et al. Contribution of Relapse-Independent Progression vs Relapse-Associated Worsening to Overall Confirmed Disability Accumulation in Typical Relapsing Multiple Sclerosis in a Pooled Analysis of 2 Randomized Clinical Trials. *JAMA Neurol*. 2020;77(9):1132. doi:10.1001/jamaneurol.2020.1568
  21. Tur C, Carbonell-Mirabent P, Cobo-Calvo Á, et al. Association of Early Progression Independent of Relapse Activity With Long-term Disability After a First Demyelinating Event in Multiple Sclerosis. *JAMA Neurol*. 2023;80(2):151. doi:10.1001/jamaneurol.2022.4655
  22. Chen B, Ji S-Q, Shen F, Tian D-S, Bu B-T. Contribution of relapse-associated worsening to overall disability accrual in patients with relapsing-onset multiple sclerosis: A mediation analysis. *Mult Scler Relat Disord*. 2022;59:103555. doi:10.1016/j.msard.2022.103555
  23. Haider L, Zrzavy T, Hametner S, et al. The topography of demyelination and neurodegeneration in the multiple sclerosis brain. *Brain*. 2016;139(3):807-815. doi:10.1093/brain/awv398
  24. Traboulsee A, Simon JH, Stone L, et al. Revised Recommendations of the Consortium of MS Centers Task Force for a Standardized MRI Protocol and Clinical Guidelines for the Diagnosis and Follow-Up of Multiple Sclerosis. *Am J Neuroradiol*. 2016;37(3):394-401. doi:10.3174/ajnr.A4539
  25. Wattjes MP, Ciccarelli O, Reich DS, et al. 2021 MAGNIMS–CMSC–NAIMS consensus recommendations on the use of MRI in patients with multiple sclerosis. *Lancet Neurol*. 2021;20(8):653-670. doi:10.1016/S1474-4422(21)00095-8
  26. Schumacher GA, Beebe G, Kibler RF, et al. PROBLEMS OF EXPERIMENTAL TRIALS OF THERAPY IN MULTIPLE SCLEROSIS: REPORT BY THE PANEL ON THE EVALUATION OF EXPERIMENTAL TRIALS OF THERAPY IN MULTIPLE SCLEROSIS. *Ann N Y Acad Sci*. 1965;122(1):552-568. doi:10.1111/j.1749-6632.1965.tb20235.x
  27. Barkhof F. Comparison of MRI criteria at first presentation to predict conversion to clinically definite multiple sclerosis. *Brain*. 1997;120(11):2059-2069. doi:10.1093/brain/120.11.2059
  28. Tintoré M, Rovira A, Martínez MJ, et al. Isolated demyelinating syndromes: comparison of different MR imaging criteria to predict conversion to clinically definite multiple sclerosis. *AJNR Am J Neuroradiol*. 2000;21(4):702-706. <http://www.ncbi.nlm.nih.gov/pubmed/10782781>
  29. Thompson AJ, Banwell BL, Barkhof F, et al. Diagnosis of multiple sclerosis: 2017 revisions of the McDonald criteria. *Lancet Neurol*. 2018;17(2):162-173. doi:10.1016/S1474-4422(17)30470-2
  30. Polman CH, Reingold SC, Banwell B, et al. Diagnostic criteria for multiple sclerosis: 2010 Revisions to the McDonald criteria. *Ann Neurol*. 2011;69(2):292-302. doi:10.1002/ana.22366
  31. Weier K, Mazraeh J, Naegelin Y, et al. Biplanar MRI for the assessment of the spinal cord in multiple sclerosis. *Mult Scler J*. 2012;18(11):1560-1569. doi:10.1177/1352458512442754
  32. Vidal-Jordana A, Rovira A, Calderon W, et al. Adding the Optic Nerve in Multiple Sclerosis Diagnostic Criteria. *Neurology*. 2024;102(1). doi:10.1212/WNL.0000000000207805
  33. Brownlee WJ, Miszkiel KA, Tur C, Barkhof F, Miller DH, Ciccarelli O. Inclusion of optic nerve involvement in dissemination in space criteria for multiple sclerosis. *Neurology*. 2018;91(12). doi:10.1212/WNL.0000000000006207
  34. Sriwastava S, Kataria S, Srivastava S, et al. Disease-modifying therapies and progressive

## 10. Bibliography

---

- multifocal leukoencephalopathy in multiple sclerosis: A systematic review and meta-analysis. *J Neuroimmunol.* 2021;360:577721. doi:10.1016/j.jneuroim.2021.577721
35. Krämer J, Brück W, Zipp F, Cerina M, Groppa S, Meuth SG. Imaging in mice and men: Pathophysiological insights into multiple sclerosis from conventional and advanced MRI techniques. *Prog Neurobiol.* 2019;182:101663. doi:10.1016/j.pneurobio.2019.101663
  36. Filippi M, Preziosa P, Banwell BL, et al. Assessment of lesions on magnetic resonance imaging in multiple sclerosis: practical guidelines. *Brain.* 2019;142(7):1858-1875. doi:10.1093/brain/awz144
  37. Granziera C, Wuerfel J, Barkhof F, et al. Quantitative magnetic resonance imaging towards clinical application in multiple sclerosis. *Brain.* 2021;144(5):1296-1311. doi:10.1093/brain/awab029
  38. Filippi M, Preziosa P, Langdon D, et al. Identifying Progression in Multiple Sclerosis: New Perspectives. *Ann Neurol.* 2020;88(3):438-452. doi:10.1002/ana.25808
  39. Kalincik T, Cutter G, Spelman T, et al. Defining reliable disability outcomes in multiple sclerosis. *Brain.* 2015;138(11):3287-3298. doi:10.1093/brain/awv258
  40. Inojosa H, Proschmann U, Akgün K, Ziemssen T. A focus on secondary progressive multiple sclerosis (SPMS): challenges in diagnosis and definition. *J Neurol.* 2021;268(4):1210-1221. doi:10.1007/s00415-019-09489-5
  41. Meyer-Moock S, Feng Y-S, Maeurer M, Dippel F-W, Kohlmann T. Systematic literature review and validity evaluation of the Expanded Disability Status Scale (EDSS) and the Multiple Sclerosis Functional Composite (MSFC) in patients with multiple sclerosis. *BMC Neurol.* 2014;14(1):58. doi:10.1186/1471-2377-14-58
  42. Noseworthy JH, Vandervoort MK, Wong CJ, Ebers GC. Interrater variability with the Expanded Disability Status Scale (EDSS) and Functional Systems (FS) in a multiple sclerosis clinical trial. *Neurology.* 1990;40(6):971-971. doi:10.1212/WNL.40.6.971
  43. Hutchinson J, Hutchinson M. The functional limitations profile may be a valid, reliable and sensitive measure of disability in multiple sclerosis. *J Neurol.* 1995;242(10):650-657. doi:10.1007/BF00866915
  44. Lorscheider J, Buzzard K, Jokubaitis V, et al. Defining secondary progressive multiple sclerosis. *Brain.* 2016;139(9):2395-2405. doi:10.1093/brain/aww173
  45. Cutter GR. Development of a multiple sclerosis functional composite as a clinical trial outcome measure. *Brain.* 1999;122(5):871-882. doi:10.1093/brain/122.5.871
  46. Brochet B, Deloire M, Bonnet M, et al. Should SDMT substitute for PASAT in MSFC? A 5-year longitudinal study. *Mult Scler J.* 2008;14(9):1242-1249. doi:10.1177/1352458508094398
  47. Bin Sawad A, Seoane-Vazquez E, Rodriguez-Monguio R, Turkistani F. Evaluation of the Expanded Disability Status Scale and the Multiple Sclerosis Functional Composite as clinical endpoints in multiple sclerosis clinical trials: quantitative meta-analyses. *Curr Med Res Opin.* 2016;32(12):1969-1974. doi:10.1080/03007995.2016.1222516
  48. Lerede A, Rodgers J, Middleton RM, et al. Patient-reported outcomes in multiple sclerosis: a prospective registry cohort study. *Brain Commun.* 2023;5(4). doi:10.1093/braincomms/fcad199
  49. McKenna SP. Measuring patient-reported outcomes: moving beyond misplaced common sense to hard science. *BMC Med.* 2011;9(1):86. doi:10.1186/1741-7015-9-86
  50. Bricchetto G, Zaratini P. Measuring outcomes that matter most to people with multiple sclerosis: the role of patient-reported outcomes. *Curr Opin Neurol.* 2020;33(3):295-299. doi:10.1097/WCO.0000000000000821

## 10. Bibliography

---

51. Midaglia Fernández L, Sastre Garriga J, Montalban Gairin X. Monitorización clínica del paciente con esclerosis múltiple a través de la tecnología digital, un campo en plena revolución. *Rev Neurol.* 2021;73(06):210. doi:10.33588/rn.7306.2021136
52. Flachenecker F, Gaßner H, Hannik J, et al. Objective sensor-based gait measures reflect motor impairment in multiple sclerosis patients: Reliability and clinical validation of a wearable sensor device. *Mult Scler Relat Disord.* 2020;39:101903. doi:10.1016/j.msard.2019.101903
53. Montalban X, Graves J, Midaglia L, et al. A smartphone sensor-based digital outcome assessment of multiple sclerosis. *Mult Scler J.* 2022;28(4):654-664. doi:10.1177/13524585211028561
54. Sahraian MA, Radue E-W, Haller S, Kappos L. Black holes in multiple sclerosis: definition, evolution, and clinical correlations. *Acta Neurol Scand.* 2010;122(1):1-8. doi:10.1111/j.1600-0404.2009.01221.x
55. Tam R, Traboulsee A, Riddehough A, Sheikhzadeh F, DKB Li. The impact of intensity variations in T1-hypointense lesions on clinical correlations in multiple sclerosis. *Mult Scler J.* 2011;17(8):949-957. doi:10.1177/1352458511402113
56. Giorgio A, Stromillo ML, Bartolozzi ML, et al. Relevance of hypointense brain MRI lesions for long-term worsening of clinical disability in relapsing multiple sclerosis. *Mult Scler J.* 2014;20(2):214-219. doi:10.1177/1352458513494490
57. Rocca MA, Comi G, Filippi M. The Role of T1-Weighted Derived Measures of Neurodegeneration for Assessing Disability Progression in Multiple Sclerosis. *Front Neurol.* 2017;8. doi:10.3389/fneur.2017.00433
58. Kerbrat A, Gros C, Badji A, et al. Multiple sclerosis lesions in motor tracts from brain to cervical cord: spatial distribution and correlation with disability. *Brain.* 2020;143(7):2089-2105. doi:10.1093/brain/awaa162
59. Healy BC, Buckle GJ, Ali EN, et al. Characterizing Clinical and MRI Dissociation in Patients with Multiple Sclerosis. *J Neuroimaging.* 2017;27(5):481-485. doi:10.1111/jon.12433
60. Lublin FD, Reingold SC, Cohen JA, et al. Defining the clinical course of multiple sclerosis. *Neurology.* 2014;83(3):278-286. doi:10.1212/WNL.0000000000000560
61. Tintore M, Rovira A, Arrambide G, et al. Brainstem lesions in clinically isolated syndromes. *Neurology.* 2010;75(21):1933-1938. doi:10.1212/WNL.0b013e3181feb26f
62. Arrambide G, Rovira A, Sastre-Garriga J, et al. Spinal cord lesions: A modest contributor to diagnosis in clinically isolated syndromes but a relevant prognostic factor. *Mult Scler J.* 2018;24(3):301-312. doi:10.1177/1352458517697830
63. Brownlee WJ, Altmann DR, Prados F, et al. Early imaging predictors of long-term outcomes in relapse-onset multiple sclerosis. *Brain.* 2019;142(8):2276-2287. doi:10.1093/brain/awz156
64. Elliott C, Wolinsky JS, Hauser SL, et al. Slowly expanding/evolving lesions as a magnetic resonance imaging marker of chronic active multiple sclerosis lesions. *Mult Scler J.* 2019;25(14):1915-1925. doi:10.1177/1352458518814117
65. Kuhlmann T, Ludwin S, Prat A, Antel J, Brück W, Lassmann H. An updated histological classification system for multiple sclerosis lesions. *Acta Neuropathol.* 2017;133(1):13-24. doi:10.1007/s00401-016-1653-y
66. Calvi A, Carrasco FP, Tur C, et al. Association of Slowly Expanding Lesions on MRI With Disability in People With Secondary Progressive Multiple Sclerosis. *Neurology.* 2022;98(17). doi:10.1212/WNL.0000000000200144
67. Elliott C, Belachew S, Wolinsky JS, et al. Chronic white matter lesion activity predicts clinical progression in primary progressive multiple sclerosis. *Brain.* 2019;142(9):2787-2799.

## 10. Bibliography

---

- doi:10.1093/brain/awz212
68. Absinta M, Sati P, Masuzzo F, et al. Association of Chronic Active Multiple Sclerosis Lesions With Disability In Vivo. *JAMA Neurol.* 2019;76(12):1474. doi:10.1001/jamaneurol.2019.2399
  69. Hametner S, Wimmer I, Haider L, Pfeifenbring S, Brück W, Lassmann H. Iron and neurodegeneration in the multiple sclerosis brain. *Ann Neurol.* 2013;74(6):848-861. doi:10.1002/ana.23974
  70. Yao B, Ikonomidou VN, Cantor FK, Ohayon JM, Duyn J, Bagnato F. Heterogeneity of Multiple Sclerosis White Matter Lesions Detected With T2\*-Weighted Imaging at 7.0 Tesla. *J Neuroimaging.* 2015;25(5):799-806. doi:10.1111/jon.12193
  71. Clarke MA, Pareto D, Pessini-Ferreira L, et al. Value of 3T Susceptibility-Weighted Imaging in the Diagnosis of Multiple Sclerosis. *Am J Neuroradiol.* 2020;41(6):1001-1008. doi:10.3174/ajnr.A6547
  72. Zhang Y, Gauthier SA, Gupta A, et al. Quantitative Susceptibility Mapping and R2\* Measured Changes during White Matter Lesion Development in Multiple Sclerosis: Myelin Breakdown, Myelin Debris Degradation and Removal, and Iron Accumulation. *Am J Neuroradiol.* 2016;37(9):1629-1635. doi:10.3174/ajnr.A4825
  73. Dal-Bianco A, Grabner G, Kronnerwetter C, et al. Long-term evolution of multiple sclerosis iron rim lesions in 7 T MRI. *Brain.* 2021;144(3):833-847. doi:10.1093/brain/awaa436
  74. Meaton I, Altokhis A, Allen CM, et al. Paramagnetic rims are a promising diagnostic imaging biomarker in multiple sclerosis. *Mult Scler J.* 2022;28(14):2212-2220. doi:10.1177/13524585221118677
  75. Calvi A, Clarke MA, Prados F, et al. Relationship between paramagnetic rim lesions and slowly expanding lesions in multiple sclerosis. *Mult Scler J.* 2023;29(3):352-362. doi:10.1177/13524585221141964
  76. Maggi P, Kuhle J, Schädelin S, et al. Chronic White Matter Inflammation and Serum Neurofilament Levels in Multiple Sclerosis. *Neurology.* 2021;97(6). doi:10.1212/WNL.0000000000012326
  77. Calabrese M, Filippi M, Gallo P. Cortical lesions in multiple sclerosis. *Nat Rev Neurol.* 2010;6(8):438-444. doi:10.1038/nrneurol.2010.93
  78. Filippi M, Rocca MA. Cortical Lesions on 7-T MRI in Multiple Sclerosis: A Window into Pathogenetic Mechanisms? *Radiology.* 2019;291(3):750-751. doi:10.1148/radiol.2019190398
  79. Filippi M, Rocca MA, Calabrese M, et al. Intracortical lesions. *Neurology.* 2010;75(22):1988-1994. doi:10.1212/WNL.0b013e3181ff96f6
  80. Calabrese M, Poretto V, Favaretto A, et al. Cortical lesion load associates with progression of disability in multiple sclerosis. *Brain.* 2012;135(10):2952-2961. doi:10.1093/brain/awz246
  81. Eden D, Gros C, Badji A, et al. Spatial distribution of multiple sclerosis lesions in the cervical spinal cord. *Brain.* 2019;142(3):633-646. doi:10.1093/brain/awy352
  82. Ouellette R, Treaba CA, Granberg T, et al. 7 T imaging reveals a gradient in spinal cord lesion distribution in multiple sclerosis. *Brain.* 2020;143(10):2973-2987. doi:10.1093/brain/awaa249
  83. Andorra M, Nakamura K, Lampert EJ, et al. Assessing Biological and Methodological Aspects of Brain Volume Loss in Multiple Sclerosis. *JAMA Neurol.* 2018;75(10):1246. doi:10.1001/jamaneurol.2018.1596
  84. Miller DH. Measurement of atrophy in multiple sclerosis: pathological basis, methodological aspects and clinical relevance. *Brain.* 2002;125(8):1676-1695. doi:10.1093/brain/awf177
  85. Azevedo CJ, Pelletier D. Whole-brain atrophy. *Curr Opin Neurol.* 2016;29(3):237-242.

## 10. Bibliography

---

- doi:10.1097/WCO.0000000000000322
86. Losseff NA, Wang L, Lai HM, et al. Progressive cerebral atrophy in multiple sclerosis A serial MRI study. *Brain*. 1996;119(6):2009-2019. doi:10.1093/brain/119.6.2009
  87. van Waesberghe JH, van Walderveen MA, Castelijns JA, et al. Patterns of lesion development in multiple sclerosis: longitudinal observations with T1-weighted spin-echo and magnetization transfer MR. *AJNR Am J Neuroradiol*. 1998;19(4):675-683. <http://www.ncbi.nlm.nih.gov/pubmed/9576653>
  88. Rudick RA, Fisher E, Lee J-C, Simon J, Jacobs L. Use of the brain parenchymal fraction to measure whole brain atrophy in relapsing-remitting MS. *Neurology*. 1999;53(8):1698-1698. doi:10.1212/WNL.53.8.1698
  89. Gau K, Schmidt CSM, Urbach H, et al. Accuracy and practical aspects of semi- and fully automatic segmentation methods for resected brain areas. *Neuroradiology*. 2020;62(12):1637-1648. doi:10.1007/s00234-020-02481-1
  90. Vrenken H, Jenkinson M, Horsfield MA, et al. Recommendations to improve imaging and analysis of brain lesion load and atrophy in longitudinal studies of multiple sclerosis. *J Neurol*. 2013;260(10):2458-2471. doi:10.1007/s00415-012-6762-5
  91. Smith SM, Zhang Y, Jenkinson M, et al. Accurate, Robust, and Automated Longitudinal and Cross-Sectional Brain Change Analysis. *Neuroimage*. 2002;17(1):479-489. doi:10.1006/nimg.2002.1040
  92. Rocca MA, Battaglini M, Benedict RHB, et al. Brain MRI atrophy quantification in MS. *Neurology*. 2017;88(4):403-413. doi:10.1212/WNL.0000000000003542
  93. Wahl M, Hübers A, Lauterbach-Soon B, et al. Motor callosal disconnection in early relapsing-remitting multiple sclerosis. *Hum Brain Mapp*. 2011;32(6):846-855. doi:10.1002/hbm.21071
  94. Delgado AF, Delgado AF. Neuroimaging lesion assessment by pseudo-subtraction of overlaid semi-transparent volumes: A technical description and feasibility series. *Neuroradiol J*. 2021;34(2):128-130. doi:10.1177/1971400920975730
  95. Ontaneda D, Raza PC, Mahajan KR, et al. Deep grey matter injury in multiple sclerosis: a NAIMS consensus statement. *Brain*. 2021;144(7):1974-1984. doi:10.1093/brain/awab132
  96. Pérez-Miralles FC, Sastre-Garriga J, Vidal-Jordana A, et al. Predictive value of early brain atrophy on response in patients treated with interferon  $\beta$ . *Neurol Neuroimmunol Neuroinflammation*. 2015;2(4). doi:10.1212/NXI.0000000000000132
  97. Vollmer T, Signorovitch J, Huynh L, et al. The natural history of brain volume loss among patients with multiple sclerosis: A systematic literature review and meta-analysis. *J Neurol Sci*. 2015;357(1-2):8-18. doi:10.1016/j.jns.2015.07.014
  98. Pérez-Miralles F, Sastre-Garriga J, Tintoré M, et al. Clinical impact of early brain atrophy in clinically isolated syndromes. *Mult Scler J*. 2013;19(14):1878-1886. doi:10.1177/1352458513488231
  99. Sastre-Garriga J, Ingle GT, Chard DT, et al. Grey and white matter volume changes in early primary progressive multiple sclerosis: a longitudinal study. *Brain*. 2005;128(6):1454-1460. doi:10.1093/brain/awh498
  100. Rao SM, Leo GJ, Houghton VM, Aubin-Faubert P St., Bernardin L. Correlation of magnetic resonance imaging with neuropsychological testing in multiple sclerosis. *Neurology*. 1989;39(2):161-161. doi:10.1212/WNL.39.2.161
  101. Radü E, Bendfeldt K, Mueller-Lenke N, Magon S, Sprenger T. Brain atrophy: an in-vivo measure of disease activity in multiple sclerosis. *Swiss Med Wkly*. Published online November 21, 2013. doi:10.4414/smw.2013.13887

## 10. Bibliography

---

102. Fisher E, Lee J, Nakamura K, Rudick RA. Gray matter atrophy in multiple sclerosis: A longitudinal study. *Ann Neurol*. 2008;64(3):255-265. doi:10.1002/ana.21436
103. Charil A, Dagher A, Lerch JP, Zijdenbos AP, Worsley KJ, Evans AC. Focal cortical atrophy in multiple sclerosis: Relation to lesion load and disability. *Neuroimage*. 2007;34(2):509-517. doi:10.1016/j.neuroimage.2006.10.006
104. Salat DH. Thinning of the Cerebral Cortex in Aging. *Cereb Cortex*. 2004;14(7):721-730. doi:10.1093/cercor/bhh032
105. Comi G, Dadon Y, Sasson N, et al. CONCERTO: A randomized, placebo-controlled trial of oral laquinimod in relapsing-remitting multiple sclerosis. *Mult Scler J*. 2022;28(4):608-619. doi:10.1177/13524585211032803
106. Chataway J, Schuerer N, Alsanousi A, et al. Effect of high-dose simvastatin on brain atrophy and disability in secondary progressive multiple sclerosis (MS-STAT): a randomised, placebo-controlled, phase 2 trial. *Lancet*. 2014;383(9936):2213-2221. doi:10.1016/S0140-6736(13)62242-4
107. Uher T, Krasensky J, Vaneckova M, et al. A Novel Semiautomated Pipeline to Measure Brain Atrophy and Lesion Burden in Multiple Sclerosis: A Long-Term Comparative Study. *J Neuroimaging*. 2017;27(6):620-629. doi:10.1111/jon.12445
108. Bican O, Minagar A, Pruitt AA. The Spinal Cord. *Neurol Clin*. 2013;31(1):1-18. doi:10.1016/j.ncl.2012.09.009
109. Ali F, Reddy V, Dublin AB. *Anatomy, Back, Anterior Spinal Artery.*; 2023. <http://www.ncbi.nlm.nih.gov/pubmed/28616230>
110. Longatti P, Fiorindi A, Marton E, Sala F, Feletti A. Where the central canal begins: endoscopic in vivo description. *J Neurosurg*. 2022;136(3):895-904. doi:10.3171/2020.12.JNS203649
111. Kato F, Yukawa Y, Suda K, Yamagata M, Ueta T. Normal morphology, age-related changes and abnormal findings of the cervical spine. Part II: Magnetic resonance imaging of over 1,200 asymptomatic subjects. *Eur Spine J*. 2012;21(8):1499-1507. doi:10.1007/s00586-012-2176-4
112. SASAKI T, KADOYA S, IIZUKA H. Roentgenological Study of the Sagittal Diameter of the Cervical Spinal Canal in Normal Adult Japanese. *Neurol Med Chir (Tokyo)*. 1998;38(2):83-89. doi:10.2176/nmc.38.83
113. Stroman PW, Wheeler-Kingshott C, Bacon M, et al. The current state-of-the-art of spinal cord imaging: Methods. *Neuroimage*. 2014;84:1070-1081. doi:10.1016/j.neuroimage.2013.04.124
114. Hakky M, Pandey S, Kwak E, Jara H, Erbay SH. Application of Basic Physics Principles to Clinical Neuroradiology: Differentiating Artifacts From True Pathology on MRI. *Am J Roentgenol*. 2013;201(2):369-377. doi:10.2214/AJR.12.10394
115. Casserly C, Seyman EE, Alcaide-Leon P, et al. Spinal Cord Atrophy in Multiple Sclerosis: A Systematic Review and Meta-Analysis. *J Neuroimaging*. 2018;28(6):556-586. doi:10.1111/jon.12553
116. Taheri K, Vavasour IM, Abel S, et al. Cervical Spinal Cord Atrophy can be Accurately Quantified Using Head Images. *Mult Scler J - Exp Transl Clin*. 2022;8(1):205521732110707. doi:10.1177/20552173211070760
117. Losseff NA, Webb SL, O’Riordan JI, et al. Spinal cord atrophy and disability in multiple sclerosis. *Brain*. 1996;119(3):701-708. doi:10.1093/brain/119.3.701
118. Amann M, Pezold S, Naegelin Y, et al. Reliable volumetry of the cervical spinal cord in MS patient follow-up data with cord image analyzer (Cordial). *J Neurol*. 2016;263(7):1364-1374. doi:10.1007/s00415-016-8133-0

## 10. Bibliography

---

119. Ashburner J, Hutton C, Frackowiak R, Johnsrude I, Price C, Friston K. Identifying global anatomical differences: deformation-based morphometry. *Hum Brain Mapp.* 1998;6(5-6):348-357. doi:10.1002/(SICI)1097-0193(1998)6:5/6<#x0003c;348::AID-HBM4<#x0003e;3.0.CO;2-P
120. De Leener B, Lévy S, Dupont SM, et al. SCT: Spinal Cord Toolbox, an open-source software for processing spinal cord MRI data. *Neuroimage.* 2017;145:24-43. doi:10.1016/j.neuroimage.2016.10.009
121. Sastre-Garriga J, Pareto D, Alberich M, et al. Spinal cord grey matter atrophy in Multiple Sclerosis clinical practice. *Neurosci Informatics.* 2022;2(2):100071. doi:10.1016/j.neuri.2022.100071
122. Prados F, Cardoso MJ, Yiannakas MC, et al. Fully automated grey and white matter spinal cord segmentation. *Sci Rep.* 2016;6(1):36151. doi:10.1038/srep36151
123. Tsagkas C, Horvath-Huck A, Haas T, et al. Fully Automatic Method for Reliable Spinal Cord Compartment Segmentation in Multiple Sclerosis. *Am J Neuroradiol.* 2023;44(2):218-227. doi:10.3174/ajnr.A7756
124. Schlaeger R, Papinutto N, Panara V, et al. Spinal cord gray matter atrophy correlates with multiple sclerosis disability. *Ann Neurol.* 2014;76(4):568-580. doi:10.1002/ana.24241
125. Papinutto N, Asteggiano C, Bischof A, et al. Intersubject Variability and Normalization Strategies for Spinal Cord Total Cross-Sectional and Gray Matter Areas. *J Neuroimaging.* 2020;30(1):110-118. doi:10.1111/jon.12666
126. Papinutto N, Schlaeger R, Panara V, et al. Age, Gender and Normalization Covariates for Spinal Cord Gray Matter and Total Cross-Sectional Areas at Cervical and Thoracic Levels: A 2D Phase Sensitive Inversion Recovery Imaging Study. Fehlings M, ed. *PLoS One.* 2015;10(3):e0118576. doi:10.1371/journal.pone.0118576
127. Nell C, Bülow R, Hosten N, Schmidt CO, Hegenscheid K. Reference values for the cervical spinal canal and the vertebral bodies by MRI in a general population. Espinoza Orías AA, ed. *PLoS One.* 2019;14(9):e0222682. doi:10.1371/journal.pone.0222682
128. Oh J, Seigo M, Saidha S, et al. Spinal Cord Normalization in Multiple Sclerosis. *J Neuroimaging.* 2014;24(6):577-584. doi:10.1111/jon.12097
129. Papinutto N, Schlaeger R, Panara V, et al. Age, gender and normalization covariates for spinal cord gray matter and total cross-sectional areas at cervical and thoracic levels: A 2D phase sensitive inversion recovery imaging study. *PLoS One.* 2015;10(3):1-18. doi:10.1371/journal.pone.0118576
130. Moccia M, Valsecchi N, Ciccarelli O, Van Schijndel R, Barkhof F, Prados F. Spinal cord atrophy in a primary progressive multiple sclerosis trial: Improved sample size using GBSI. *NeuroImage Clin.* 2020;28:102418. doi:10.1016/j.nicl.2020.102418
131. Mina Y, Azodi S, Dubuche T, et al. Cervical and thoracic cord atrophy in multiple sclerosis phenotypes: Quantification and correlation with clinical disability. *NeuroImage Clin.* 2021;30:102680. doi:10.1016/j.nicl.2021.102680
132. Zurawski J, Glanz BI, Healy BC, et al. The impact of cervical spinal cord atrophy on quality of life in multiple sclerosis. *J Neurol Sci.* 2019;403:38-43. doi:10.1016/j.jns.2019.04.023
133. Rocca MA, Valsasina P, Meani A, et al. Clinically relevant cranio-caudal patterns of cervical cord atrophy evolution in MS. *Neurology.* 2019;93(20):e1852-e1866. doi:10.1212/WNL.00000000000008466
134. Ruggieri S, Petracca M, Miller A, et al. Association of Deep Gray Matter Damage With Cortical and Spinal Cord Degeneration in Primary Progressive Multiple Sclerosis. *JAMA*

## 10. Bibliography

---

- Neurol.* 2015;72(12):1466. doi:10.1001/jamaneurol.2015.1897
135. Oh J, Sotirchos ES, Saidha S, et al. Relationships between quantitative spinal cord MRI and retinal layers in multiple sclerosis. *Neurology.* 2015;84(7):720-728. doi:10.1212/WNL.0000000000001257
136. Vidal-Jordana A, Pareto D, Cabello S, et al. Optical coherence tomography measures correlate with brain and spinal cord atrophy and multiple sclerosis disease-related disability. *Eur J Neurol.* 2020;27(11):2225-2232. doi:10.1111/ene.14421
137. Ghione E, Bergsland N, Dwyer MG, et al. Brain Atrophy Is Associated with Disability Progression in Patients with MS followed in a Clinical Routine. *Am J Neuroradiol.* 2018;39(12):2237-2242. doi:10.3174/ajnr.A5876
138. Bischof A, Papinutto N, Keshavan A, et al. Spinal Cord Atrophy Predicts Progressive Disease in Relapsing Multiple Sclerosis. *Ann Neurol.* 2022;91(2):268-281. doi:10.1002/ana.26281
139. Barkhof F. The clinico-radiological paradox in multiple sclerosis revisited. *Curr Opin Neurol.* 2002;15(3):239-245. doi:10.1097/00019052-200206000-00003
140. Woo MS, Engler JB, Friese MA. The neuropathobiology of multiple sclerosis. *Nat Rev Neurosci.* Published online May 24, 2024. doi:10.1038/s41583-024-00823-z
141. Satz P. Brain reserve capacity on symptom onset after brain injury: A formulation and review of evidence for threshold theory. *Neuropsychology.* 1993;7(3):273-295. doi:10.1037/0894-4105.7.3.273
142. Bennett DA, Schneider JA, Arvanitakis Z, et al. Neuropathology of older persons without cognitive impairment from two community-based studies. *Neurology.* 2006;66(12):1837-1844. doi:10.1212/01.wnl.0000219668.47116.e6
143. Sumowski JF, Rocca MA, Leavitt VM, et al. Brain reserve and cognitive reserve in multiple sclerosis. *Neurology.* 2013;80(24):2186-2193. doi:10.1212/WNL.0b013e318296e98b
144. Haug H. Brain sizes, surfaces, and neuronal sizes of the cortex cerebri: A stereological investigation of man and his variability and a comparison with some mammals (primates, whales, marsupials, insectivores, and one elephant). *Am J Anat.* 1987;180(2):126-142. doi:10.1002/aja.1001800203
145. Langella S, Sadiq MU, Mucha PJ, Giovanello KS, Dayan E. Lower functional hippocampal redundancy in mild cognitive impairment. *Transl Psychiatry.* 2021;11(1):61. doi:10.1038/s41398-020-01166-w
146. MacLulich AMJ, Ferguson KJ, Deary IJ, Seckl JR, Starr JM, Wardlaw JM. Intracranial capacity and brain volumes are associated with cognition in healthy elderly men. *Neurology.* 2002;59(2):169-174. doi:10.1212/WNL.59.2.169
147. Perneczky R, Wagenpfeil S, Lunetta KL, et al. Head circumference, atrophy, and cognition. *Neurology.* 2010;75(2):137-142. doi:10.1212/WNL.0b013e3181e7ca97
148. STERN Y. What is cognitive reserve? Theory and research application of the reserve concept. *J Int Neuropsychol Soc.* 2002;8(3):448-460. doi:10.1017/S1355617702813248
149. Kuhlmann T, Moccia M, Coetzee T, et al. Multiple sclerosis progression: time for a new mechanism-driven framework. *Lancet Neurol.* 2023;22(1):78-88. doi:10.1016/S1474-4422(22)00289-7
150. Rocca MA, Amato MP, De Stefano N, et al. Clinical and imaging assessment of cognitive dysfunction in multiple sclerosis. *Lancet Neurol.* 2015;14(3):302-317. doi:10.1016/S1474-4422(14)70250-9
151. Deloire MSA, Ruet A, Hamel D, Bonnet M, Dousset V, Brochet B. MRI predictors of



## 10. Bibliography

---

- cognitive outcome in early multiple sclerosis. *Neurology*. 2011;76(13):1161-1167. doi:10.1212/WNL.0b013e318212a8be
152. Benedict RHB, Bruce JM, Dwyer MG, et al. Neocortical Atrophy, Third Ventricular Width, and Cognitive Dysfunction in Multiple Sclerosis. *Arch Neurol*. 2006;63(9):1301. doi:10.1001/archneur.63.9.1301
153. Sumowski JF, Rocca MA, Leavitt VM, et al. Brain reserve and cognitive reserve protect against cognitive decline over 4.5 years in MS. *Neurology*. 2014;82(20):1776-1783. doi:10.1212/WNL.0000000000000433
154. SUMOWSKI JF, CHIARAVALLIOTTI N, WYLIE G, DELUCA J. Cognitive reserve moderates the negative effect of brain atrophy on cognitive efficiency in multiple sclerosis. *J Int Neuropsychol Soc*. 2009;15(4):606-612. doi:10.1017/S1355617709090912
155. Martins Da Silva A, Cavaco S, Moreira I, et al. Cognitive reserve in multiple sclerosis: Protective effects of education. *Mult Scler J*. 2015;21(10):1312-1321. doi:10.1177/1352458515581874
156. Sumowski JF, Chiaravallotti N, DeLuca J. Cognitive reserve protects against cognitive dysfunction in multiple sclerosis. *J Clin Exp Neuropsychol*. 2009;31(8):913-926. doi:10.1080/13803390902740643
157. Rocca MA, Riccitelli GC, Meani A, et al. Cognitive reserve, cognition, and regional brain damage in MS: A 2 -year longitudinal study. *Mult Scler J*. 2019;25(3):372-381. doi:10.1177/1352458517750767
158. Pinter D, Sumowski J, DeLuca J, et al. Higher Education Moderates the Effect of T2 Lesion Load and Third Ventricle Width on Cognition in Multiple Sclerosis. Weber MS, ed. *PLoS One*. 2014;9(1):e87567. doi:10.1371/journal.pone.0087567
159. O'Brien C, Holtzer R. Physical reserve: construct development and predictive utility. *Aging Clin Exp Res*. 2023;35(5):1055-1062. doi:10.1007/s40520-023-02371-5
160. Sastre-Garriga J, Rovira A, García-Vidal A, et al. Spinal cord reserve in multiple sclerosis. *J Neurol Neurosurg Psychiatry*. Published online January 23, 2023:jnnp-2022-330613. doi:10.1136/jnnp-2022-330613
161. Ullmann E, Pelletier Paquette JF, Thong WE, Cohen-Adad J. Automatic Labeling of Vertebral Levels Using a Robust Template-Based Approach. *Int J Biomed Imaging*. 2014;2014:1-9. doi:10.1155/2014/719520
162. De Leener B, Fonov VS, Collins DL, Callot V, Stikov N, Cohen-Adad J. PAM50: Unbiased multimodal template of the brainstem and spinal cord aligned with the ICBM152 space. *Neuroimage*. 2018;165:170-179. doi:10.1016/j.neuroimage.2017.10.041
163. Tukey JW. *Exploratory Data Analysis*.; 1977. [https://scholar.google.com/scholar\\_lookup?title=Exploratory+Data+Analysis&author=Tukey,+J.W.&publication\\_year=1977](https://scholar.google.com/scholar_lookup?title=Exploratory+Data+Analysis&author=Tukey,+J.W.&publication_year=1977)
164. Zou KH, Warfield SK, Bharatha A, et al. Statistical validation of image segmentation quality based on a spatial overlap index1. *Acad Radiol*. 2004;11(2):178-189. doi:10.1016/S1076-6332(03)00671-8
165. Koo TK, Li MY. A Guideline of Selecting and Reporting Intraclass Correlation Coefficients for Reliability Research. *J Chiropr Med*. 2016;15(2):155-163. doi:10.1016/j.jcm.2016.02.012
166. Rocca MA, Valsasina P, Meani A, et al. Association of Gray Matter Atrophy Patterns With Clinical Phenotype and Progression in Multiple Sclerosis. *Neurology*. 2021;96(11):e1561-e1573. doi:10.1212/WNL.00000000000011494
167. Lublin FD. New Multiple Sclerosis Phenotypic Classification. *Eur Neurol*. 2014;72(Suppl.

## 10. Bibliography

---

- 1):1-5. doi:10.1159/000367614
168. Liu Y, Lukas C, Steenwijk MD, et al. Multicenter Validation of Mean Upper Cervical Cord Area Measurements from Head 3D T1-Weighted MR Imaging in Patients with Multiple Sclerosis. *Am J Neuroradiol*. 2016;37(4):749-754. doi:10.3174/ajnr.A4635
169. Mongay-Ochoa N, Pareto D, Alberich M, et al. Validation of a New Semiautomated Segmentation Pipeline Based on the Spinal Cord Toolbox DeepSeg Algorithm to Estimate the Cervical Canal Area. *Am J Neuroradiol*. Published online 2023:1-6. doi:10.3174/ajnr.a7899
170. Cadotte DW, Cadotte A, Cohen-Adad J, et al. Characterizing the Location of Spinal and Vertebral Levels in the Human Cervical Spinal Cord. *Am J Neuroradiol*. 2015;36(4):803-810. doi:10.3174/ajnr.A4192
171. Papinutto N, Bakshi R, Bischof A, et al. Gradient nonlinearity effects on upper cervical spinal cord area measurement from 3D T1-weighted brain MRI acquisitions. *Magn Reson Med*. 2018;79(3):1595-1601. doi:10.1002/mrm.26776
172. Miller DH, Leary SM. Primary-progressive multiple sclerosis. *Lancet Neurol*. 2007;6(10):903-912. doi:10.1016/S1474-4422(07)70243-0
173. Rovaris M, Confavreux C, Furlan R, Kappos L, Comi G, Filippi M. Secondary progressive multiple sclerosis: current knowledge and future challenges. *Lancet Neurol*. 2006;5(4):343-354. doi:10.1016/S1474-4422(06)70410-0
174. Valsasina P, Rocca MA, Horsfield MA, Copetti M, Filippi M. A longitudinal MRI study of cervical cord atrophy in multiple sclerosis. *J Neurol*. 2015;262(7):1622-1628. doi:10.1007/s00415-015-7754-z
175. Aymerich FX, Auger C, Alonso J, et al. Cervical Cord Atrophy and Long-Term Disease Progression in Patients with Primary-Progressive Multiple Sclerosis. *Am J Neuroradiol*. 2018;39(2):399-404. doi:10.3174/ajnr.A5495
176. Dekker I, Sombekke MH, Balk LJ, et al. Infratentorial and spinal cord lesions: Cumulative predictors of long-term disability? *Mult Scler J*. 2020;26(11):1381-1391. doi:10.1177/1352458519864933
177. Ruggieri S, Prosperini L, Petracca M, et al. The added value of spinal cord lesions to disability accrual in multiple sclerosis. *J Neurol*. Published online June 29, 2023. doi:10.1007/s00415-023-11829-5
178. Iglesias JE, Billot B, Balbastre Y, et al. SynthSR: A public AI tool to turn heterogeneous clinical brain scans into high-resolution T1-weighted images for 3D morphometry. *Sci Adv*. 2023;9(5). doi:10.1126/sciadv.add3607
179. Nouri A, Tessitore E, Molliqaj G, et al. Degenerative Cervical Myelopathy: Development and Natural History [AO Spine RECODE-DCM Research Priority Number 2]. *Glob Spine J*. 2022;12(1):39S-54S. doi:10.1177/21925682211036071
180. Guan Q, Xing F, Long Y, Xiang Z. Cervical intradural disc herniation: A systematic review. *J Clin Neurosci*. 2018;48:1-6. doi:10.1016/j.jocn.2017.10.024

## **11. ANNEX**

---

# 11. Annex

## 11.1 Publication

Mongay-Ochoa N, Pareto D, Alberich M, Tintore M, Montalban X, Rovira À, Sastre-Garriga J. **Validation of a New Semiautomated Segmentation Pipeline Based on the Spinal Cord Toolbox DeepSeg Algorithm to Estimate the Cervical Canal Area.** *AJNR Am J Neuroradiol.* 2023 Jul;44(7):867-872. doi: 10.3174/ajnr.A7899. Epub 2023 Jun 8. PMID: 37290816; PMCID: PMC10337626.

ORIGINAL RESEARCH  
SPINE

### Validation of a New Semiautomated Segmentation Pipeline Based on the Spinal Cord Toolbox DeepSeg Algorithm to Estimate the Cervical Canal Area

N. Mongay-Ochoa, D. Pareto, M. Alberich, M. Tintore, X. Montalban, À. Rovira, and J. Sastre-Garriga

#### ABSTRACT

**BACKGROUND AND PURPOSE:** As in the brain reserve concept, a larger cervical canal area may also protect against disability. In this context, a semiautomated pipeline has been developed to obtain quantitative estimations of the cervical canal area. The aim of the study was to validate the pipeline, to evaluate the consistency of the cervical canal area measurements during a 1-year period, and to compare cervical canal area estimations obtained from brain and cervical MRI acquisitions.

**MATERIALS AND METHODS:** Eight healthy controls and 18 patients with MS underwent baseline and follow-up 3T brain and cervical spine sagittal 3D MPRAGE. The cervical canal area was measured in all acquisitions, and estimations obtained with the proposed pipeline were compared with manual segmentations performed by 1 evaluator using the Dice similarity coefficient. The cervical canal area estimations obtained on baseline and follow-up T1WI were compared; brain and cervical cord acquisitions were also compared using the individual and average intraclass correlation coefficients.

**RESULTS:** The agreement between the manual cervical canal area masks and the masks provided by the proposed pipeline was excellent, with a mean Dice similarity coefficient mean of 0.90 (range, 0.73–0.97). The cervical canal area estimations obtained from baseline and follow-up scans showed a good level of concordance (intraclass correlation coefficient = 0.76; 95% CI, 0.44–0.88); estimations obtained from brain and cervical MRIs also had good agreement (intraclass correlation coefficient = 0.77; 95% CI, 0.45–0.90).

**CONCLUSIONS:** The proposed pipeline is a reliable tool to estimate the cervical canal area. The cervical canal area is a stable measure across time; moreover, when cervical sequences are not available, the cervical canal area could be estimated using brain T1WI.

**ABBREVIATIONS:** CCaA = cervical canal area; FA = flip angle; GT = ground truth; HC = healthy controls; ICC = intraclass correlation coefficient; LoA = limits of agreement; pwMS = patients with multiple sclerosis; SCT = Spinal Cord Toolbox; SD = standard deviation

In patients with MS, the progression of neurologic disability cannot be explained only by the accumulation of brain white matter lesions.<sup>1</sup> Because neurodegenerative damage of the cervical cord is present in most patients with MS,<sup>2</sup> recent work has demonstrated the value of cervical cord atrophy as an independent prognostic factor for disability.<sup>3</sup>

In homology to the brain reserve concept, which implies that individuals with a larger premorbid brain (estimated using total intracranial volume as a proxy of maximal lifetime brain growth) have a lower risk of MS-related cognitive and physical impairment,<sup>4</sup>

a larger cervical canal area (CCaA), which may be taken as a proxy for maximal lifetime spinal cord growth, may also protect against disability.<sup>5</sup>

In this context, a semiautomated pipeline has been developed to obtain quantitative estimations of the CCaA based on brain and cervical 3D T1WI, using the Spinal Cord Toolbox (SCT; <https://www.nitrc.org/projects/sct/>). To validate the reproducibility of the proposed pipeline, we compared CCaA measurements obtained with the SCT with those obtained with the manual ground truth (GT), both in healthy controls (HC) and patients with MS. Then, the performance of the pipeline was evaluated by assessing the CCaA at baseline and 1-year follow-up (scan-rescan test) and evaluating CCaA measurements obtained with brain and cervical T1WI.

#### MATERIALS AND METHODS

##### Data Acquisition

An initial set of 10 HC and 21 patients with MS underwent baseline and follow-up brain and cervical spine sagittal 3D MPRAGE. All MRI scans were acquired in a 3T system (Tim Trio; Siemens)

Received November 12, 2022; accepted after revision May 11, 2023.

From the Department of Neurology (N.M.-O., M.T., X.M., J.S.-G.), Multiple Sclerosis Centre of Catalonia, and Section of Neuroradiology (D.P., M.A., À.R.), Department of Radiology, Hospital Universitari Vall d'Hebron, Barcelona, Spain.

Please address correspondence to Deborah Pareto Onghena, PhD, Section of Neuroradiology, Department of Radiology (IDI), Vall d'Hebron, University Hospital, Pg Vall d'Hebron 119-129, 08035 Barcelona, Spain; e-mail: [deborah.pareto.idi@gencat.cat](mailto:deborah.pareto.idi@gencat.cat)

Indicates article with online supplemental data.

<http://dx.doi.org/10.3174/ajnr.A7899>

AJNR Am J Neuroradiol •• • 2023 www.ajnr.org 1

using the following acquisition parameters: TR = 2300 ms, TE = 2.98 ms, TI = 900 ms, flip angle = 9°, voxel size =  $1 \times 1 \times 1 \text{ mm}^3$ ; brain FOV =  $240 \times 256 \times 176$ , cervical FOV =  $240 \times 25 \times 128$ . Additionally, all subjects underwent a brain 2D FLAIR scan (TR = 9000 ms, TE = 93 ms, TI = 2500 ms, flip angle = 120°, voxel size =  $0.49 \times 0.49 \times 3.0 \text{ mm}^3$ ). The positioning protocol was the same across all subjects. The project was approved by the local ethics committee, and subjects signed an informed consent.

## Image Processing

The CCaA was measured in all acquisitions using the following in-house pipeline based on the SCT (Version 5.0.1):<sup>6</sup> First, a segmentation of the cervical cord was obtained with the DeepSeg algorithm. Then, the posterior tip of the C2–C3 intervertebral disc was manually labeled by 2 evaluators (a neurologist with a 7 years' experience and an MRI technician with 11 years' experience). The output from the DeepSeg algorithm, along with these manual intervertebral disc landmarks, was used to normalize the images to the PAM50 atlas,<sup>7</sup> an unbiased multimodal MRI template of the full spinal cord (C1–L2 vertebral level) and brainstem where several spinal cord structures have been predefined. Previously, a spinal canal template covering from C1 to C5 was created by our research group in the same space as the PAM50 atlas and was added to the predefined structures (PAM50\_41; Online Supplemental Data). A spinal canal segmentation mask was created in the same space as the atlas and added to the predefined structures, including the spinal canal template. Then, the images were normalized using the inverse normalization matrix, as proposed by SCT, and finally, the spinal canal mask was transferred from the atlas space to the native space (Fig 1).

Additionally, the total intracranial volume was assessed in all subjects using the T1WI sequences with statistical parametric mapping software (SPM; <http://www.fil.ion.ucl.ac.uk/spm/software/spm12>); the lesion volume was estimated using 2D FLAIR MRI with the Lesion Segmentation Toolbox, included in the SPM software (<https://www.applied-statistics.de/lst.html>).

## Statistical Analysis

CCaA was then estimated as the mean cross-sectional area across either 5, 11, or 17 slices centered on the C2–C3 intervertebral disc, representing the 3 groups of comparisons. Anatomically, 5 slices usually cover the C2–C3 cervical disc, 11 slices cover from the lower margin of C2 to the upper margin of C3; and 17 slices cover from the odontoid basis to the midpoint of the posterior arch of C3 (a certain intersubject variability is detected in those limits according to the individual anatomy).

To identify outlier CCaA estimations, we removed all measures with a value beyond 1.5 times the interquartile range.<sup>8</sup>

Then, CCaA estimations in HC and patients with MS were compared by a multivariable regression model adjusted for age and sex; CCaA estimations from baseline and follow-up cervical cord scans and from brain and cervical MRIs were also compared using a paired *t* test.

To assess the reproducibility of the proposed pipeline, we compared the CCaA estimations obtained from the cervical cord and brain T1WI at 2 different time points with the proposed pipeline manual segmentations performed by 1 evaluator, considered the

GT, using the Dice similarity coefficient.<sup>9</sup> In addition, a second evaluator manually outlined the CCaA to assess the interoperator variability. Additionally, we compared the CCaA mean obtained with the manual GT at baseline for the cervical cord and brain scans using a paired *t* test. The GT, considered the reference value, was measured at the midpoint of C2–C3.

Finally, CCaA estimations obtained on baseline and follow-up cervical cord T1WI were compared; brain and cervical cord acquisitions were also compared using the individual and average intraclass correlation coefficient (ICC)<sup>10</sup> and the Bland-Altman method with their limits of agreement (LoA). Statistical analysis was performed with STATA 16.1 software (StataCorp). Before we performed a *t* test, the normal distribution of different variables was evaluated using the Shapiro-Wilk test, and the homogeneity of variances was determined by the Levene test. To appraise assumptions of linear regression, we checked the normality of residuals using the Shapiro-Wilk test; homoscedasticity was evaluated with the Breusch-Pagan test; independence of observations was determined using the Durbin-Watson test; and collinearity was assessed by the variance inflation factor. The *P* value for significance was set at  $P < .05$ .

## RESULTS

The proposed pipeline failed in only 3 subjects when using 17 slices to obtain the mean CCaA, because the position of the brain scan was too high and did not cover the upper segment of the cervical cord completely.

After we removed 2 HC and 3 patients with MS, the final cohort included CCaA estimations from 8 HC and 18 patients with MS. Clinical and MRI data are shown in the Table. After we evaluated assumptions of linear regression (Shapiro-Wilk test,  $P = .80$ ; Levene test,  $P = .74$ ; Breusch-Pagan test,  $P = .94$ ; Durbin-Watson test,  $P = .84$ ; and variance inflation factor = 1.07), age- and sex-adjusted linear regression models confirmed that there were no significant differences in the CCaA between HC and patients with MS, estimated in both the cervical cord (mean absolute difference =  $0.33 \text{ mm}^2$ ,  $\beta = 0.10$ ,  $P = .54$ ) and brain acquisitions (mean absolute difference =  $2.18 \text{ mm}^2$ ,  $\beta = 0.36$ ,  $P = .14$ ). Consequently, to perform the statistical analysis between different sequences with a larger sample size, we considered HC and patients with MS as a single group (26 subjects).

In the assessment of the reproducibility of the proposed pipeline, the degree of overlap between the CCaA masks generated by the proposed pipeline and the manual GT was excellent with a Dice similarity coefficient mean of 0.90 (range, 0.73–0.97). The distribution across the 4 different acquisitions is shown in Fig 2. Agreement between the 2 evaluators was also excellent, with a Dice similarity coefficient of 0.95 (range, 0.78–1). Furthermore, we did not find significant differences when comparing CCaA estimations obtained with the pipeline and the GT by a *t* test, either at the baseline cervical cord T1WI (mean absolute difference =  $9.56 \text{ mm}^2$ ,  $t[25] = 1.77$ ,  $P = .09$ ) or brain T1WI (mean absolute difference =  $6.35 \text{ mm}^2$ ,  $t[25] = 0.82$ ,  $P = .42$ ).

When we compared CCaA estimations obtained from baseline and 1-year follow-up cervical cord MRIs, the highest agreement was obtained with 11 and 17 slices (ICC = 0.76; 95% CI, 0.44–0.88, and ICC = 0.78; 95% CI, 0.56–0.90, respectively).

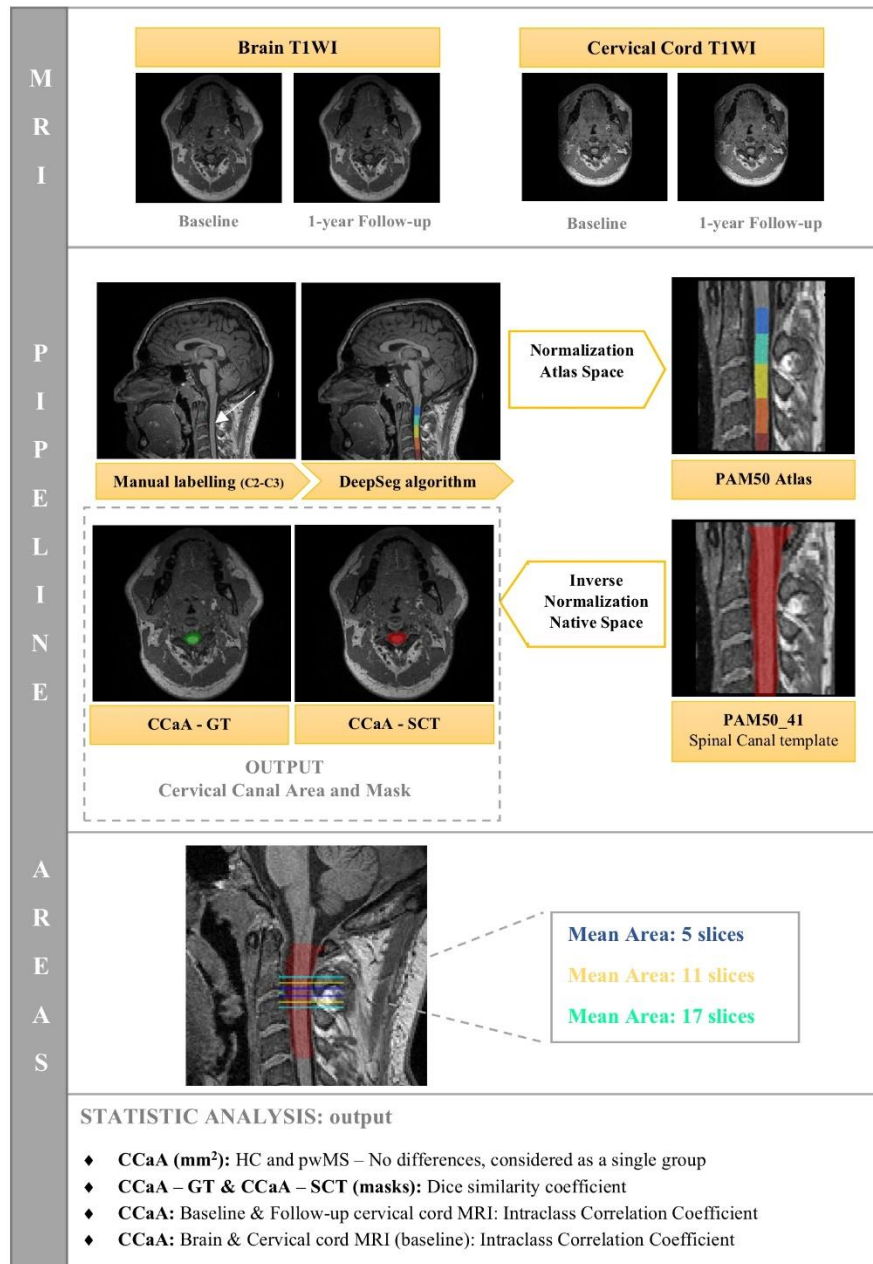


**FIG 1.** Graphical representation of the proposed pipeline to estimate the cervical canal, including the MRI sequences, a flowchart, the assessment of the mean cervical canal area across the different number of slices, and the statistical analysis performed.

Average ICCs are represented in Fig 3, and they are consistently higher than individual ICCs. Estimations of the CCaA with 17 and 11 slices were also highly similar when using the Bland-Altman method, in contrast to LoA obtained with 5 slices, with a narrower and better-centered LoA (Fig 4, left side). When comparing CCaA estimations obtained from cervical cord T1WI

acquisitions at baseline (mean = 218.37 [SD, 5.02] mm<sup>2</sup>) and follow-up (mean = 217.09 [SD, 5.62] mm<sup>2</sup>), we did not find significant differences (mean absolute paired difference = 1.28 mm<sup>2</sup>,  $t[25] = 1.22, P = .23$ ).

CCaA estimations obtained from brain and cervical cord MRIs had a high agreement, independent of the number of slices

# 11. Annex

**Demographic, clinical, and radiologic characteristics of HC and patients with MS**

|   | HC (n = 8)    | Patients with MS (n = 18) | P Value <sup>a</sup> |
|---|---------------|---------------------------|----------------------|
| Sex (female) (No.) (%)                          | 5 (62.5%)     | 11 (61.1%)                | .97                  |
| Age (mean) (SD) (yr)                            | 30.89 (1.44)  | 33.84 (1.98)              | .36                  |
| CCaA (mean) (SD) (mm <sup>2</sup> )             |               |                           |                      |
| Cervical MRI acquisition                        | 218.15 (4.84) | 218.47 (5.23)             | .73                  |
| Brain MRI acquisition                           | 214.57 (3.97) | 216.75 (3.47)             | .48                  |
| Total intracranial volume (mean) (SD) (mL)      | 1422.3 (0.10) | 1392.9 (0.12)             | .55                  |
| T2 lesion volume (mean) (SD) (mm <sup>3</sup> ) | —             | 2.31 (4.09)               | —                    |

**Note:** —Dash indicates not information available; HC: healthy controls; pwMS, patients with multiple sclerosis; SD, standard deviation.

<sup>a</sup> Values correspond to univariate comparisons using parametric and non-parametric tests, as convenience.

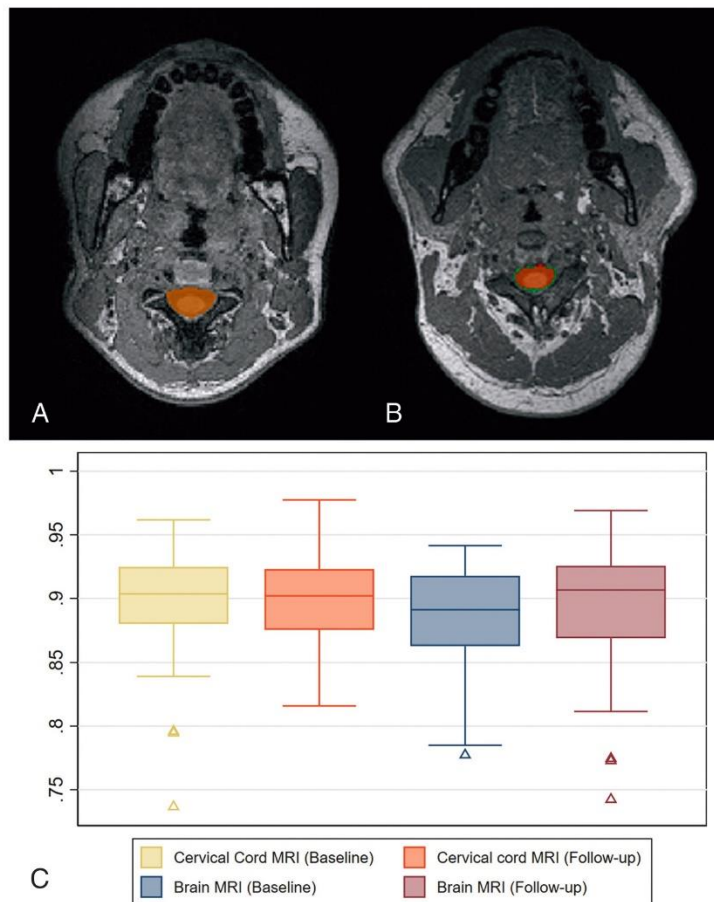


**FIG 2.** CCaA masks obtained with the proposed pipeline (green) versus the manual segmentation (red) in a patient with MS. A, Spinal MRI acquisition shows a Dice similarity coefficient of 0.92. B, Brain MRI acquisition shows a Dice similarity coefficient of 0.88. C, Distribution of Dice similarity coefficients between CCaA masks from the in-house pipeline and the GT across the 4 acquisitions, both in HC and patients with MS.

used to estimate the CCaA (Fig 3). However, the Bland-Altman method showed a better agreement with CCaA estimations of 17 and 11 slices, than with those obtained with 5 slices (Fig 4). When analyzing absolute means, we found minimal-but-significant

differences between CCaA estimations from brain (mean = 216.07 [SD, 3.7] mm<sup>2</sup>) and cervical MRIs (mean = 218 [SD, 5.0]2 mm<sup>2</sup>) (mean absolute paired difference = 2.30,  $t[25] = 2.97$ ,  $P = .006$ ).

## DISCUSSION

In the present study, we validated a semiautomated segmentation pipeline to estimate the CCaA on the basis of the SCT by comparing the generated masks with a manual GT. The overlap was excellent, and significant differences were not found when comparing both measurement methods, indicating that the proposed pipeline seems to appropriately measure the CCaA. Additionally, we have shown that the CCaA is stable for a 1-year period in all subjects. Finally, the CCaA could be properly estimated using either brain or cervical cord MRIs.

To our knowledge, CCaA variations across time have not been analyzed before, though changes were not expected a priori.<sup>11</sup> We verified its consistency during a 1-year period by assessing the measurement in baseline and follow-up cervical T1WIs. Consequently, the CCaA could be used in future studies as a proxy for the premorbid status of the spinal cord, because stability across time is a prerequisite for such use. Because it is usually done in other cervical cord area measurement methods,<sup>12</sup> we considered more appropriated to calculate the mean area over several sections instead of only in 1 section. An increase in the number of sections used would reduce the variability of the measurement, but in the case of the spinal canal, variability could increase because sections may cover a region where the canal area physiologically increases toward the foramen magnum. To check what number of sections would provide the best compromise, we calculated ICCs using CCaA estimations with the SCT across 5, 7, and 11 slices centered at the midpoint of the C2–C3 vertebral disc. The study showed a good level of concordance between time points, obtaining

the highest individual ICC when using 11 and 17 slices for the analysis, compared with 5 slices. We considered that differences in the ICC between the number of slices are related to minor inaccuracies in subject repositioning; hence, the lower the number of slices used

# 11. Annex

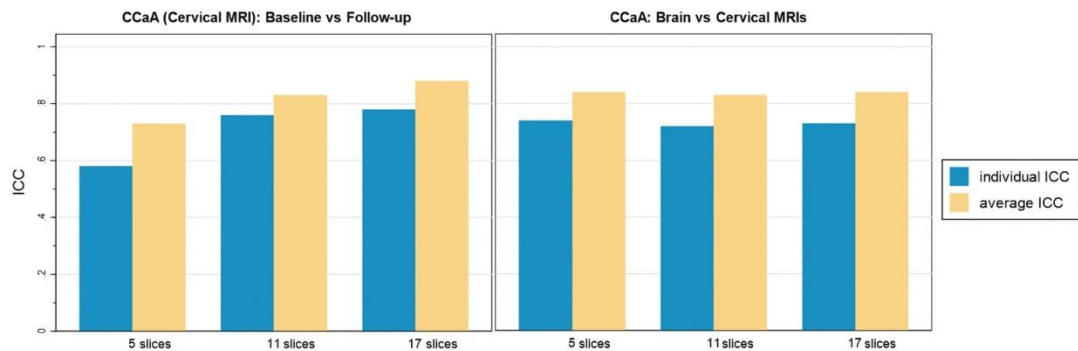


**FIG 3.** Representation of individual ICC (blue) and average (yellow) ICCs, calculated in 5, 11, and 17 slices. On the left, the ICC between baseline and follow-up cervical MRIs. On the right, degree of concordance of the CCaA analyzed in brain and cervical acquisitions.

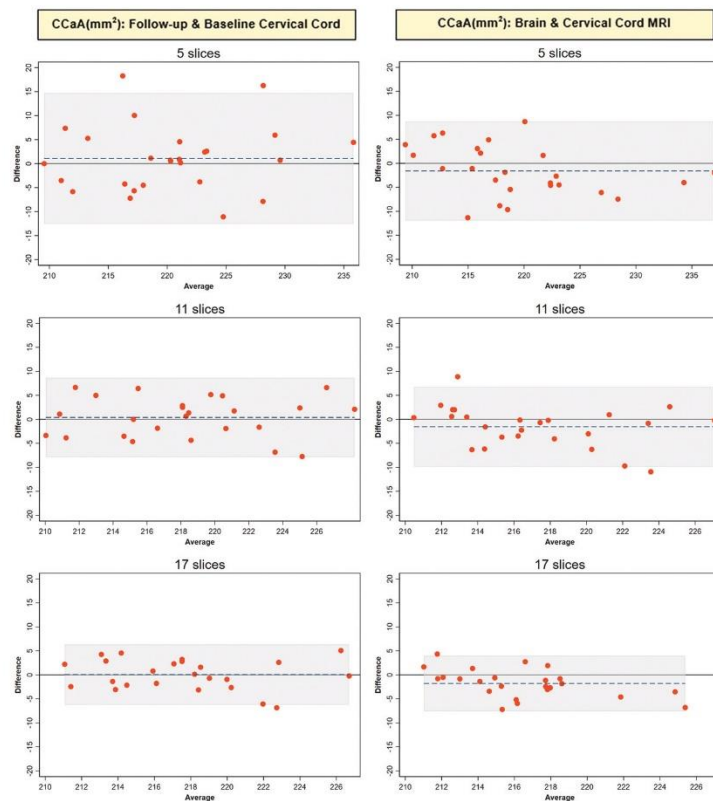


**FIG 4.** Bland-Altman plots showing the agreement between CCaA estimations assessed in different numbers of slices. On the left, the agreement between baseline and follow-up cervical cord MRI is shown; on the right, between brain and cervical cord MRIs. Notice that the x-axis scale of the plot analyzing CCaA estimations on 5 slices is larger than the others.

to calculate the CCaA, the greater the variability found among patients.

Despite the spinal cord being located in the periphery of the FOV on brain T1WI, where gradient nonlinearity distortion effects are substantial,<sup>13</sup> it has already been proved that it is possible to reliably measure the cervical cord area using brain

acquisitions.<sup>14</sup> Therefore, we tested the robustness of CCaA estimations obtained from brain and spine scans, obtaining good agreement between them. Similar ICC values across the different numbers of slices used to calculate the CCaA may be because no repositioning is needed between brain and spine acquisitions.



Overall, ICCs obtained were lower than those reported in other validation studies.<sup>13,14</sup> A possible explanation might be that the individual ICC has been reported instead of the average, which tends to minimize variations and provides higher ICCs. Moreover, although the degree of agreement between CCaA estimations from brain and cervical MRIs was not excellent and there were significant differences between both measurements, the mean difference was inferior to 3 mm<sup>2</sup> in the paired *t* test analysis. Therefore, results seem to suggest that brain CCaA estimations might be considered when dedicated cervical sequences are not available, though both acquisitions may not be fully interchangeable when analyzing the CCaA of a single subject, possibly because the cervical canal is differently located in the FOV of cervical cord and brain T1WIs. Because the in-house pipeline failed in 3 subjects when using 17 slices, it might be advisable to use the 11-slice approach, which provides similar reproducibility parameters.

Several limitations should be mentioned. First, the sample size is small and could explain the range of ICCs obtained. Second, our pipeline includes manual labeling of the C2–C3 intervertebral disc, which may be a limiting factor when dealing with large cohorts because it clearly increases processing time. Third, we performed the image acquisition with the same scanner and positioning protocol; therefore, we have not tested the pipeline under other conditions. Finally, we adjusted measurements by age and sex, but not height, because normalization using anthropometric parameters still remains controversial.<sup>15,16</sup>

## CONCLUSIONS

This study validates a new semiautomated algorithm to estimate the CCaA based on the SCT. An excellent agreement was obtained between the manual segmentations and those provided by the pipeline. We used this algorithm to demonstrate the consistency of CCaA measurements across time, showing no changes during a 1-year period. Finally, results suggested that brain CCaA estimations might be considered when dedicated cervical sequences are not available.

## ACKNOWLEDGMENTS

We wish to thank the subjects who kindly agreed to take part in this study. We acknowledge the support of the Department of Neuroradiology and the Centre of Multiple Sclerosis of Catalonia of the Vall Hebron University Hospital (Barcelona, Spain).

Disclosure forms provided by the authors are available with the full text and PDF of this article at [www.ajnr.org](http://www.ajnr.org).

## REFERENCES

1. Liu Z, Yaldizli Ö, Pardini M, et al. **Cervical cord area measurement using volumetric brain magnetic resonance imaging in multiple sclerosis.** *Mult Scler Relat Disord* 2015;4:52–57 CrossRef Medline
2. Eden D, Gros C, Badji A, et al. **Spatial distribution of multiple sclerosis lesions in the cervical spinal cord.** *Brain* 2019;142:633–46 CrossRef Medline
3. Arrambide G, Rovira A, Sastre-Garriga J, et al. **Spinal cord lesions: a modest contributor to diagnosis in clinically isolated syndromes but a relevant prognostic factor.** *Mult Scler* 2018;24:301–12 CrossRef Medline
4. Sumowski JF, Rocca MA, Leavitt VM, et al. **Brain reserve against physical disability progression over 5 years in multiple sclerosis.** *Neurology* 2016;86:2006–09 CrossRef Medline
5. Sastre-Garriga J, Rovira A, García-Vidal A, et al. **Spinal cord reserve in multiple sclerosis.** *J Neurol Neurosurg Psychiatry* 2023 Jan 23 [Epub ahead of print] CrossRef Medline
6. De Leener B, Lévy S, Dupont SM, et al. **SCT: Spinal Cord Toolbox, an open-source software for processing spinal cord MRI data.** *Neuroimage* 2017;145:24–43 CrossRef Medline
7. De Leener B, Fonov VS, Collins DL, et al. **PAM50: unbiased multimodal template of the brainstem and spinal cord aligned with the ICBM152 space.** *Neuroimage* 2018;165:170–79 CrossRef Medline
8. Tukey JW. *Exploratory Data Analysis.* Addison-Wesley; 1977:43–44
9. Zou KH, Warfield SK, Bharatha A, et al. **Statistical validation of image segmentation quality based on a spatial overlap index 1.** *Acad Radiol* 2004;11:178–89 CrossRef Medline
10. Koo TK, Li MY. **A guideline of selecting and reporting intraclass correlation coefficients for reliability research.** *J Chiropr Med* 2016;15:155–63 CrossRef Medline
11. Kato F, Yukawa Y, Suda K, et al. **Normal morphology, age-related changes and abnormal findings of the cervical spine, Part II: magnetic resonance imaging of over 1,200 asymptomatic subjects.** *Eur Spine J* 2012;21:1499–507 CrossRef Medline
12. Rocca MA, Valsasina P, Meani A, et al; MAGNIMS Study Group. **Clinically relevant cranio-caudal patterns of cervical cord atrophy evolution in MS.** *Neurology* 2019;93:e1852–66 CrossRef Medline
13. Papinutto N, Bakshi R, Bischof A, et al; North American Imaging in Multiple Sclerosis Cooperative (NAIMS). **Gradient nonlinearity effects on upper cervical spinal cord area measurement from 3D T1-weighted brain MRI acquisitions.** *Magn Reson Med* 2018;79:1595–601 CrossRef Medline
14. Liu Y, Lukas C, Steenwijk MD, et al. **Multicenter validation of mean upper cervical cord area measurements from head 3D T1-weighted MR imaging in patients with multiple sclerosis.** *AJNR Am J Neuroradiol* 2016;37:749–54 CrossRef Medline
15. Oh J, Seigo M, Saidha S, et al. **Spinal cord normalization in multiple sclerosis.** *J Neuroimaging* 2014;24:577–84 CrossRef Medline
16. Papinutto N, Schlaeger R, Panara V, et al. **Age, gender and normalization covariates for spinal cord gray matter and total cross-sectional areas at cervical and thoracic levels: a 2D phase sensitive inversion recovery imaging study.** *PLoS One* 2015;10:e0118576–18 CrossRef Medline

## 11.2 Oral communication

Magnims ES. MSMilan2023 – Oral Presentations. O105/2315 (pages 80-81). *Mult Scler J*. 2023;29(3\_suppl):4-136. doi:10.1177/13524585231196191

**Methods:** In this monocentric retrospective study, we performed manual lesion delineation on SC MRI with full sagittal and axial coverage in people between 18 and 60 years of age with relapsing-remitting MS and clinical follow-up data of five years. The first CDA event after baseline, determined by a sustained increase in the Expanded Disability Status Scale (EDSS) over six months, was classified as either PIRA or RAW. SC lesion parameters were compared between groups with and without CDA as well as between patients with RAW and patients with PIRA. The prognostic values of SCLN and SCLV were assessed via receiver operating characteristic curves and their respective areas under the curve.

**Results:** 204 patients were included, 148 of which had at least one SC lesion and 59 experienced CDA. Patients without any SC lesions experienced significantly less CDA (OR = 5.8,  $p < 0.001$ ). SCLN and SCLV were closely correlated ( $r_s = 0.91$ ,  $p < 0.001$ ) and were both significantly associated with CDA on follow-up ( $p < 0.001$ ). Subgroup analyses confirmed this association for patients with PIRA on CDA (34 events,  $p < 0.001$  for both SC lesion measures) but not for RAW (25 events,  $p = 0.077$  and  $p = 0.22$ ).

**Conclusion:** Patients without any SC lesions are notably less likely to experience CDA. Both the number and volume of SC lesions on MRI are associated with future accumulation of disability largely independent of relapses.

**Disclosure of interest:** Lauerer: nothing to disclose

Bussas: nothing to disclose

El Hussein: nothing to disclose

Harabacz: nothing to disclose

Pineker: nothing to disclose

Pongratz: nothing to disclose

Berthele: AB has received consulting and/or speaker fees from Alexion, Biogen, Celgene, Horizon, Novartis, Roche and Sandoz/Hexal. His institution has received compensation for clinical trials from Alexion, Biogen, Merck, Novartis, Roche, and Sanofi Genzyme.

Riederer: nothing to disclose

Kirschke: nothing to disclose

Zimmer: nothing to disclose

Hemmer: Bernhard Hemmer is associated with DIFUTURE (Data Integration for Future Medicine) [BMBF 01ZZ1804[A-I]]. Bernhard Hemmer received funding from the Deutsche Forschungsgemeinschaft (DFG, German Research Foundation) under Germany's Excellence Strategy within the framework of the Munich Cluster for Systems Neurology [EXC 2145 SyNergy – ID 390857198] and the European Union's Horizon 2020 Research and Innovation Program [grant MultipleMS, EU RIA 733161]. He has served on scientific advisory boards for Novartis; he has served as DMSC member for AllergyCare, Sandoz, Polpharma and TG therapeutics; he or his institution have received speaker honoraria from Desitin; his institution received research grants from Regeneron for multiple sclerosis research. He holds part of two patents; one for the detection of antibodies against KIR4.1 in a subpopulation of patients with multiple sclerosis and one for genetic determinants of neutralizing antibodies to interferon.

Mühlau: German Research Foundation, DFG Priority Programme 2177, Radiomics: Next Generation of Biomedical Imaging (project number 428223038), German Federal Ministry of Education

and Research (BMBF), Medical Informatics Initiative (MII), Data Integration for Future Medicine (DIFUTURE) consortium (grants 01ZZ1603[A-D] and 01ZZ1804[A-I]), The National Institutes of Health (grant 1R01NS112161-01 [subinvestigator]), Bavarian State Ministry for Science and Art, Collaborative Bilateral Research Program Bavaria – Québec: AI in medicine (project number F.4-V0134.K5.1/86/45)

## O105/2315

## The role of the spinal cord in multiple sclerosis: a multicentric study

Neus Mongay-Ochoa<sup>1</sup>, Deborah Pareto<sup>2</sup>, Manel Alberich<sup>2</sup>, Pere Carbonell<sup>3</sup>, Paola Valsasina<sup>4</sup>, Massimo Filippi<sup>4,5</sup>, Angela Vidal-Jordana<sup>3</sup>, Cristina Auger<sup>2</sup>, Mar Tintoré<sup>3</sup>, Alessandro Meani<sup>6</sup>, Claudio Gobbi<sup>7,8</sup>, Chiara Zecca<sup>7,8</sup>, Frederik Barkhof<sup>9,10,11</sup>, Menno Schoonheim<sup>11</sup>, Eva Strijbis<sup>11</sup>, Hugo Vrenken<sup>9,10,11</sup>, Antonio Gallo<sup>12</sup>, Alvino Biseco<sup>12</sup>, Olga Ciccarelli<sup>10,12</sup>, Marios Yiannaikas<sup>14</sup>, Jacqueline Palace<sup>15</sup>, Lucy Matthews<sup>15</sup>, Achim Gass<sup>16</sup>, Philipp Eisele<sup>16</sup>, Carsten Lukas<sup>17</sup>, Barbara Bellenberg<sup>17</sup>, MONICA MARGONI<sup>18</sup>, Paolo Preziosa<sup>5,6</sup>, Xavier Montalban<sup>3</sup>, Maria Assunta Rocca<sup>5,6</sup>, Alex Rovira Caffellas<sup>2</sup>, Jaume Sastre-Garriga<sup>3</sup>

<sup>1</sup>Multiple Sclerosis Centre of Catalonia-Vall Hebron University Hospital, Barcelona, Spain, <sup>2</sup>Dept. of Radiology-Vall Hebron University Hospital, Magnetic Resonance Unit, Barcelona, Spain, <sup>3</sup>Multiple Sclerosis Centre of Catalonia-Vall Hebron University Hospital, Barcelona, Spain, <sup>4</sup>Institute of Experimental Neurology, Division of Neuroscience, and Neurology Unit, IRCCS San Raffaele Scientific Institute, Section of Neuroradiology, Milan, Italy, <sup>5</sup>Vita-Salute San Raffaele University, Milano, Italy, <sup>6</sup>Neuroimaging Research Unit, Institute of Experimental Neurology, Division of Neuroscience, and Neurology Unit, IRCCS San Raffaele Scientific Institute, Milan, Italy, <sup>7</sup>Multiple Sclerosis Center (MSC), Department of Neurology, Neurocenter of Southern Switzerland, Department of Neurology, Lugano, Switzerland, <sup>8</sup>USI Università della Svizzera italiana, Faculty of Biomedical Science, Lugano, Switzerland, <sup>9</sup>Faculty of Brain Sciences, University College London Queen Square Institute of Neurology, University College London, London, United Kingdom, <sup>10</sup>National Institute for Health Research University College London Hospitals Biomedical Research Centre, London, United Kingdom, <sup>11</sup>Amsterdam UMC, location VUmc, MS Center Amsterdam, Radiology and Nuclear Medicine, Vrije Universiteit Amsterdam, Amsterdam Neuroscience, Amsterdam, Netherlands, <sup>12</sup>Clinic of Neurology, Second University of Naples, Italy. MRI Research Center SUN-FISM, Second University of Naples, Naples, Italy, <sup>13</sup>Queen Square MS Centre, Department of Neuroinflammation, UCL Queen Square Institute of Neurology, Faculty of Brain Sciences, University College London, London, United Kingdom, <sup>14</sup>National Institute for Health Research, Biomedical Research Centre, University College London Hospitals, London, United Kingdom, <sup>15</sup>John Radcliffe Hospital, University of Oxford, Nuffield Department of Clinical Neurosciences, Oxford, United Kingdom, <sup>16</sup>Department of Neurology, Mannheim Center of Translational Neurosciences (MCTN), Medical Faculty Mannheim, Heidelberg

University, Mannheim, Germany, <sup>17</sup>Institute of Neuroradiology, St. Josef-Hospital Bochum, Ruhr University Bochum, Bochum, Germany

**Introduction:** Our recent work demonstrated that the cervical canal area (CCaA), a potential proxy of the spinal cord reserve, is associated to disability, measured by the Patient Determined Disease steps (PDDS) in patients with MS.

**Objectives/Aims:** The main objectives of the present study are: i) to compare CCaA between healthy controls (HC) and different MS phenotypes, and ii) to test the association between the CCaA and disability, measured by the Expanded Disability Status Scale (EDSS).

**Methods:** Clinical and MRI data were obtained at 9 European sites (Magnims.eu) from 177 HC and 428 MS patients (289 relapsing MS, and 139 progressive MS), recruited between 2010 and 2016. The CCaA in each subject was measured in a sagittal 3D T1-weighted scan covering the entire cervical cord using our validated in-house pipeline based on the Spinal Cord Toolbox. CCaA was estimated as the mean cross-sectional area over 11 slices centred on the C2-C3 intervertebral disc. A coefficient of variation (CV) was then calculated for each measurement, removing those subjects displaying a CV > 0.075. Afterwards, a visual quality check of all segmentations was performed. Multivariable regression models adjusted for age and sex were used to evaluate mean CCaA differences between groups, and to study the association between EDSS and CCaA.

**Results:** After quality control, the final cohort comprised 135 HC and 304 MS patients. When comparing the CCaA between groups, there were no significant differences between HC and relapsing MS (214.62mm<sup>2</sup> vs. 213.68mm<sup>2</sup>, p=0.40), but progressive MS showed significantly lower CCaA (214.62mm<sup>2</sup> vs. 210.51mm<sup>2</sup>, p=0.007). There was a significant correlation between CCaA and EDSS (Spearman's rho -0.19, p=0.007), also when adjusted by age and sex ( $\beta$  = -0.11; p=0.023).

**Conclusion:** No differences in CCaA were observed between HC and relapsing MS patients, a prerequisite to consider CCaA a valid proxy of spinal cord reserve. However, progressive patients displayed a lower CCaA, suggesting that a lower spinal cord reserve might be a feature of progressive MS phenotype. Overall, CCaA is related to EDSS, confirming the existence of spinal cord reserve.

**Disclosure of interest:** NMO: has a predoctoral grant Rio Hortega, from the Instituto de Salud Carlos III (CM21/00018). She also has received speaking honoraria and travel expenses from Merck and Roche.

DP: has received a research contract from Biogen Idec and a grant from Fondo de Investigaciones Sanitarias (PI18/00823, PI22/01709).

MA has nothing to disclose.

PCM: he is yearly salary is supported by a grant from Biogen to Fundació privada Cemcat for statistical analysis.

PV: received speakers' honoraria from Biogen Idec.

MF: is Editor-in-Chief of the Journal of Neurology, Associate Editor of Human Brain Mapping, Associate Editor of Radiology, and Associate Editor of Neurological Sciences; received compensation for consulting services from Alexion, Almirall, Biogen, Merck, Novartis, Roche, Sanofi; speaking activities from Bayer,

Biogen, Celgene, Chiesi Italia SpA, Eli Lilly, Genzyme, Janssen, Merck-Serono, Neopharmed Gentili, Novartis, Novo Nordisk, Roche, Sanofi, Takeda, and TEVA; participation in Advisory Boards for Alexion, Biogen, Bristol-Myers Squibb, Merck, Novartis, Roche, Sanofi, Sanofi-Aventis, Sanofi-Genzyme, Takeda; scientific direction of educational events for Biogen, Merck, Roche, Celgene, Bristol-Myers Squibb, Lilly, Novartis, Sanofi-Genzyme; he receives research support from Biogen Idec, Merck-Serono, Novartis, Roche, Italian Ministry of Health, Fondazione Italiana Sclerosi Multipla, and ARISLA (Fondazione Italiana di Ricerca per la SLA).

AVJ: has received support has received support for contracts Juan Rodes (JR16/00024) and from Fondo de Investigación en Salud (PI17/02162 and PI22/01589) from Instituto de Salud Carlos III, Spain, and has engaged in consulting and/or participated as speaker in events organized by Roche, Novartis, Merck, and Sanofi.

CA: MT: has received compensation for consulting services, speaking honoraria and research support from Almirall, Bayer Schering Pharma, Biogen-Idec, Genzyme, Janssen, Merck-Serono, Novartis, Roche, Sanofi-Aventis, Viela Bio and Teva Pharmaceuticals. Data Safety Monitoring Board for Parexel and UCB Biopharma

AM: nothing to disclose

CG: reports that the Ente Ospedaliero Cantonale (employer) received compensation for speaking activities, consulting fees, or research grants from Almirall, Biogen Idec, Bristol Meyer Squibb, Lundbeck, Merck, Novartis, Sanofi, Teva Pharma, Roche.

CZ: reports that the Ente Ospedaliero Cantonale (employer) received compensation for speaking activities, consulting fees, or research grants from Almirall, Biogen Idec, Bristol Meyer Squibb, Lundbeck, Merck, Novartis, Sanofi, Teva Pharma, Roche.

FB: serves on the steering committee and is iDMC member for Biogen, Merck, Roche, EISAL. He acts as a consultant for Roche, Biogen, Merck, IXICO, Jansen, Combinostics. He has research agreements with Novartis, Merck, Biogen, GE, Roche. He is co-founder and share-holder of Queen Square Analytics LTD

MMS: Serves on the editorial board of Neurology and Frontiers in Neurology; receives research support from the Dutch MS Research Foundation, Eurostars-EUREKA, ARSEP, Amsterdam Neuroscience, MAGNIMS and ZonMW (Vidi grant, project number 09150172010056) and has served as a consultant for or received research support from Atara Biotherapeutics, Biogen, Celgene/Bristol Meyers Squibb, EIP, Sanofi, MedDay and Merck.

EMS: nothing to disclose

HV: AG: AB: has received speaker honoraria and/or compensation for travel grant and consulting service from Biogen, Merck, Genzyme, Novartis, Alexion and Roche

OC: is a member of independent DSMB for Novartis, gave a teaching talk on McDonald criteria in a Merck local symposium, and contributed to an Advisory Board for Biogen; she is Deputy Editor of Neurology, for which she receives an honorarium.

MY: nothing to disclose

JP: LM: AG: PE: Has received travel expenses from Bayer Health Care and is member of the Editorial Board of the Journal of Neuroimaging.

CL: received a research grant by the German Federal Ministry for Education and Research, BMBF, German Competence Network

# 11. Annex

## 11.3 Funding and scholarships

Rio Hortega Grant, from the Instituto de Salud Carlos III (CM21/00018).



Anexo 1 (concedidos) a la Resolución de la Dirección del Instituto de Salud Carlos III, O.A., M.P. por la que se conceden Contratos Río Hortega de la convocatoria 2021 de la Acción Estratégica en Salud 2017 – 2020.

| EXPEDIENTE | MODALIDAD   | PERSONA CANDIDATA               | CENTRO SOLICITANTE  | NIF       | CENTRO DE REALIZACIÓN  | COMUNIDAD AUTÓNOMA | CENTRO DE ADSCRIPCIÓN DEL JEFE DE GRUPO                       |
|------------|---|---------------------------------|---|-----------|--|--------------------|---|
| CM21/00007 | Grupo Habitual  | FRAILE RIBOT, PABLO ARTURO      | FUNDACION INSTITUTO DE INVESTIGACION SANITARIA ILLES BALEARS                                    | G57326324 | INSTITUTO DE INVESTIGACION SANITARIA ILLES BALEARS (IISBa)                 | BALEARES           | HOSPITAL UNIVERSITARIO SON ESPASES                            |
| CM21/00012 | Grupo Habitual  | UDAONDO GASCON, CLARA ISABEL    | FUNDACION INVESTIGACION BIOMEDICA HOSPITAL LA PAZ   | G83727057 | HOSPITAL LA PAZ  | MADRID             |   |
| CM21/00013 | Grupo Habitual  | FACAL MOLINA, FERNANDO          | FUNDACION INSTITUTO DE INVESTIGACION SANITARIA DE SANTIAGO DE COMPOSTELA                        | G15796683 | COMPLEJO HOSPIT. UNIVERSITARIO DE SANTIAGO                                 | GALICIA            |   |
| CM21/00016 | Grupo Habitual  | GUASP VERDAGUER, MAR            | INSTITUTO DE INVESTIGACIONES BIOMEDICAS AUGUST PI I SUNYER (IDIBAPS)                            | O5856414G | INSTITUTO DE INVESTIGACIONES BIOMEDICAS AUGUST PI I SUNYER (IDIBAPS)       | CATALUÑA           | HOSPITAL CLINICO Y PROVINCIAL DE BARCELONA                    |
| CM21/00017 | Grupos dirigidos por investigadores nacidos en 1976 o posterior | ANMELLA DIAZ, GERARD            | INSTITUTO DE INVESTIGACIONES BIOMEDICAS AUGUST PI I SUNYER (IDIBAPS)                            | O5856414G | INSTITUTO DE INVESTIGACIONES BIOMEDICAS AUGUST PI I SUNYER (IDIBAPS)       | CATALUÑA           | HOSPITAL CLINICO Y PROVINCIAL DE BARCELONA                    |
| CM21/00018 | Grupo Habitual  | MONGAY OCHOA, NEUS              | FUNDACION INSTITUTO DE INVESTIGACION VALLE DE HEBRON  | G60594009 | INSTITUTO DE INVESTIGACION HOSPITAL UNIVERSITARIO VALLE DE HEBRON (VHIR)   | CATALUÑA           | FUNDACION INSTITUTO DE INVESTIGACION VALLE DE HEBRON          |
| CM21/00019 | Grupo Habitual  | MORENO JUSTE, AIDA              | FUNDACION INSTITUTO DE INVESTIGACION SANITARIA ARAGON   | G99426132 | INSTITUTO DE INVESTIGACION SANITARIA ARAGON                                | ARAGON             | HOSPITAL MIGUEL SERVET  |
| CM21/00021 | Grupo Habitual  | LOPEZ RUIZ, ROCIO               | FUNDACION PUBLICA ANDALUZA PARA LA GESTION DE LA INVESTIGACION EN SALUD DE SEVILLA              | G41918830 | HOSPITAL VIRGEN MACARENA   | ANDALUCIA          |   |
| CM21/00024 | Grupo Habitual  | FALGAS MARTINEZ, NEUS           | INSTITUTO DE INVESTIGACIONES BIOMEDICAS AUGUST PI I SUNYER (IDIBAPS)                            | O5856414G | INSTITUTO DE INVESTIGACIONES BIOMEDICAS AUGUST PI I SUNYER (IDIBAPS)       | CATALUÑA           | HOSPITAL CLINICO Y PROVINCIAL DE BARCELONA                    |
| CM21/00025 | Grupo Habitual  | RUBIN DE CELIX VARGAS, CRISTINA | FUNDACION INVESTIGACION BIOMEDICA HOSPITAL DE LA PRINCESA                                       | G83727081 | INSTITUTO DE INVESTIGACION BIOMEDICA HOSPITAL UNIVERSITARIO DE LA PRINCESA | MADRID             | HOSPITAL DE LA PRINCESA                                       |
| CM21/00027 | Grupo Habitual  | MOLINA RAMOS, ANA ISABEL        | FUNDACION PARA LA INVESTIGACION DE MALAGA EN BIOMEDICINA Y SALUD (FINABIS)                      | G29830643 | INSTITUTO DE INVESTIGACION BIOMEDICA DE MALAGA (IBMA)                      | ANDALUCIA          | COMPLEJO HOSPITALARIO DE ESPECIALIDADES VIRGEN DE LA VICTORIA |
| CM21/00028 | Grupo Habitual  | RODRIGUEZ CALLE, CARMEN         | FUNDACION INVESTIGACION BIOMEDICA HOSPITAL RAMON Y CAJAL  | G83726984 | HOSPITAL RAMON Y CAJAL   | MADRID             |   |
| CM21/00030 | Grupo Habitual  | MARCELO CALVO, CRISTINA         | FUNDACION INVESTIGACION BIOMEDICA HOSPITAL LA PAZ   | G83727057 | HOSPITAL LA PAZ  | MADRID             | FUNDACION INVESTIGACION BIOMEDICA HOSPITAL LA PAZ             |
| CM21/00033 | Grupo Habitual  | GUINART MULERO, DANIEL          | FUNDACION INSTITUTO HOSPITAL DEL MAR DE INVESTIGACIONES MEDICAS (FIMIM)                         | G60072253 | INSTITUTO HOSPITAL DEL MAR DE INVESTIGACIONES MEDICAS (IMIM)               | CATALUÑA           | HOSPITAL DEL MAR  |
| CM21/00034 | Grupo Habitual  | OTERINO MANZANAS, ARMANDO       | FUNDACION INSTITUTO DE ESTUDIOS DE CIENCIAS DE LA SALUD DE CASTILLA Y LEON                      | G42152405 | INSTITUTO DE INVESTIGACION BIOMEDICA DE SALAMANCA (BSAL)                   | CASTILLA Y LEON    | HOSPITAL UNIVERSITARIO DE SALAMANCA                           |
| CM21/00035 | Grupo Habitual  | MORTE ROMEA, ELENA              | FUNDACION INSTITUTO DE INVESTIGACION SANITARIA ARAGON   | G99426132 | INSTITUTO DE INVESTIGACION SANITARIA ARAGON                                | ARAGON             | HOSPITAL CLINICO UNIVERSITARIO LOZANO BLESA                   |
| CM21/00036 | Grupos dirigidos por investigadores nacidos en 1976 o posterior | PRIETO-MORENO PFEIFER, ANA      | FUNDACION PARA LA INV. INNOVACION BIOMEDICA H. U. INFANTA LEONOR- H. U. DEL SURESTE             | G88098678 | HOSPITAL UNIVERSITARIO INFANTA LEONOR                                      | MADRID             |   |
| CM21/00038 | Grupo Habitual  | ALEMANY MARTI, MONTSERRAT       | FUNDACION IDIBELL   | G58863317 | HOSPITAL DE BELLVITGE  | CATALUÑA           |   |
| CM21/00041 | Grupos dirigidos por investigadores nacidos en 1976 o posterior | JUANOLA MAYOS, EDUARD           | FUNDACION INSTITUTO INV GERMANS TRIAS I PUJOL   | G60805462 | HOSPITAL GERMANS TRIAS I PUJOL   | CATALUÑA           |   |
| CM21/00042 | Grupo Habitual  | SALAZAR LEON, JUAN DIEGO        | FUNDACION PARA EL FOMENTO DE LA INV. SANITARIA Y BIOMEDICA DE LA COMUNIDAD VALENCIANA (FISABIO) | G98073760 | HOSPITAL DOCTOR PESET  | COM. VALENCIANA    |   |
| CM21/00043 | Grupos dirigidos por investigadores nacidos en 1976 o posterior | RUANO ZARAGOZA, MARIA           | INSTITUTO DE INVESTIGACIONES BIOMEDICAS AUGUST PI I SUNYER (IDIBAPS)                            | O5856414G | INSTITUTO DE INVESTIGACIONES BIOMEDICAS AUGUST PI I SUNYER (IDIBAPS)       | CATALUÑA           | HOSPITAL CLINICO Y PROVINCIAL DE BARCELONA                    |
| CM21/00047 | Grupo Habitual  | ABELENDA ALONSO, GABRIELA       | FUNDACION IDIBELL   | G58863317 | HOSPITAL DE BELLVITGE  | CATALUÑA           |   |
| CM21/00049 | Grupos dirigidos por investigadores nacidos en 1976 o posterior | BUESA LORENZO, JULIA            | FUNDACION PARA LA INVESTIGACION DEL HOSPITAL LA FE  | G97067557 | INSTITUTO DE INVESTIGACION SANITARIA HOSPITAL LA FE                        | COM. VALENCIANA    | HOSPITAL LA FE  |
| CM21/00051 | Grupo Habitual  | MUÑOZ DELGADO, LAURA            | FUNDACION PUBLICA ANDALUZA PARA LA GESTION DE LA INVESTIGACION EN SALUD DE SEVILLA              | G41918830 | INSTITUTO DE BIOMEDICINA DE SEVILLA - IBIS                                 | ANDALUCIA          | HOSPITAL UNIVERSITARIO VIRGEN DEL ROCIO                       |
| CM21/00057 | Grupo Habitual  | CARBAYO VIEJO, ALVARO           | IB-SANT PAU. INSTITUTO DE INVESTIGACION HOSPITAL SANTA CRUZ Y SAN PABLO                         | G60136934 | IB-SANT PAU. INSTITUTO DE INVESTIGACION HOSPITAL SANTA CRUZ Y SAN PABLO    | CATALUÑA           | HOSPITAL DE LA SANTA CRUZ Y SAN PABLO                         |
| CM21/00058 | Grupo Habitual  | BENITEZ QUINTANILLA, LETICIA    | INSTITUTO DE INVESTIGACIONES BIOMEDICAS AUGUST PI I SUNYER (IDIBAPS)                            | O5856414G | INSTITUTO DE INVESTIGACIONES BIOMEDICAS AUGUST PI I SUNYER (IDIBAPS)       | CATALUÑA           | HOSPITAL CLINICO Y PROVINCIAL DE BARCELONA                    |